ANNUAL REPORT

2002

CORROSION RESEARCH

Materials Science and Engineering

Published

by

THE CORROSION RESEARCH GROUP HOKKAIDO UNIVERSITY

......

For additional copies and more information, please write to the group members

Prof. T. Ohtsuka; CORROSION ENGINEERING LABORATORY

Prof. M. Seo; INTERFACIAL ELECTROCHEMISTRY LABORATORY

Prof. T. Narita; DISSIMILAR MATERIALS INTERFACE ENGINEERING LABORATORY

Prof. H. Takahashi; INTERFACE MICRO-STRUCTURE ANALYSIS LABORATORY

Prof. H. Konno; LABORATORY OF ADVANCED MATERIALS CHEMISTRY

Assoc.Prof. H. Tamura

Graduate School of Engineering, Hokkaido University Kita13, Nishi8, Kita-ku, Sapporo 060-8628, Japan

Prof. F. Watari; DENTAL MATERIALS AND ENGINEERING LABORATORY

Graduate School of Dental Medicine, Hokkaido University Kita13, Nishi7, Kita-ku, Sapporo 060-8586, Japan

CONTENTS

Page
CURRENT ACTIVITIES and PRESENTATIONS
CORROSION ENGINEERING LABORATORY 3
INTERFACIAL ELECTROCHEMISTRY LABORATORY 14
DISSIMILAR MATERIALS INTERFACE ENGINEERING LABORATORY 24
INTERFACE MICRO-STRUCTURE ANALYSIS LABORATORY 33
DENTAL MATERIALS AND ENGINEERING LABORATORY 47
LABORATORY OF ADVANCED MATERIALS CHEMISTRY 62
OTHER CORRESPONDING MEMBER
Assoc. Prof. Dr. Hiroki Tamura 73
ABSTRACTS of PUBLICATIONS
CORROSION
Corrosion of Tin Alloys in Sulfuric and Nitric Acids
Improvement of Corrosion Property and Structual Change in
304 Stainless Steel by means of Ion-Mixing
Double-Pulse Technique as an Electrochemical Tool for
Controlling the Preparation of Metallic Nanoparticles
Evaluation of Corrosion Behavior of Iron by
Scanning Electrochemical Microscopy 80
Application of AC Resistmetry to Localized Corrosion on Iron 81

Crevice Corrosion of Types of 304L and 316L Stainless Steel in	
Nitric Acid Solutions	82
PASSIVATION and ANODIC OXIDE FILM	
Localized Corrosion of Zn-Al Alloy Coated Steels by	
Photon Rupture Method - Effect of Chloride Ions	83
Luminescence from Band-gap Photo-excitation of	
Titanium Anodic Oxide	84
Electrochemo-mechanical Properties of Passive Metal Surfaces ······	85
Mechanical Properties of Amorphous Anodic Alumina and	
Tantala Films Using Nanoindentation	86
Enrichment Behaviour of Gallium in Heat and	
Surface Treatments of Al-Ga Foils	87
Formation of Anodic Films on Magnesium Alloys in	
an Alkaline Phosphate Electrolyte ······	88
Enrichment of Alloying Elements in Anodized Magnesium Alloys	89
Behavior of Impurity and Minor Alloying Elements During	
Surface Treatments of Aluminum	90
Surface Nanotextures on Aluminium ······	91
Characterization of Electrodeposited WO ₃ Films and	
its Application to Electrochemical Wastewater Treatment ······	92
Ionic Mobilities in Amorphous Anodic Titania	93

Ionic Transport in Amorphous Anodic Titania Stabilised by Incorporation of Silicon Species
Materials for Global Carbon Dioxide Recycling
Ionic Transport in Anodically Oxidized Al/W Layers 96
Transient Anodic Oxidation of an Al-W Alloy: Effects of Current Ratio 97
Molybdate/Al (III) Composite Films on Steel and Zinc-Plated Steel by Chemical Conversion
Detachment of Alumina Films from Aluminium by 100 keV H ⁺ Ions 99
Anodic Film Growth on an Al-21at.%Mg Alloy100
Porous Tantala and Alumina Films from Non-Thickness Limited Anodising in Phosphate/Glycerol Electrolyte
Anodic Film Growth on Tantalum in Dilute Phosphoric Acid Solution at 20 and 85°C
Transmission Electron Microscopy of Non-Thickness-Limited Anodic Films on Tantalum
Anodically Deposited Manganese Molybdenum Tungsten Oxide Anodes for Oxygen Evolution in Seawater Electrolysis
Radio Frequency GDOES Depth Profiling Analysis of a B-Doped Diamond Film Deposited onto Si by Microwave Plasma CVD105

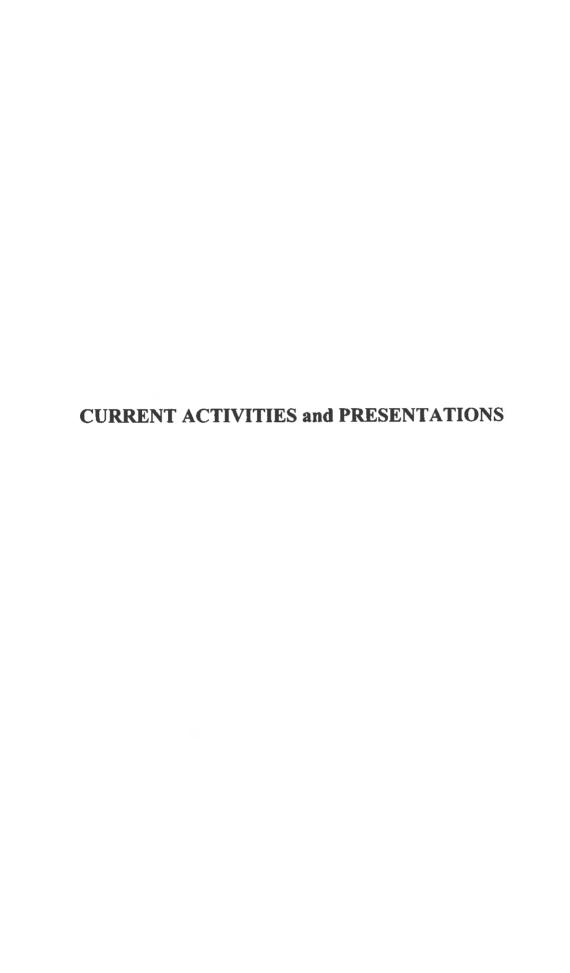
Radio Frequency Glow Discharge Optical Emission Spectroscopy
-Depth Profiling Analysis of Thin Anodic Alumina Films as
Potential Reference Materials ······106
Role of Metal Ion Impurities in Generation of Oxygen Gas
Within Anodic Alumina ······107
Oxygen Evolution Within Barrier Oxide Films108
Oxygen Evolution within Barrier Oxide Films108
Visible Light Responsibility of Titanium Dioxide Photocatalyst by
Metal Ion Decoration and Basic Research into Its Dental Application109
Modeling the Kinetics of Lithium Ion Incorporation into Tunnel Vacancies of
Spinel-Type Manganese Dioxide λ-MnO ₂ from Aqueous Solutions ·······110
Ion Freshones Bernetics of Transite in Add the form
Ion-Exchange Properties of Tetratitanic Acid with a Layer Structure for
Alkali Metal Ions ······111
Ion Complexation at Oxide-Solution Interfaces112
Potential Modulation Reflectance of Manganese Holgenated Tetrphenylporphyrin
Derivatives Assembled on Gold Electrodes ······113
Hydrogen Generation from a Single Crystal Magnetite Coupled Galvanically
with a Carbon Steel in Sulfate Solution114
Effects of Dichromate Treatment on Mechanical Properties of
Passivated Single Crystal Iron (100) and (110) Surfaces115
Tabbrated Single Crystal Iron (100) and (110) Surfaces
Scanning Electrochemical Microscopic Study of Detecting
Non-homogeneity in Surface Reactions of Metals116

Monitoring of Hydrogen Absorption into Titanium using Resistmetry117
Effects of Iron (III) Ions on Corrosion of Stainless Steel in Concentrated Nitric Acid Solutions at High Temperature
Formation of Anodic Oxide Films on Aluminum in Diluted KOH Solutions119
Increase in Breakdown Potential of Anodic Oxide Film on Aluminum by Pore-Filling Method
Repairing of Anodic Oxide Films on Al - Zn Alloy Coated Steel After Removal with Photon Rupture in Solutions
Anodizing of Aluminum Covered with SiO ₂ by Sol-Gel Coating. -Formation Mechanism of composite Oxide Films with High Potential Sustainability-
Scanning Confocal Laser Microscopy of the Surface of Anodized Al5052 Alloy
Effect of Mg and Si on the Microstructure and Corrosion Behavior of Zn-Al Hot Dip Coatings on Low Carbon Steel
Effect of Carbon Content on the Reaction Behavior of Hot Dipped Carbon Steel in Molten Zn-6mass%Al Bath
SURFACE FINISHING
Effect of Spark Plasma Sintering Pressure on the Properties of
Functionally Graded Implant and Its Biocompatibility126
Structual Analysis of Arabinogalactan from Japanese Larch in Hokkaido
and Chemical Functionalization of Arabinogalactans127

	Effects of Ti ions and Particles on Neutrophil Function and Morphology ······128
	Effects of Particle Size on Cell Function and Morphology in Ti and Ni
	Surface Properties and Biocompatibility of Nitrided Titanium for Abrasion Resistant Implant Materials
	Mechanical Properties of Surface Nitrided Titanium for Abrasion Resistant Implant Materials
	Development of Arch Form Esthetic Orthodontic Wires by Light Polymerization 132
	The Development of the Estetic Orthodontic Wire ······133
	Effect of the Addition on Intermediate Oxide on Firing Contraction of Porcelain Inlay Processed by Cold Isostatic Pressing Method
	Effect of Debindered Spherical Particle on Porcelain Inlay Processed by Cold Isostatic Pressing
]	HIGH TEMPERATURE OXIDATION and SULFIDATION
	Roles of Aluminium and Chromium in Sulfidation and Oxidation of
	Sputter-Deposited Al- and Cr-Refractory Metal Alloys
	Oxidation Behavior of Mo ₅ SiB ₂ -Based Alloy at Elevated Temperatures ······138
	Sorption and Recovery of Heavy Oils Using Carbonized
	Fir Fibers and Recycling ······139

Microstructure and Oxidation Behavior of ReSi _{1.75} Synthesized by Spark Plasma Sintering140
Degradation of Cr ₂ O ₃ Scale Formed on Stainless Steel in H ₂ O-Containing Atmospheres ······141
High-Temperature Oxidation Behavior of ReSi _{1,75} 142
Oxidation Behavior of Fe-25Cr Alloy under Mechanical Loading in Atmosphere Containing SO ₂ at High Temperature143
High Temperature Oxidation Behavior of TiAl Coated by Al-Cr Alloy in Molten Salt144
Coating of Ni-Aluminides on TiAl Intermetallics Through Up-hill Diffusion
Sulfidation Properties of TiAl-2at.%X (X=Si, Mn, Ni, Ge, Y, Zr, La and Ta) Alloys at 1173K and 1.3Pa sulfur Pressure in an H ₂ S-H ₂ Gas Mixture146
SOLIDIFICATION Modifying Solidification Structures of Sn-Ag Alloys with Third Elements147
Growth Direction of Cellular and Dendritic Interface in a Constrained Growth Condition
Investigation of the Mechanism of Alloy Dendrite Deflection due to Flowing Melt by Phase-Field Simulation
Probabilistic Parameter for Nucleation during Solidification of Al Alloys150
Tempetature-enthalpy Curves of Multicomponent Casting Alloys151

Reactive Ca	sting and	Welding of	of High-Meltin	g-Point		
Intermetallic	Compour	nds ······	• • • • • • • • • • • • • • • • • • • •	*****	•••••	152



CORROSION ENGINEERING LABORATORY

Prof. Dr. Toshiaki Ohtsuka TEL/FAX: +81-11-706-6351

E-mail: ohtsuka@elechem1-mc.eng.hokudai.ac.jp

Assoc. Prof. Dr. Takeshi Sasaki

TEL: +81-11-706-6352

: +81-11-706-7813 FAX: +81-11-706-7813

E-mail: txsasaki@eng.hokudai.ac.jp

Lecturer Dr. Takenori Notoya

TEL/FAX: +81-11-706-6353

E mail: tnotoya@eng.hokudai.ac.jp

Res. Assoc. Dr. Mikito Ueda

TEL/FAX:+81-11-706-7813

E mail: mikito@eng.hokudai.ac.jp

Technician Dr. Shoichi Konda

TEL: +81-11-706-7236

FAX: +81-11-706-7813

E mail: konda@eng.hokudai.ac.jp

Research Fellow

Masaru Matsuda

Students

M. Nagata, K. Hayakawa, K. Hioki, T. Domyo, H. Kigawa, T. Komatsu, M. Ito, G. Ando, M. Iida, Y. Horiguchi, M. Yosimatsu

Facilities and Capabilities

Ellipsometer: Rotating-analyser type of automated ellipsometer with 632.8 nm

wavelength of light.

Potential Modulation Reflectance: Wavelength region from 350 to 800 nm.

Raman Scattering Spectrometer: JASCO R-800T, triple type of spectrometer equipped with an Argon gas laser of 2W power.

FT-IR Spectrometer: JASCO FT/IR 550 equipped with MCT detector for in-situ measurement of corrosion layers on metals.

QCM system for in-situ gravimetry of surface layer on metals.

Electrochemical AC Impedance: NF Circuit Design 5020 FRA equipped with a specially designed potentiostat.

Spectrophotometer: JASCO V-520 in a wavelength region from 200 to 900 nm.

Electrochemistry apparatuses.

Optical Microscopy

Electrochemical Corrosion-Rate Monitor System.

Our research activities are concerned with corrosion and corrosion prevention of metals, molten salt electrolysis and modeling of artificial photosynthesis system.

Research programs in progress are as follows:

(1) New corrosion resistive films consisting of conductive polymers

A conductive polymer coating was applied to corrosion prevention of carbon steels. A bilayered polypyrrole (PPy) film doped by polymolibdate (PMo) ions at the inner side and by 1,5-naphtharendisulfonic (NDS) ions at the outer side was successfully formed on the steel plate by electropolymerization from pyrrole monomers in aqueous solutions. PMo in the inner layer enhances the formation of ppasive oxide film on the steel and NDS in the outer layer suppresses leaching of the PMo into aqueous solutions. The bilayer PPy film greatly decreases the corrosion rate of the steel plate to a level of the passive current in 3.5 wt% NaCl solution and keep the open circuit potential high enough for the passive region, although the respective single PPy films do not induce any decrease of the

corrosion rate.

(2) Artificial model for photosynthesis

In the bioreaction, the quinone and porphyrin derivatives are surrounded by a hydrophobic protein environment. The hydrophobic environment was realized by using phopholipid bilayer membrane on electrodes. The electron transfer of the quinone and metallic porphyrin derivatives was measured in the membrabe in which the quinone or manganese porphyrin derivatives were occluded. Photo-induced current was also measured in the membrane electrode consisting of the phopholipid occluding zinc or magnesium porophyrins. Photocurrent action spectra corresponding to the absorption spectra coud be measured, although the conversion efficiency from photon to electronic current is not enough large.

(3) Monitoring of corrosion layer on zinc by Raman spectroscopy

Corrosion layer on zinc and zinc alloy covering steels formed in a model atmosphere was monitored by Raman scattering spectroscopy under the in-situ condition. At the presence of NaCl, aqueous ZnCl₂ layer is at first formed by the electrochemical reaction between zinc and oxygen in the water layer adsorbed from the humidified air. When the concentration of ZnCl₂ in the aqueous surface layer increases and reaches the saturation, simonkolleite begins to form. The time periods to the formation of aqueous ZnCl₂ layer at enough high concentration and of simonkollite greatly depended on the composition of alloys. Addition of Al and Ni into zinc coatings delays the formation of ZnCl₂ layer and simonkollite.

(4) Evaluation of corrosion rate of steels in solutions containing snow-melt salts

Corrosion Rate of Steels was evaluated in solutions containing snow-melt salts of NaCl-CaCl₂ and NaCl-MgCl₂ by an electrochemical polarization technique. Various inhibitors were attempted to suppress the corrosion of steels in the solutions. The poly-phosphate salt was found to be one of the effective inhibitors for decreasing the corrosion loss in this solution.

(5) Passive film on nickel by ellipsometry

The passive oxide film anodicaly formed on nickel was measured in acidic sulfate solutions at pH 2 and 3 by an automated ellispometry. The thickness of the film was about 1.5 to 2.0 nm, not clearly depending on potential and solution pH. The potential change from anodic passive region to a cathodic potential, the film changed in refractive index to a lower values in the initial 30 s period, accompanied by increase of the thickness. The reduction of the film thickness gradually takes place after the initial change. The behavior of the cathodic reduction of the film can be explained by the initial hydration from NiO passive film to a hydrated film, followed by dissolution of the hydrated oxide.

(6) Improvement of Corrosion resistance of TiAl inter-metallic compound by coating of Al-Cr alloy from a molten salt electrolysis

A coating layer of Al-Cr alloy was cathodically formed at 423 K on the TiAl inter-metallic coumpound in an AlCl₃-NaCl-KCl molten salt mixture containing CrCl₂. A large improvement for oxidation resistance of the TiAl compound at 1173 K was obtained by the coating of the Al-Cr alloy layer.

(7) Electrophoretic deposition for preperation of functional oxide films

Oxide powder with perovskite structure was deposited electrophoretically in an organic solvent to prepare the oxygen permeability membrane. For estimation of the electrophoretic deposition mechanism, a potential profile in the organic solution containing the oxide powder was measured by a probe electrode the position of which can be controlled. It was found that a potential drop about 15 V was required at the solution/ electrode interfacial layer.

(8) Corrosion products on copper in humid air containing sulfur dioxide

Surface layers initially formed on copper in air containing SO₂ have been investigated by in situ IR-RAS. The identification of the corrosion products and determination of their formation rates was achieved by combining in situ IR-RAS

and QCM measurements. The layer-thickness of the physically adsorbed water was also determined as a function of time. The layer-thickness increased with time under the constant relative humidity. This was explained by the capillary effects of the corrosion products and/or the large affinity of the corrosion products with water.

(9) Adsorption of thiourea on a gold electrode in perchloric acid

Adsorption of thiourea on gold in percholric acids and its structure changes with potential were investigated using in situ surface-enhanced infrared absorption spectroscopy together with the electrochemical technique. The results have been verified by ab initio molecular orbital calculation.

Other Activities

Prof. Ohtsuka attended the 2nd Intern. Conf. on Environment Sensitive Cracking and Corrosion Damage, Hiroshima, 29 Oct.-2 Nov., 2001 and presented a paper entitled by Luminescence with Band Gap Energy by UV-Light Excitation to Anodic Oxide Films on Titanium.

Associate professor T. Sasaki attended the 8th Joint Seminar between University of Science and Technology Beijing and Hokkaido University, Beijing/China, 24-26 April and presented a paper entitled by in situ IR-RAS investigation of corrosion of tin in air containing H₂O, NO₂ and SO₂ at room temperature. He also attended the 7th International Symposium on Advances in Electrochemical Science and Technology, Chennai/India, 27-29 November and presented a paper entitled by corrosion of tin in humid air containing NO₂ and SO₂ in room temperature as investigated by in situ IR-RAS and a paper entitled by adsorption of thiourea on gold electrode in perchloric acids studied by in situ surface-enhanced infrared absorption spectroscopy. After the symposium he visited the Central Electrochemical Research Institute in Karaikudi/India and presented a paper entitled by quantitative determination of corrosion products on copper in gaseous

Current Activities and Presentations

environments by using IR-RAS and QCM.

Dr. M. Ueda attended the 13th international symposium on Molten Salt (The Electrochemical Society), Philadelphia, U. S. A. 12 – 17 May and presented a paper entitled by High Temperature Oxidation Behavior of TiAl Coated by Al-Cr Alloy in Molten Salt. He also attended the 53rd Annual meeting of the International Society of Electrochemistry, Duesserdorf, Germany 15-20 September and presented a paper entitled by Preparation of Silver Nano-particles by using a Double-pulse Technique.

Presentations

Measurement of Reaction Rates of Self-assembled Redox Monolayers by Potentialmodulation Reflectance; T. Yamada, M.Nango, T. Ohtsuka: The Joint Meeting of The Hokkaido Sections of ECS Jpn, Surf. Finish. Soc. Jpn, and Jpn Soc. Corros. Eng., Sapporo, Jan., 2002.

Corrosion Prevention of Carbon Steels by a Composite Coating of Polypyrrole and Polymolibdate; T. Domyo, T. Ohtsuka: The Joint Meeting of The Hokkaido Sections of ECS Jpn, Surf. Finish. Soc. Jpn, and Jpn Soc. Corros. Eng., Sapporo, Jan., 2002.

Improvement of Surface Properties of Various Stainless Steels by Ion Mixing Technique; Y. Masumoto, M. Takeda, T. Suda, S. Watanabe, S. Ohnuki, and T. Ohtsuka: Winter Meeting of Hokkaido Branch of Jpn Inst. Metals and ISIJ, Jan., 2002.

Adsoption of Thiourea on Gold Electrodes; M. Kondo, H. Tachikawa, T. Sasaki, and T. Ohtsuka: Winter Meeting of Hokkaido Branch of Jpn Inst. Metals and ISIJ, Jan., 2002.

Insertion of LH Complex into Lipidbilayers and its Photocurrent; M. Nagata, T. Ohtsuka, Y. Yoshimura, N. Kajiwara, K. Dewa, K. Yamashita, and M. Nango: The 81st Annual Meeting of the Chemical Soc. Jpn, Tokyo, March, 2002.

Organization of LH Protein-Bacteriachrolofil Complex in lipidbilayer; J. Inagaki, Y. Yoshimura, M. Nagata, T. Ohtsuka, K. Dewa, K. Yamashita, M. Nango: The 81st Annual Meeting of the Chemical Soc. Jpn, Tokyo, March, 2002.

Self-assembled Monolayer of LH Complex and its Photocurrent; T. Ochiai, Y.

Yabuki, M. Nagata, T. Ohtsuka, K. Dewa, K. Yamashita, M. Nango: The 81st Annual Meeting of the Chemical Soc. Jpn, Tokyo, March, 2002.

Film Structure of Benzotriazole Derivatives on Cupper Surface; T. Notoya, M. Satake, T. Ohtsuka, H. Yashiro, T. Yamauchi, and D. P. Schweinberg: The 69th Annual Meeting of Electrochem. Soc. Jpn., Sendai, April, 2002.

Relation between Applied Potential and Electromigration Deposition of La-Sr-Co Oxides; K. Hayakawa, M. Ueda, and T. Ohtsuka: The 69th Annual Meeting of Electrochem. Soc. Jpn., Sendai, April, 2002.

Complex Plane Plots of Potential Modulation Reflectance of Manganese Porphyrin Monolayers with Redox Response; T. Ohtsuka and T. Yamada: The 69th Annual Meeting of Electrochem. Soc. Jpn., Sendai, April, 2002.

In Situ IR-RAS Investigation of Corrosion of Tin in Air Containing H₂O, NO₂ and SO₂ at Room Temperature; T. Sasaki, R. Kanagawa, and T. Ohtsuka: The 8th Joint Seminar between University of Science and Technology Beijing and Hokkaido University, University of Science and Technology Beijing, Beijing/ China, April, 2002.

High Temperature Oxidation Behavior of TiAl Coated by Al-Cr Alloy in Molten Salt, M. Ueda, D. Susukida, S. Konda, and T. Ohtsuka, The 13th International Symposium on Molten Salt, Philadelphia U.S.A. May 12-17,2002.

Raman Spectroscopy for Corrosion Products Formed on Zinc and Zinc-Coated Steels in Humid Air with NaCl Particles; T. Ohtsuka and M. Matsuda, The 1st International Conference on Advanced Structural Steels: Tsukuba International Congress Center, Tsukuba, Japan, May 22-24, 2002.

Evaluation of Protection Ability of Iron Rust Layers by AC Conductance; T_{et} Ohtsuka: The 2002 Annual Meeting of Jpn Soc. Corros. Eng., Kawasaki, May, 2002.

Luminescence of Anodic Oxide Films on Titanium by Uv Light Excitation; M. Ueda and T. Ohtsuka: The 2002 Annual Meeting of Jpn Soc. Corros. Eng., Kawasaki, May, 2002.

Corrosion Prevention of Polypyrrole-Polymolibdate Composite Films; T. Domyo and T. Ohtsuka: The 2002 Annual Meeting of Jpn Soc. Corros. Eng., Kawasaki, May, 2002.

Effect of Electrode Configuration for the Preparation of Oxide Layers by Electromigration Deposition; K. Hayakawa, M. Ueda, and T. Ohtsuka: Summer Meeting of Hokkaido Branches of Jpn Inst. Metals and ISIJ, Jun., 2002.

Construction of Photosynthetic Antenna Complex in Lipid Bilayers; Morio Nagata, Junichi Inagaki, Yoshimi Yoshimura, Toshiaki Ohtsuka, Kouji Iida and Mamoru Nango: 2nd International Conference on Porphyrins and Phthalocyanines, Kyoto, July, 2002.

Photocurrent of Light-harvesting Complex in Lipid Bilayers Assembled on Electrodes; Morio Nagata, Mamoru Nango, and Toshiaki Ohtsuka:14th International Conference on Photochemical Conversion and Storage of Solar Energy, Sapporo, 2002.

Laboratory Cell for Metallic Electrochemistry; T. Ohtsuka: Symposium for Training of Technicians in the Universities at Hokkaido Area, July, 2002.

Adsorption of Water Vaper on Various Fe(III) Oxyhydroxides; T. Komatsu, T.

Sasaki, and T. Ohtsuka: The 49th Discussion Meeting of Jpn. Soc. Corros. Eng., Sept. 2002.

Preparation of Silver Nano-particles by using a Double-pulse Technique, M.Ueda, A. Anders, H. Dietz and W. Plieth, 53rd annual meeting of the International Society of Electrochemistry, Duesseldorf Geramny, Sept. 2002.

Effect of Inhibitors on thr Corrosion Prevention of Steels in Aqueous Solution Containing Chloride Snow Melts; S. Konda, T. Ohtsuka, M. Kubota, and N. Yoshimoto: The 49th Discussion Meeting of Jpn. Soc. Corros. Eng., Sept. 2002.

Infra-red Spectra of Water Adsorbed on Gold; T. Sasaki, M. Yokoyama, and T. Ohtsuka: The 49th Discussion Meeting of Jpn. Soc. Corros. Eng., Sept. 2002. Analysis of Solid-liquid Interfaces by Using Light Reflection in Visible Region; T. Ohtsuka: The 33rd Joint Meeting of Chubu Branches of Chemistry Related Societies, Oct., 2002.

Kinetics of Charge Transfer Reaction at Solid-liquid Interface; T. Ohtsuka: Simposium of the 19th Committee for Steel Making of JSPS, Oct, 2002.

Formation Sequence to Simonkollite during Atmospheric Corrosion of Zinc by Raman Spectroscopy; T. Ohtsuka and M. Matsuda: The 140th ISIJ Autumn Meeting, Intern. Session, Nov., 2002.

Redox Reaction Rate on the Electrode covered by Manganese Porphyrin Monolayer; T. Ohtsuka: The 13th Symposium of Catalysis Research Center of Hokksaido Unversity, "Nonotechnology and Catalytic Chemistry", Nov., 2002.

Corrosion of Tin in Humid Air Containing NO₂ and SO₂ in Room Temperature as Investigated by in situ IR-RAS, T. Sasaki, R. Kanagawa and T. Ohtsuka, The 7th

International Symposium on Advances in Electrochemical and Science Technology, Chennai, India, Nov., 2002.

Adsorption of Thiourea on Gold Electrode in Perchloric Acids Studied by in situ Surface-enhanced Infrared Absorption Spectroscopy, T. Sasaki, M. Kondo, H. Tachikawa, M. Osawa and T. Ohtsuka, ibid.

Effect of Electric Field Direction and Number of Deposition in Formation of Perovskite Type Oxide Layer Using a Electrophoretic Deposition, M. Ueda, K. Hayakawa and T. Ohtsuka, 34th sympsium on Molten Salt Chemistry, Toyohashi, Nov. 2002.

Quantitative Determination of Corrosion Products on Copper in Gaseous Environments by Using IR-RAS and QCM, T. Sasaki, Post-symposium of ISAEST-VII, Karaikudi, India, Dec., 2002.

INTERFACIAL ELECTROCHEMISTRY LABORATORY

Prof. Dr. Masahiro Seo TEL/FAX: +81-11-706-6735

E-mail: seo@elechem1-mc.eng.hokudai.ac.jp

Assoc. Prof. Dr. Kazuhisa Azumi TEL/FAX: +81-11-706-6736

E-mail: azumi@elechem1-mc.eng.hokudai.ac.jp

Res. Assoc. Dr. Koji Fushimi TEL/FAX: +81-11-706-6737

E-mail: fushimi@elechem1-mc.eng.hokudai.ac.jp

Foreign Researcher

Dr. Joong-Do Kim

Students

M. Chiba, K. Iokibe, T. Ueno, N. Kikuchi, Y. Kurata, T. Kurihara A. Kanada, M. Yamazaki, K. Yamaya, M. Hagioi, Y. Hosin and N. Munakata

Equipments

Atomic Force Microscope: Digital Instruments Nanoscope-III

Nano-indentation Apparatus: Hysitron Inc.

EQCM System.

Laser-Bending Beam Apparatus for Stress Measurement.

Piezo-electric Detection Apparatus for Surface Stress Measurement

Scanning Electrochemical Microscope System.

The research activity of the laboratory still continues to be directed towards a

better understanding of the interfacial properties of metal and semiconductor electrodes in relation to the interfacial electrochemistry involving adsorption, corrosion, passivation, anodic oxidation, hydrogen adsorption / absorption, and surface finishing.

Current topics on research are as follows:

(1) Mechano-Electrochemical Properties of Passive Iron Surfaces Evaluated by an *In-situ* Nano-Scratching Test.

In-situ (as kept at 0.25 V vs. SHE in solution) and ex-situ (in air) nano-scratching tests were performed to the iron single crystal (110) and (100) surfaces passivated at 0.25 V (SHE) in pH 8.4 borate solution to evaluate the mechanical and electrochemical properties. correlated i.e., mechano-electrochemical properties of the passive surfaces. The friction coefficient of the passive iron (100) surface was larger than that of the passive iron (110) surface, irrespective of in-situ or ex-situ nano-scratching. The friction coefficient obtained with *in-situ* nano-scratching for both the passive iron (110) and (100) surfaces were significantly larger than that obtained with ex-situ nano-scratching. The increase in friction coefficient due to in-situ nano-scratching was explained in terms of a series of mechano-electrochemical reaction taking place at the moving front of the indenter such as active dissolution from the film rupture sites followed by repassivation.

(2) Measurement of Stress Changes during Electrodeposition of Multi-layers of Cu and Cu₂O.

The potential oscillation was observed during cathodic polarization of a gold electrode at a constant current density of $i_c = 1.0$ mA cm⁻² in pH 7.0, 0.02 M CuSO₄ + 0.2 M lactic acid solution. The derivative of mass change with cathodic charge obtained with EQCM suggested that multi-layers of Cu and Cu₂O were electrodeposited on the gold. The oscillation of stress changes synchronized with

the potential oscillation was also found by using a bending beam method. The stress changed to the tensile direction when the potential dropped, i.e., Cu was deposited, while the stress changed to the compressive direction when the potential raised, i.e., Cu₂O was deposited.

(3) Effect of Trace Amount of Pb on Corrosion of Nickel Thin Film.

The effect of trace amount of Pb on corrosion of nickel thin film in pH 3.0 perchlorate solution was investigated by an EQCM. It was found from comparison between the polarization curve and gravimetrical curve that the addition of 10⁻⁴ M Pb²⁺ in solution retarded the active dissolution of nickel, while it lowered the stability of passive film on nickel. The retardation of active dissolution was ascribed to the adsorption of Pb²⁺ on nickel.

(4) Local Formation of Porous Layer on n-Type InP with Electrochemical Etching after Scratching.

A surface scratching of n-type InP (100) wafer with a diamond pencil, followed by an electrochemical etching in 0.5 M HCl was performed to find the optimum condition for preparation of a porous layer on the specified local area. The porous layer could be formed only on the scratched area by a potentiostatic etching at 1.1 V (SHE) for 300 s. The line width of the porous layer changed from 1.5 μ m to 10 μ m, depending on the load level normal to the surface. The micro-structure of the porous layer was oriented normal to the scratching direction. The defective zones were also observed along the out side edge of the porous layer.

(5) Direct Plating of Ni-P onto Sputter Deposited Al Alloy Films

Electroless Ni-P plating was directly deposited on various kind of Al alloy films formed on glass plate using magnetron sputter deposition method. On Al-Ni, Al-Cu, Al-Pt and Al-Pd films, Ni-P layers were successfully deposited without double zincate pretreatment. Peeling test showed that good adhesion strength of plating layer with the substrate of Al alloy films was acheived. On Al-Fe alloy film,

however, sparsely dispersed dome-like depositions were formed on the surface probably due to lower catalytic activity of Fe for deposition reaction. Considerably flat interface between the plating layer and the substrate of Al alloy films observed with AFM proposed that the strong adhesion strength of the plating layer was brought by not the anchor effect but the metallic binding at the nucleation points that were formed in the initial stage of the plating process.

(6) Application of Resistmetry to Al Dissolution under Hydrogen Evolution Reaction.

Resistmetry was applied to the Al dissolution during the condition of hydrogen evolution under cathodic polarization. Decomposition reaction of water forms OH ions resulting in increase of pH around the electrode surface. This causes dissolution of Al surface due to local alkalization of electrolyte solution. The dissolution rate of thin-wire form Al electrode during potential sweep in the potential range between –5 and 5 V_{RHE} was evaluated as a function of composition of electrolyte solutions. Specimen surface after experiments showed formation of large pits in the borate solution at pH 6.5, and depositions of Al hydroxide layer in the sulfate solutions. In the polarization curve measured in the sulfate solutions a cathodic current peak appeared depending on the concentration of H₂SO₄, i.e., pH of the solution. After appearence of this peak the cathodic current in the subsequent cycles of the potential sweep decreased and the dissolution of Al was also suppressed. This phenomena was named as the "cathodic passivation" phenomena.

(7) Preferential Sputtering of Oxide Film on Metal under Plasma Discharge

SUS electrodes were oxidized at high temperature in air to form thick oxide film and then immersed in the aqueous electrolyte solution to be polarized cathodically at the cell voltage higher than 100 V. In this condition high temperature plasma layer was formed at the interface of electrode and solution. Charged particles in the plasma layer bombarded the electrode surface resulting in sputtering of the surface. Since the work function of the oxide film is lower than that of metal surface, the

oxide layer was preferentially sputtered by the plasma. The oxide films with a few µm in thickness were sputtered within 10 s. Spectra of the light emitted from the plasma layer was continuously measured during sputtering using a CCD spectrometer. Change in intensities of atomic emission lines with sputtering time reflected the change in surface composition of the oxide layer such as Fe, Cr and O. Determination of depth profile of atomic composition from the spectral change was, however, difficult because the sputtering was occurred too rapidly and non-uniformly.

(8) Initiation of Localised Corrosion on Copper Thin Film Electrode by Combinational Use of an EQCM with a Liquid-Phase Ion Gun

A new method allowing simultaneous observation of anodic currents and small mass changes during initiation was developed to discuss early growth of a single localised corrosion site. An electrochemical quartz crystal microbalance (EQCM) was combined with a liquid-phase ion gun (LPIG) consisting of an Ag/AgCl microelectrode which produces chloride ions, causing local breakdown of passive film and pit growth. The method was applied to copper thin films polarized anodically at +600 or +800 mV (SHE). It was found from comparison between coulometry and gravimetry that copper dissolves as Cu²⁺ during the pit growth.

Other Activities

In February, Prof. M. Seo received the 2002 Japan Surface Finishing Society Award for the Study on Specific Adsorption and Anodic Oxidation of Metals by Piezo-electric Response and Surface Stress Methods. In April, Dr. K. Fushimi visited the Max-Planck-Institut für Eisenforschung, Düsseldorf, Germany to conduct a postdoctoral work for 14 months under supervision of Prof. M. Stratmann. In May, Prof. M. Seo participated in the first International Conference on Advanced Structural Steels, Tsukuba, Japan and presented the lecture entitled "Novel Methods of Determining Non-Homogeneity in Surface Film". Dr. K. Fushimi received the 2002 Advanced Award of the Japan Society of Corrosion

Engineering for the Study on Evaluation of Heterogeneity and Local Breakdown of Passive Film by Scanning Electrochemical Microscopy. In July, Prof. M. Seo paid a visit to Dr. B. MacDougall at the Institute for Chemical Process and Environmental Technology, National Research Council Canada, Ottawa and presented the seminar entitled "Fundamental Electrochemistry of Metal Electrodes". In August, Dr. J. –D. Kim left this laboratory after the postdoctoral work as JSPS foreign researcher for two years and belonged to Samsung Techwin Co. Ltd., Korea. In September, Prof. M. Seo, Mr. M. Chiba (Ph. D. Student) and Mr. Y. Kurata (Msc. Student) participated in the 53rd Annual Meeting of International Society of Electrochemistry held in Düsseldorf, Germany to present one oral and two poster papers, and visited the Max-Planck-Institut für Eisenforschung. Furthermore, Prof. M. Seo participated in the 15 th International Corrosion Congress held in Granada, Spain and presented the plenary lecture entitled "Electrochemo-mechanical Properties of Passive Metal Surfaces".

The following foreign scientists visited this laboratory: Mr. S. -B. Lee and Mr. C.-H. Kim (Ph.D. Students of Prof. S.-I Pyun), Department of Materials Science and Engineering, Korea Advanced Institute of Science and Technology (KAIST), Korea, from January 14 to 17, Dr. C.A. Melendres, California, USA, on January 29, Prof. Y. Shacham-Diamand, Research Institute of Nano-Science and Nano-Technology, Telaviv University, Israel, on October 30, Prof. K. Nisancioglu, Department of Electrochemistry, Faculty of Chemistry and Biology, Norwegian University of Science and Technology Trondheim, Norway, on November 13.

Presentations

- K. Yamaya, M. Seo and A. W. Hassel: Changes in Micro-structure due to Cathodic Polarization for Porous n-type InP Prepared with Anodic Etching, The 2002 Joint Meeting of Hokkaido Section of Electrochem. Soc. Jpn., Surf. Finish. Soc. Jpn., and Jpn. Corrosion Eng., Sapporo, Jan., 2002.
- J. -D. Kim and M. Seo: Stresses in Anodic Oxide Film on Nickel, ibid.
- Y. Kurata, J.-Y. Go, M. Chiba, S.-I. Pyun and M. Seo: Nano-indentation of Tantalum Surfaces Subjected to Anodic Oxidation, ibid.
- M. Yamazaki and M. Seo: Measurement of Changes in Surface Stress of Gold Electrode during Underpotential Deposition of Pb, ibid.
- H. Mitani, S. -I. Pyun and M. Seo: Fundamental Study on Electrochemical Reaction of Positive Electrode in Nickel-Hydrogen Battery, ibid.
- T. Ueno, K. Azumi and M. Seo: Analysis of Cathodic Dissolution Mechanism of Al by Resistometry, ibid.
- A. Kanada, K. Azumi and M. Seo: Preparation of Ultra-fine Particles of Metals and Semiconductors by a High-voltage Cathodic Discharging, ibid.
- T. Kurihara, K. Azumi and M. Seo: Electroless Plating of Ni-P on Al Alloys and Relation between Morphology and Adhesion at the Plating layer and Substrate Interface, ibid.
- T. Yugiri, K. Azumi and M. Seo: Direct Nickel Plating on Al-Ni Alloy Thin Films, ibid.

- N. Kikuchi and M. Seo: Analysis of Passivation Process of Electroplated Nickel Thin Film in Sulfate Solutions with Different pH Values, The 2002 Joint Hokkaido Section Winter Meeting of the Japan Analytical Society and Japan Chemical Society, Sapporo, Feb., 2002.
- M. Seo: Study on Specific Adsorption and Anodic Oxidation of Metal Surfaces by Piezo-electric Response and Surface Stress Methods, The 105 th Annual Meeting of Surface Finishing Society of Japan, Hitachi, Mar., 2002.
- T. Ueno, K. Azumi and M. Seo: Analysis of Cathodic Dissolution of Al by Resistmetry, ibid.
- K. Azumi, T. Kurihara, M. Seo and T. Kawashima: Observation of the Interface between Ni-P deposition layer and Al Alloy Substrat, ibid.
- K. Azumi, T. Yugiri, M. Seo and T. Kawashima: Direct Electroless Ni-P Plating on Sputter-deposited Al-Ni Alloy Films, ibid.
- Y. Kurata and M. Seo: Evaluation of Mechanical Properties of Titanium Surfaces by In-situ Nano-indentation and Nano-scratching, ibid.
- J. -D. Kim and M. Seo: Changes of Stress in Anodic Oxide Film on Nickel during Anodic and Cathodic Polarization, ibid.
- M. Seo and M. Yamazaki: Changes in Surface Stress of Gold Electrode during Underpotential Deposition of Pb, The 69th Annual Meeting of the Electrochem. Soc. Jpn., Sendai, April, 2002.
- M. Seo and T. Yamaya: Changes in Micro-morphology of Porous n-Type InP due to Cathodic and Anodic Polarization, ibid.

- K. Azumi, M. Kawaguchi, A. Kanada and M. Seo: Trial of Preparation of Metal and Semiconductor Fine Particles by Using a High-voltage Discharging Electrode in Aqueous Solution, ibid.
- M. Seo: Novel Methods of Determining Non-Homogeneity in Surface Film, The First International Conference on Advanced Structural Steels, Tsukuba, May, 2002.
- J. -D. Kim and M. Seo: Changes in Stress of Anodic Oxide Film on Ni by Potential Steps, The 2002 Annual Meeting of Jpn. Soc. Corrosion Eng., Kawasaki, May, 2002.
- N. Kikuchi and M. Seo: Analysis of Passive and Trans-passive Processes of Electroplated Nickel Thin Film, ibid.
- M. Chiba and M. Seo: Evaluation of Mechano-electrochemical Properties of Passive Iron Surfaces by Nano-indentation and Nano-scratching, ibid.
- K. Azumi and M. Seo: Corrosion Characteristics of Carbon Steel-Titanium Clad in Neutral Aqueous Solutions, ibid.
- Y. Kurata, J.-Y. Go, S.-I. Pyun and M. Seo: Nano-indentation of Tantalum Surfaces Anodically Oxidized, The 53 rd. Annual Meeting of the International Society of Electrochemistry, Dusseldorf, Germany, Sept., 2002.
- M. Chiba and M. Seo: Nano-mechano-electrochemical Properties of Passive Iron Surfaces Evaluated by an *In-situ* Nano-scratching Test, ibid.
- K. Fushimi and M. Seo: Micro-fabrication of Steel Surface by liquid-phase Ion Gun, ibid.

- A. Mingers, A. W. Hassel and M. Seo: The Kinetics of Simultaneous Indium Deposition and Hydrogen Evolution on Indium Phosphide and Gold, ibid.
- M. Seo and Y. Kurata: Nano-mechano-electrochemical Properties of Passive Titanium Surfaces Evaluated by In-situ Nano-indentation and Nano-scratching, ibid.
- M. Seo: Electrocheme-mechanical Properties of Passive Metal Surfaces, The 15th International Corrosion Congress, Granada, Spain, Sept., 2002.

DISSIMILAR MATERIALS INTERFACE ENGINEERING LABORATORY

Prof. Dr. T. Narita

Tel.:+81-11-706-6355 Fax.:+81-11-706-7814 E-mail:narita@eng.hokudai.ac.jp Assoc. Prof. Dr. K. Ohsasa

Tel.:+81-11-706-6356 Fax.:+81-11-706-7814 E-mail:sasa@eng.hokudai.ac.jp Res. Assoc. H. Taumi

Tel.:+81-11-706-6356 Fax.:+81-11-706-7814 E-mail:taumi@eng.hokudai.ac.jp Res. Assoc. Dr. S. Hayashi

Tel.:+81-11-706-6357 Fax.:+81-11-706-7814 E-mail: hayashi@eng.hokudai.ac.jp
Tech. Staff J. Tanaka

Tel.:+81-11-706-6357 Fax.:+81-11-706-7814 E-mail: jtanaka@eng.hokudai.ac.jp

Foreign Researchers

Zane Zhenyu Liu

Students

F. Lang, S. Gun Su, M. T.Izumi, Y.Natsume H.Shirosawa, S.Tominaga, S.Narita T.Nishimoto D.Iino, Y.Matsumura, N.Nishiguchi N.Suzuki, D.Sumoyama, Y.Taguwa and K.Nakagawa

The research activities of the laboratory are directed to an understanding of the mechanism of the high temperature corrosion in super alloys, inter-metallic compounds and iron-based alloys, and to the development of the corrosion resistant alloys and corrosion protection of materials with coating and surface modification. The research activity is also directed to an understanding of the solidification mechanism of metals and Alloys and to develop the modeling of casting structure using Phase-field, Cellular Automata, MonteCalro and Molecular Dynamics

methods.

Current topics on research are in the following:

(1) High temperature sulfidation of alloys

Sulfidation properties of stainless steels, nickel alloys, and Ti-Al intermetallic compounds were investigated at relatively low sulfur pressures in H₂S-H₂ atmospheres.

(2) High temperature oxidation resistance of sulfidation processed Ti-Al alloys.

High temperature oxidation behavior of sulfidation processed Ti-Al intermetallic compound was investigated. Effect of the third element addition on the oxidation behavior was extensively investigated.

(3) High temperature corrosion under the atmosphere containing water vapor.

Oxidation behavior in Fe-Al and Fe-Si alloys under the atmosphere containing water vapor was studied. Acceleration of the oxidation was observed and its mechanism was investigated.

(4) Effect of Re coating on high temperature oxidation of super alloy.

Re was coated on the surface of a super alloy, and the oxidation behavior of the alloy was examined. A new method for coating Re on the surface of alloys based on electric plating was also investigated.

(5) Characterization of thermal barrier coatings

Thermal barrier coatings of the NiCrAlY-Zirconia composite were prepared by using Plasma Splay Coating Method and their mechanical and physical properties were investigated.

(6) Galvanizing process of steels by two step hot dipping

Current Activities and Presentations

Galvanizing of steels was carried out by using a Zn-Al and a Zn-Al-Mg-Si molten alloys, and the optimum condition was investigated to make the galvanized layer having high corrosion resistance.

(7) Pb-free solder

Change in microstructure of a Pb-free solder due to composition and cooling rate during solidification was investigated. Effect of heat treatment on elastic modulus, microstructure and hardness of the solder was studied.

(8) TLP Bonding

Dissolution and isothermal solidification behavior during transient liquid phase bonding process of Ni, Ni base alloys and Al were investigated based on both experiment and computer simulation.

(9) Prediction of solidification structure of casting

A method to simulate the macro structure of a casting was investigated by combining thermodynamics analysis, heat transfer calculation, Monte-Calro Method and Cellular Automata Method.

(10) Simulation of microstructure development in solidifying alloy by Phase-field model.

The dendrite growth in the solidification process of an alloy was investigated by using a Phase-Field Model. Change in dendrite morphology due to thermal, solutal and fluid flow conditions was examined.

Presentations

Probabilistic Parameter for Nucleation during Solidification of Al Alloys; K.Ohsasa, H.Shirosawa and T.Narita: 5th Pacific Rim International Conference on Modeling of Casting & Solidification Processes, Nagoya, Jan. 2002.

Inner scale Formation and Its Effect on Oxidation Behavior of Fe-based Si and Al Alloys in Atmospheres Containing Water Vapour; T.Narita: TMS Meeting, Seattle, USA, Feb. 2002.

Novel coatings on TiAl and Ni-Cr alloys; T.Narita and T.Izumi: The International Conference in Commemoration for the 50th Anniversary of Chungnum National University, Daejon, Korea, May 2002.

Heat Transfer Analysis for Aluminum Base Multi-component Alloys Based on Enthalpy Method; H.Shirosawa, K.Ohsasa and T.Narita: Commemorative Meeting of The Hokkaido Sec. of Jpn. Inst. Light Metals for the 50th Anniversary of the Institute., Sapporo, Jan. 2002.

Analysis of Transient Liquid Diffusion Bonding Process using Phase-field Method; Y.Natsume, K.Ohsasa and T.Narita: Commemorative Meeting of The Hokkaido Sec. of Jpn. Inst. Light Metals for the 50th Anniversary of the Institute., Sapporo, Jan. 2002.

Improvement of the High Temperature Corrosion Resistance of Fe-24Al Alloy Foil unde Mixed Gas Atmosphere; F.Lang, T.Narita, Yu Zhiming, S.Gedevanshvili and S.C. Deevi The 130th Annual Meeting of Jpn. Inst. Metals; Tokyo, Mar. 2002.

Formation of Anti-oxidation Coating Layer on Nb base Alloy; Y.Matsumura, M.Fukumoto, S.Hayashi, T.Narita, I.Iwanaga, A.Kasama and R.Tanaka: ibid.

Current Activities and Presentations

Anti-oxidation Properties of Cr,Al Vapour Diffusion Processed TiAl Alloy; T.Nishimoto, T.Izumi and T.Narita: ibid.

Anti-oxidation Properties of TiAl Alloy with Ni-Al Coating; T.Izumi, T.Nishimoto and T.Narita: ibid.

Effect of Oxide Film and Corrosion Morphology on Mechanical Strength; I. Sohn and T.Narita: ibid.

Oxidation Behavior of Ni base Alloy under the Atmosphere Containing Water Vapor: S.Tominaga, S.Hayashi and T.Narita: ibid.

Inter-diffusion in High melting Point Metal System(Re,W-Ni); S.Narita, S.Hayashi and T.Narita: ibid.

Solute Partition in Ni base Alloy; M.Koizumi, M.Kudoh and K.Ohsasa: ibid. Analysis of Dendrite Deflection using Phase-field Method; Y.Natsume: 5th Young Scientist Forum, The 143th Annual Meeting of Iron and Steel Inst. Jpn., Tokyo, Mar. 2002.

Present State of the Prediction Method of Casting Structure and Heterogeneous Nucleation; K.Ohsasa and H.Shirosawa: The 143th Annual Meeting of Iron and Steel Inst. Jpn., Tokyo, Mar. 2002.

Application of Anti-oxidation NiAl Coating to TiAl; T.Izumi, T.Nishimoto and T.Narita: Annual Meeting of 123 Committee of Jpn. Soc. Promotion of Science, Tokyo, Mar. 2002.

Prediction of the Solidification Structure of Casting and Heterogeneous

Nucleation; K. Ohsasa, H.Shirosawa and T.Narita: 8th Hokkaido University-Beijing Science and Thechnology University Joint Seminar, Beijing, China, Apr. 2002.

Coating by Electroplating Process and Its Application to Niobium based Alloys; T.Narita: The 16th International Symposium on Ultra-high Temperature Materials UBE2002, Ube, Japan, May 2002.

Solidification Path of AC4C Aluminum Alloy Containing Iron; M.Kudoh, M.Komatsu and K.Ohsasa: The 102th Annual Meeting of Jpn. Inst. Light Metals, Sapporo, May 2002.

Growth Direction of Cell or Dendrite Under Positive Thermal Gradient; H.Esaka, K.Ohsasa, H.Daimon, Y.Natsume and M.Tamura: Annual Meeting of 19 Committee of Jpn. Soc. Promotion of Science, Tokyo, May 2002.

High Temperature Sulfidation Behavior of Fe-24Wt.%Al Foil; F.Lang, T.Narita, Yu Zhiming, S.Gedevanshvili and S.C. Deevi: The Summer Joint Meeting of The Hokkaido Secs. of Jpn. Inst. Metals and Iron and Steel Inst. Jpn., Tomakomai, July 2002.

Application of Anti-oxidation Coating Layer to Nb base Alloy; Y.Matsumura, S.Hayashi and T.Narita: ibid.

High Temperature Oxidation Behavior of Pt-Ti Alloy; D.Iino, T.Tanaka and T.Narita: ibid.

Anti-oxidation Ni-Al Coating on TlAl Alloy; T.Izumi, T.Nishimoto and T.Narita: ibid.

Comparison between Moving Boundary and Phase-field Models for the Analysis of TLP Bonding Process; Y.Natsume, T.Shinmura, K.Ohsasa and T.Narita: ibid.

Heat Transfer Analysis of Solidifying Multi-component Alloys with Application of Thermodynamic Analysis; H.Shirosawa, K.Ohsasa, K.Matsuura and T.Narita: Commemorative Meeting of the Hokkaido Sec. of Jpn. Foundry Engineering Soc. for the 50th Anniversary, Sapporo, July 2002.

Prediction of Casting Structure of Unidirectionally Solidified Al Base Alloy with Heating of Top Region; N.Nishiguchi K.Ohsasa and T.Narita: ibid.

Coatings of Ni-Aluminides on Heat Ressitant Alloys due to Up-hill Diffusion Application to TiAl intermetallics and Ni-Cr alloys; T. Narita, T.Izumi, T.Nishimoto, D.Yoshida, and S.Hayashi: International Symposium on High Temperature Corrosion in Energy Related Systems, Rio de Janeiro, Brazil, Sept. 2002.

-

Effect of Addition of Elements on Anti-oxidation Properties of Cr,Al Vapor Diffusion Processed TiAl Alloy; T.Izumi, T.Nishimoto and T.Narita: Annual Meeting of Jpn. Soc. Corro. Eng. Himeji, Sept. 2002.

Application of up-hill diffusion Process for TiAl and Ti Alloys; T.Izumi, T.Nishimoto and T.Narita: ibid.

Coating of Ni-Aluminides on TiAl intermtallics through up-hill diffusion; T.Izumi, T.Nishimoto and T.Narita: 7th Liege conference Materials for advanced power engineering, Liege Belgium, Sept. 2002.

Coatings on Niobium Based Alloys; T.Narita: The 43rd International Symposium on Assembly Related Technology, Kyoto, Japan, Oct. 2002.

Heat Transfer Analysis of Solidifying Al•Fe Base Multi-component Alloys Based on Thermodynamic Analysis; H.Shirosawa, K.Ohsasa, K.Matsuura and T.Narita: The 141th Annual Meeting of Jpn. Foundry Engineering Soc., Yamagata, Oct. 2002.

Temperature-Enthalpy Curves of Multicomponent Casting Alloys; K.Ohsasa, K.Matsuura and H.Shirosawa: 65th World Foundry Congress, Gyeongju, Korea, Oct. 2002.

Reactive Casting and Welding of High-Melting-Point Intermetallic Compounds; K.Matsuura, K.Ohsasa and M.Kudoh: ibid.

Diffusion path of the coating on TiAl alloy and Ni-Cr alloys; T.Narita: International Workshop on Designing of Interfacial Structures in Advanced Materials and their Joints, Osaka, Nov. 2002.

High Temperature Oxidation Behavior of Fe-40%Al Foil; F.Lang, T.Narita, Yu Zhiming, S.Gedevanshvili and S.C. Deevi: The 131th Annual Meeting of Jpn. Inst. Metals, Osaka, Nov. 2002.

Effect of Al Content in Mother Material on the Anti-oxidation property of Cr,Al Vapour Diffusion Processed TiAl Alloy; T.Nishimoto, T.Izumi and T.Narita: ibid. Effect of up-hill diffusion Process on Heat Resistant Ti Alloy; T.Izumi, T.Nishimoto and T.Narita: ibid.

High Temperature Oxidation Behavior of Pt-Ti Alloy in Air; D.Iino, T.Tanaka and T.Narita: ibid.

Effect of Water Vapor on the High Temperature Oxidation Behavior of Ni-lowAl Alloy; S.Tominaga, S.Hayashi and T.Narita: ibid.

Current Activities and Presentations

Inter-Diffusion Behavior between Re base Alloy/Ni, NiAl: S.Narita, S.Hayashi and T.Narita: ibid.

Micro Segregation in Ni base Super Alloy; M.Koizumi, M.Kudoh and K.Ohsasa: ibid.

Evaluation of Heterogeneous Nucleation Frequency in Al base Alloy using Unidirectional Solidification Technique with Heating of Top Region; N.Nishiguchi K.Ohsasa and T.Narita: ibid.

Analysis of Deflection Phenomenon of Dendrite or Cell from Heat Flow Direction using Phase-field Method; Y.Natsume, H.Esaka and K.Ohsasa: 6th Young Scientist Forum, The 144th Annual Meeting of Iron and Steel Inst. Jpn., Osaka, Nov. 2002.

Analysis of Dissolution and Isothermal Solidification Behavior of base Metal during Transient Liquid Phase Diffusion Bonding Process; Y.Natsume, T.Shinmura, K.Ohsasa and T.Narita: The 144th Annual Meeting of Iron and Steel Inst. Jpn., Osaka, Nov. 2002.

Oxidation Resistant Properties of up-hill diffusion Processed TiAl and Ti Alloys: T.Izumi, T.Nishimoto and T.Narita: Annual Meeting of 123 Committee of Jpn. Soc. Promotion of Science, Tokyo, Nov. Mar. 2002.

Analysis of Transient Liquid Phase Diffusion Bonding Process (TLP); Y.Natsume, K.Ohsasa and T.Narita: North Forum of The Hokkaido Sec. of Iron and Steel Inst. Jpn., Muroran, Dec. 2002.

INTERFACE MICRO-STRUCTURE ANALYSIS LABORATORY

Prof. Dr. H. Takahashi

Tel +81-11-706-7110, Fax +81-11-706-7881

E-mail: takahasi@elechem1-mc.eng.hokudai.ac.jp

Assoc. Prof. Dr. K. Kurokawa

Tel +81-11-706-7111, Fax +81-11-706-7881

E-mail: kazu@elechem1-mc.eng.hokudai.ac.jp

Res. Assoc. Dr. M. Sakairi

Tel +81-11-706-7112, Fax +81-11-706-7881

E-mail: msakairi@elechem1-mc.eng.hokudai.ac.jp

Researchers

Dr. K. Watanabe, Dr. A. Mozalev

Students

T. Kikuchi, K. Yamauchi, Z. Kato, K. Itabashi, E. Sakata, S. Matsushita, S. Nishizawa, M. Yamada, N. Takada, T. Nakagiri, K. Nagahara, M. Yamada

Equipments

Atomic Force Microscope

Conforcal Scanning Laser Microscope

Pulsed Nd - YAG Laser patterning system

Oxidation Test Equipment with Thermobalance and Ultra-High Temperature Furnace

Optical Microscope with High Temperature Furnace

Research work at "Interface Micro-Structure Analysis Laboratory (LIMSA)" directs toward 1) the examination of structure and dielectric properties of anodic oxide films on Valve metals, 2) micro- and nano-patterning of aluminum using laser irradiation and AFM probe processing, 3) high temperature oxidation of metals and intermetallics, 4) interface reactions between metals and silicides, 5) sintering and synthesis of composites, and 6) localized corrosion of coated steels.

The topics of investigation are in the following:

(1) Formation of Si-Al composite oxide films with ultra high voltage sustainability by sol-gel coating / anodizing.

Plain and etched aluminum foils were coated with SiO₂ films by sol-gel dipping method, and then anodized galvanostatically in 0.5M boric acid solutions at 333K. Anodic oxide films grew on both plain and etched foils at a high current efficiency for film formation up to 1,200 V during anodizing. Electric capacitance of the anodic oxide films formed on the etched foil after SiO₂ coating was larger than that without SiO₂ coating, while the capacitance of the anodic oxide films formed on the plain foil after SiO₂ coating was as large as that without SiO₂ coating.

(2) Selective copper deposition on aluminum surface with a diamond probe of AFM.

Aluminum specimens covered with thin barrier type anodic oxide films were scratched with diamond-probe of atomic force microscope in CuSO₄ solutions to remove the oxide film locally. After scratching, the specimen was cathodically polarized, using the prove as a counter electrode. Copper dot array was fabricated only at the film-removed areas by repeating scratching and electro-deposition.

(3) Fabrication of micro three-dimensional structures by laser irradiation and metal deposition.

Local metal deposition by anodizing / laser irradiation / electroplating was

applied on a columnar aluminum specimen with several mm diameter. During laser irradiation, the specimen was rotated and moved downwards and upwards. After metal deposition by electroplating, the specimen was immersed in NaOH solution to remove the oxide film and the metal substrate. Cylindrical and prismatic Ni network structures could be fabricated after the dissolution procedure.

(4) Formation and dielectric properties of niobium anodic oxide films

Niobium specimens were anodized in H_3PO_4 solution galvanostatically up to 100 V, and then the anode potential of the specimens was kept at 100 V for 6 hrs. The structural change of the film surface during the potentiostatic anodizing was observed by SEM, CSLM, and AFM. During the potentiostatic anodizing, sub- μ m imperfections formed at ridges of surface network structure grew to ten μ m imperfections after 6 hrs. This may be responsible for bias dependency of the capacitance of anodic oxide films.

(5) Fabrication of proto-type of aluminum electrolytic capacitor with a solid organic electrolyte.

Barrier type of anodic oxide films were formed on electropolished aluminum plates or on aluminum plates covered with SiO_2 thin films by sol gel coatings. Both anodized specimens were attached with poly poly-enedioxy-thiophene and aluminum counter electrode to examine the dielectric properties of the metal / oxide / solid electrolyte / metal systems. The electric capacity of the systems was 20 - 50 % smaller than that of metal / oxide / liquid electrolyte / metal systems. The film breakdown voltage of the system with solid electrolyte was much lower than the film formation potential. The mechanisms of decrease in the capacitance and film breakdown potential by attaching the organic polymer were discussed.

(6) Study on initial corrosion of Zn-, Zn/5%Al-, Zn/55%Al- and Al-coated steel in anion-containing solutions by photon rapture method.

Carbon steel coated with Zn, Zn/5%Al, Zn/55%Al and Al layers were covered

with a thin film of nitrocellulose. The specimens were irradiated with a pulsed Nd-YAG laser in Cl⁻ containing solutions at different pHs under potentiostatic conditions to remove the nitrocellulose film locally. Reformation of oxide film at the laser-irradiated area occurred at a low potential region in all the solutions, while localized corrosion occurred in Cl⁻ ion containing solutions at a high potential region. Oxide films formed on Zn-coated steel showed a high healing ability for a long period.

(7) Fabrication of new type plastic injection mold by anodizing, laser irradiation and Ni-P electroless plating

A novel method involving a combination of pulsed YAG laser irradiation and local Ni-P deposition by electroless plating was attempted for fabrication of a new type plastic injection mold. The plastic products obtained with the mold prepared thus showed a good performance.

(8) Anodizing of aluminum coated with Nb₂O₅ film by MOCVD

Aluminum specimens were covered with Nb_2O_5 films by the metal organic chemical vapor deposition, and then anodized galvanostatically in a neutral borate solution. Changes in the film structure during anodizing were examined by Rutherford back scattering spectroscopy (RBS), TEM and EDX, and the electric capacitance of anodic oxide films was measured by the electrochemical impedance measurements. During anodizing, Al_2O_3 layer grew at the interface between Nb_2O_5 film and the metal substrate, and the Al_2O_3 / Nb_2O_5 layer interface became obscure. The electric capacitance of anodic oxide films formed after Nb_2O_5 coating was twice as high as that formed on aluminum without Nb_2O_5 coating.

(9) Fabrication of aluminum micro electrochemical-reactors by anodizing, laser irradiation, and electroplating

Aluminum specimen covered with porous anodic oxide films was irradiated with a pulsed Nd-YAG laser to produce through-holes with 500 µm diameter, channels

with 300 μ m width, and a chamber with 2 x 2 x 0.1 mm volume on the surface, and Au layer was deposited on the surface of the chamber. Electrochemical reactors were fabricated by attaching the surface-modified specimens via an Teflon sheet, and evaluated on the electrochemical performance using a $[Fe(CN)_6]^{3-}$ / $[Fe(CN)_6]^{4-}$ solution system. A cyclic voltamogram showed redox peaks of $[Fe(CN)_6]^{3-}$ and $[Fe(CN)_6]^{4-}$ ions.

(10) High temperature oxidation of stainless steel in H₂O-containing atmospheres.

In order to clarify the mechanism of degradation of a chromia scale in H_2O -containing atmospheres, oxidation behavior of stainless steel, evaporation behavior of sintered chromia, and evolution behavior of hydrogen from chromia scales have been investigated. It was speculated that the degradation could be caused by the evaporation of chromia as $CrO_2(OH)_2$.

(11) Evaporation behavior of SiO₂ in H₂O-containing atmospheres.

In order to evaluate the oxidation resistance of SiO₂-formers such as silicides and Si-based ceramics in H₂O-containing atmospheres, the evaporation of fused and sintered crystalline SiO₂ specimens in H₂O-containing atmospheres has been investigated. The evaporation of SiO₂ as Si(OH)₄ became aggressive at 1000°C and above.

(12) Oxidation behavior of metal silicides.

In order to clarify the oxidation mechanism of metal disilicides, high-temperature oxidation tests of Re-, W-, Cr-, and Nb-silicides have been carried out in air. ReSi_{1.75} and WSi₂ formed a protective SiO₂ at high temperatures, while NbSi₂ formed the mixed oxide scale consisting of Nb and Si oxides. CrSi₂ had excellent oxidation resistance below 1100°C, but the oxidation resistance degraded drastically due to the evaporation of Cr₂O₃ above 1200°C.

Other activities

In February, Prof. Takahashi traveled in Korea to visit Prof. Kwang B. Kim at Yonsei Univ. in Seoul, Dr. Jong-Huy Kim at Energy Storage Research Center, Korea Inst. of Energy Research in Daejon, and Prof. Soo Gil Park at Chungbuk Univ. in Cheongju. He gave lectures there and discussed with them and their colleague.

In March, Ms. Y. Arai and Mr. K. Watanabe received the engineering doctor degree. Dr. Arai resumed a researcher life at Hitachi Co., and Dr. Watanabe joined again LIMSA as a postdoctoral fellowship by JSPS.

In April, Prof. Takahashi attended Symp. for the Commemory of 50th Anniversary of Foundation of Univ. of Sci. and Tech, Beijing in Beijing and presented a paper entitled "Micro and Nano-Technology on Aluminum Surface by Anodizing, Laser Irradiation and AFM Probe Processing".

In May, he attended Symp. 2002 on New Functional Material at Chungnum Univ. in Taejon, and presented a paper entitled "Micro- and Nano- Patterning of the Aluminum surface by Anodizing, Laser Irradiation and AFM Probe Processing". Assoc. Prof. Kurokawa attended the symposium in Honor of the 65th Birthday of Professor Wayne L. Worrell (The Electrochemical Society) held in Philadelphia, U. S. A. and presented a paper entitled "High-Temperature Oxidation Behavior of ReSi_{1.75}". Dr. Sakairi attended the Asian Conference on Electrochemistry, ACEC 2002, Jeju Korea, held in Jeju, Korea and presented a paper, "Repairing of Anodic Oxide Films on Al Coated Steel After Removal with Photon Rupture in Solutions".

In July, Prof. S.G. Park stayed with his students for one month for the collaboration on the development of hybrid type capacitors.

In September, Prof. Takahashi and Mr. Z. Kato traveled in Europe to visit Prof. D. Landolt at Ecole Polytech. Fed. De Lausanne in Lausanne, and Profs. H. Bohni, and S. Virtanen at Swiss Fed. Inst. of Tech. in Zurich, and also to attend the 53rd Annual Meeting of the ISE. At a poster session of the ISE meeting, they presented papers entitled "Micro-patterning of Aluminum of AFM processing and copper electroplating (Z.K.)" and "Micro patterning of Curved Surface of Aluminum by Laser Irradiation and Metal Deposition (H.T)". 'New Type Hybrid Capacitor of

Metal Oxide(Ru, Co, Mn) Electrodes with Polymer Electrolyte". Dr. A. Mozalev attended the ISE meeting to give a lecture on "Nucleation and Growth of the Nano-structured Anodic Oxides on Tantalum and Niobium Under the Porous Alumina Film". Assoc. Prof. Kurokawa attended the 15th International Corrosion Congress held in Granada, Spain, with Mr. Yamauchi, and they presented a paper entitled "Degradation of Cr₂O₃ Scale Formed on Stainless Steel in H₂O-Containing Atmospheres".

In October, Dr. A. Mozalev joined again LIMSA from Belarus as a researcher in the project of the fabrication of new type plastic injection mold by anodizing, laser irradiation and Ni-P electroless plating. Prof. Takahashi and Dr. Sakairi attended the 202nd Meeting of ECS at Salt Lake City, and represented papers entitled "Local Breakdown of Aluminum Anodic Oxide Films Contacting with Solid Electrolytes" and "Repairing of Oxide Films on Zn - 55% Al Alloy Coated Steel After Removal with Photon Rupture in Solutions". After the meeting, Dr. Sakairi visited Inst. for Chemical Process and Environmental Tech., National Research Council Canada, in Ottawa. In NRC, he presented and discussed with Dr D. B. Macdougall, Dr. S-M, Moon, Dr. Christina Bock and Dr. Macdougall's laboratory member on" Micro Surface Patterning by Laser Irradiation and AFM Tip Processing". He also met Dr. M. Graham and discussed on recent his research work.

In November, Dr. Sakairi attended Japan-China Joint Seminar on Marin Corrosion, held in Tokyo, Japan and presented a paper "Localized Corrosion of Zn-Al alloy coated steels by Photon Rupture Method.-Effect of Chloride Ions-".

Foreign scientists visited to LIMSA in 2002 are Prof. S. Park and Dr. W. K. Chei, Chungbuk Univ., Korea, in July, Prof. Y. S. Diamond, Tel Aviv Univ., in October, Prof. Przybylski, Univ. of Mining and Metallurgy, Poland, in November.

Presentations

Localized Corrosion of Zn-Al alloy Coated Steels by Photon Rupture, K. Itabashi, M. Sakairi, H. Takahahsi, The Winter Joint Meeting of The Hokkaido Secs. of Jpn. Inst. Metals and Iron and Steel Inst. Jpn., Muroran, Jan., 2002.

Formation of Ta-Al composite Oxide Film by MOCVD and Anodizing, E. Sakata, M. Sakairi and H. Takahashi, The joint Meeting of The Hokkaido Secs. of Elechtrochem. Soc. Jpn., Surf. Finish. Soc. Jpn., and Jpn. Soc. Corros. Eng., Sapporo, Jan., 2002.

The Formation and Dielectric Properties of Nanostructured Ta-Al Oxide Films, A. Mozalev, M. Sakairi and H. Takahashi, ibid.

Effect of Addition of Boron on Oxidation Resistance of ReSi_{1.75}, H. Hara, K. Kurokawa, and H. Takahashi, The Winter Joint Meeting of The Hokkaido Secs. of Jpn. Inst. Metals and Iron and Steel Inst. Jpn., Jan., Sapporo, 2002.

Growth Behavior of Inner Scale formed on Stainless Steel in H₂O-containing Atmospheres, A. Yamauchi, K. Kurokawa, and H. Takahashi, ibid.

Observation of Anodic Oxide Films Formed on Al Alloy by Confocal Scanning Laser Microscope, M. Sakairi, S. Moon and H. Takahashi, The Winter Joint Meeting of The Hokkaido Secs. of Chem. Soc. Jpn. and Jpn. Soc. Anal. Chem., Sapporo. Feb., 2002.

Microstructure Fabrication on Aluminum by Laser Irradiation and Electrochemical Technique -Correction of Spherical Aberration with Doublet Lens-, T, Kikuchi, M. Sakairi, H. Takahashi, Y. Abe, and N. Katayama, ibid.

Anodic Oxide Film Formed on Aluminum Alloy with Confocal Scanning Laser Microscopy, M. Sakairi, S. Moon, H. Takahashi, The 105th Annual Meeting of Surf. Finish. Soc. Jpn., Hitachi, Mar. 2001.

Fabrication of 3-dimensional Microstructure on Curved Surface of Aluminum with Laser Irradiation and Electrodeposition, T, Kikuchi, M. Sakairi, H. Takahashi, Y. Abe, and N. Katayama, ibid.

The Formation of Nano-structured Ta-Al Oxide Films and Their Application to Electrolytic and Thin-Films Capacitors, A. Mozalev, M.Sakairi, H. Takahashi, ibid.

Sintering Behavior of Electrically-Conductive and –Nonconductive Materials in a Spark Plasma Sintering Method, K. Kurokawa, The 9th Annual Meeting of Inst. of Applied Plasma Sci., Ube, Mar., 2002.

Structures of Scales Formed on Silicides, K. Kurokawa, The 130th Annual Meeting of Jpn. Inst. Metals, Tokyo, Mar. 2002.

Measurement of Evolution of Hydrogen from Chromia Scale Formed on Stainless Steel in H₂O-containing Atmospheres, A. Yamauchi, K. Kurokawa, and H. Takahashi, ibid.

Initial Stage of Localized Corrosion on Zn-Al Alloy Coated Steels by Photon Rupture, M. Sakairi, K. Itabashi and H. Takahashi, The 68th Annual Meeting of the Electrochem. Soc. of Jpn., Sendai, April 2002.

Formation of Al / Ta Composite Oxide Film on Al by MOCVD and Anodizing., E. Sakata, M. Sakairi, H. Takahashi and S. Nagata, ibid.

Removal of Aluminum anodic oxide film by AFM processing and electrochemical

measurement, Z. Kato, M. Sakairi, H. Takahashi, ibid.

Formation and Degradation of Protective Scale in Intermetallics, K. Kurokawa, 2002 Syukudai Theme Sympo. of Jpn. Inst. of Metals, Akita, April, 2002.

Repairing of Anodic Oxide Films on Al Coated Steel After Removal with Photon Rupture in Solutions, M. Sakairi, K. Itabashi and H. Takahashi, ACEC 2002, Jeju Koria, May. 2001.

Micro- and Nano- Patterning of the Aluminum Surface by Anodizing, Laser Irradiation and AFM Probe Processing., H. Takahashi, M. Sakairi, T. Kikuchi, and Z. Kato, Symp. 2002 on New Functional Material, Taejon, Korea, May 2002.

Initial Stage of Localized Corrosion on Zn-Al Alloy Coated Steels by Photon Rupture in SO_4^{2-} Containing Solutions, K. Itabashi, M. Sakairi and H. Takahashi, 2002 Annual Meeting of Jpn. Soc. Corros. Eng., Kawasaki, May 2002.

High-Temperature Oxidation Behavior of ReSi_{1.75}, K. Kurokawa, H. Hara, A. Shibayama, and H. Takahashi, A Sympojium in Honor of the 65th Birthday of Prof. Wayne L. Worrell (ECS), Philadelphia, U. S. A., May, 2002.

Formation of High Functional Aluminum Anodic Oxide film using Sol-Gel Coating, K. Watanabe, Lilac Seminar for Hokkaido Branch of Electrochemical Soc. of Jpn., Ootaki-mura, June 2002.

Interface Reaction Between Al Anodic Oxide Film and Conductive Polymer, M. Yamada, M. Sakairi and H. Takahashi, The Summer Joint Meeting The Hokkaido Secs. of Chem. Soc. Jpn. And Jpn. Soc. Anal. Chem. Asahikawa, July, 2002.

Structures of Scales Formed on Carbon Steels at 1473 K in H₂O-containing

Atmospheres, S. Nishizawa, K. Kurokawa, and H. Takahashi, The Summer Joint Meeting of The Hokkaido Secs. of Jpn. Inst. Metals and Iron and Steel Inst. Jpn., Jan., Tomakomai, 2002.

Micro-Surface Finishing by High Energy Photons and Probe Processing., M. Sakairi, 2002 Hokkaido Summer Seminar, Sapporo, Aug. 2002.

Micro-patterning of Aluminum by AFM Processing and Copper Electroplating, Z. Kato, M. Sakairi, H. Takahashi, 53rd Annual Meeting of the International Society of Electrochemistry, Sep. 2002.

Cross Sectional Observation of Zn Alloy Coated Steels by Ultra Microtomy., M. Sakairi, K. Itabashi and H. Takahashi, The 49th Discussion Meeting of J. Soc. Corros. Eng., Himeji, Sep. 2002.

Effect of Aggressive Anions on Initial Stage of Localized Corrosion on Zn-Al Alloy Coated Steels by Photon Rupture, K. Itabashi, M. Sakairi and H. Takahashi, ibid.

Growth Behavior of Nb Anodic Oxide Film and Its Dielectric Property, M. Sakairi, T. Miyamoto, H. Takahashi, K. Takayama, Y. Oda, The Autumn Meeting of Electrochem. Soc. of Jpn., Atsugi, Sep., 2002.

Formation of Al-Nb and Al-Ta Composite Oxide Films by Anodizing/MOCVDE, E. Sakata, M. Sakairi, H. Takahashi and S. Nagata, ibid.

Interface Reaction Between Al Anodic Oxide Film and Poly- (3,4 ethylendioxythiophene), M. Yamada, M. Sakairi, H. Takahashi, K. Nogami and H. Uchi, ibid.

Electrochemical Characteristics of Nano-particles of RuOx Electrode for Hybrid Super-capacitor, H. Kim, M. Sakairi, H. Takahashi, S. Park, ibid.

Observation of Defect in Oxide Film Formed on Al Alloy by Confocal Scanning Laser Microscope, M. Sakairi, H. Takahashi and S. Moon, The 51st Annual Meeting of Jpn. Anal. Chem., Sapporo, Sep. 2002.

Degradation of Cr₂O₃ Scale Formed on Stainless Steel in H₂O-Containing Atmospheres, A. Yamauchi, K. Kurokawa and H. Takahashi, 15th International Corrosion Congress, Spain, Sep. 2002.

Micro-patterning of Aluminum by AFM Processing and Copper Electroplating, Z. Kato, M. Sakairi, H. Takahashi, The 3rd Annual Meeting of the International Society of Electrochemistry, Dusseldorf, Sep. 2002.

Micro-patterning of Curved Surface of Aluminum by Laser Irradiation and Metal Deposition, T, Kikuchi, M. Sakairi, H. Takahashi, Y. Abe, and N. Katayama, ibid.

Nucleation and Growth of the Nanostructured Anodic Oxides on Tantalum and Niobium Under the Porous Alumina Film, A. Mozalev, M. Sakairi, I. Saeki, H. Takahashi, ibid.

New Type Hybrid Capacitor of Metal Oxide (Ru, Co, Mn) Electrodes with Polymer Electrolyte, S.G. Park, M. Sakairi, and H. Takahashi, ibid.

Fabrication of 3-dimensional Ni Microstructure with Anodizing / Laser Irradiation / Electroplating, T, Kikuchi, M. Sakairi, H. Takahashi, Y. Abe, and N. Katayama: The 106th Annual Meeting of Surf. Finish. Soc. Jpn., Kobe, Sep., 2002.

Change in Structure of Al-Si Composite Oxide Films on Aluminum under

Potentiostatic Polarization, K. Watanabe, M. Sakairi, S. Hirai, and H. Takahashi, ibid.

Anodizing of Aluminum Coated with (Nb₂O₅-SiO₂) Layer by Sol-Gel, K. Watanabe, M. Sakairi, H. Takahashi, S. Hirai, and S. Nagata, ibid.

Local Breakdown of Aluminum Anodic Oxide Films Contacting with Solid Electrolytes, Yamada, M. Sakairi, H. Takahashi, K. Nogami, and H. Uchi, 202nd ECS meeting, Salt Lake, USA, Oct., 2002.

Repairing of Oxide films on Zn-55% Al Alloy Coated Steel After Removal with Photon Rupture in Solutions, Sakairi, K. Itabashi and H. Takahashi, ibid.

Dielectric properties and break down voltage of Aluminum Electrolytic Capacitor with a Solid Organic Electrolyte, Y. Yamada, M. Sakairi, H. Takahashi, K. Nogami and H. Uchi, The 19th ARS (Anodizing Research Society, SFJ) Conference, Nagaragawa, Nov., 2002.

Microstructure Change of Silica Scale and The Related Problems, K. Kurokawa, The 131th Annual Meeting of Jpn. Inst. Metals, Suita, Nov. 2002.

Effect of Water Vapor on Degradation of Cr₂O₃ Scale Formed on Stainless Steel, A. Yamauchi, K. Kurokawa, H. Takahashi, Y. Yamauchi, Y. Hirohata, and T. Hino, The 144th Annual Meeting of The Iron and Steel Inst. Jpn., Suita, Nov., 2002.

Structure and Spalling of Oxide Scales Formed on Steels in H₂O-Containing Atmospheres, S. Nishizawa, K. Kurokawa and H. Takahashi, ibid.

Effect of Evaporation of WO₃ on Formation of SiO₂ Scale in WSi₂, K. Kurokawa, A. Shibayama, H. Tkakahashi, Inter'l Conf. on Designing of Interfacial Structures

Current Activities and Presentations

in Adv. Materials and Their Joints, Suita, Nov., 2002.

Formation of High Functional Oxide film by Sol-Gel Coating/Anodizing K. Watanabe: Special Lecture for Hokkaido Branch of Surf. Finish. Soc. Jpn., Sapporo, Dec., 2002.

DENTAL MATERIALS AND ENGINEERING LABORATORY

Prof. Dr. F. Watari Tel&Fax:+81-11-706-4251 E-mail:watari@den.hokudai.ac.jp Assoc, Prof. Dr. M.Uo. Tel&Fax:+81-11-706-4251 E-mail:uo@den.hokudai.ac.jp Res. Assoc. Dr. S.Ohkawa Tel&Fax:+81-11-706-4251 E-mail:ohkawa@den.hokudai.ac.jp Res. Assoc. Dr. T. Akasaka Tel&Fax:+81-11-706-4251 E-mail: akasaka@den.hokudai.ac.jp Technician Mr.T.Sugawara Tel&Fax:+81-11-706-4251 E-mail:stoshi@den.hokudai.ac.jp Guest Researcher, Dr. D.I.Rosca Tel&Fax:+81-11-706-4251 E-mail:rosca@den.hokudai.ac.jp

Students

Y.Tamura, Y.Tanimura, T.Tsuchiya, J.Konishi, M.K.Yamada, S.Tanaka, Y.Iwasaki, K.Tani, K.Tamura, H.Kondo, N.Kamishima

Facilities and Capabilities

XSAM: HORIBA XGT-2000V, Scanning X-ray analytical microscope for elemental mapping analysis

AFM: TopoMetrix TMX2000 Explorer, AFM for dry and wet specimens NSOM: TopoMetrix Aurora, Near field Scanning Optical Microscope

Laser Raman Spectrometer: Dilor Labram, Laser Raman Spectrometer with mapping analysis

ICP: HITACHI P-4010, ICP emission spectrometer for analysis of elements in aquaous solution

FT/IR: Jasco FT/IR-300E, FT/IR spectrometer with microscopic IR measurement Universal Testing Machine: INSTRON MODEL 4204, Testing for mechanical properties of materials

Laser Welder: ATJ TLL7000, Nd-YAG pulse laser welder with computer controlled x-y stage

Cold Isostatic Press: Hikari Koatsu Kiki (10000atm type and 20000atm type)

Kobelco, Large volume isostatic press (4000atm)

Vickers Hardness Tester: Shimadzu

Acoustic Emission: Physical Acoustic Corporation

Thermal Gravitometry and Differential Thermal Analysis(TG/DTA): Rigaku Denki

Diamond Cutter: Buehler and Struers diamond cutter

Surface Area Analyzer: Shimadzu Flowsorp III, Surface area analysis with BET method

Particle size distribution analyzer: Shimadzu SALD-7000, Particle size distribution analysis with laser scattering

The research activities cover (1)the development, evaluation and application of dental and biomaterials, (2)the development of methods and equipments for fabrication of materials and prostheses and (3)the measurement of properties. These are concerned with mechanical, thermal properties, corrosion, surface treatment, biocompatibility, bioreactivity, estheticity and various methods of imaging and microanalysis. Many researches are related to dental, biological and engineering fields and performed in collaboration with clinical departments including Removable Prosthetic Dentistry (Prof. Takao KAWASAKI), Orthodontics (Prof. Junnichiro IIDA), Operative Dentistry (Prof. Hidehiko SANO), Oral and

Maxillofacial Surgery (Prof. Yasunori TOTSUKA), Crown and Bridge Prosthodontics (Prof.Noboru OHATA) and Protective Dentistry (Prof. Manabu MORITA).

Current topics on research are as follows;

(1) Development of functionally graded dental implant

The dental implant with the structure of functionally graded materials (FGM) has been fabricated to satisfy different properties. The typical example is such that the composition changes from the biocompatible metal, Ti, at one end, increasing the content of ceramics, hydroxyapatite (HAP), principal component of bone and teeth, toward 100% HAP at the other end. This can control the functions of mechanical properties and biocompatibility, optimize them, depending on the necessity of each part of implant, without the abrupt change by the formation of discrete boundary. The effect of FGM structure Ti/HAP, Ti/Co on tissue response is investigated by the animal implantation test into rats and rabbits. The tissue reaction and new bone formation around the implant to the gradient composition is evaluated by both the conventional method using an optical microscope with stained specimens and by elemental mapping and other imaging methods using electron microprobe analysis(EPMA) and X-ray scanning analytical microscope(XSAM) with unstained specimens.

(2) Development of FRP esthetic orthodontic wire

To realize the esthetic, transparent orthodontic wire the FRP wires of the diameter 0.5mm with the multiple fiber structure has been fabricated by either drawing of fiber-polymer complex at 250 °C or photopolymerization method. Biocompatible CaO-P₂O₅-SiO₂-Al₂O₃ (CPSA) glass fibers of 8-20μm in diameter are oriented unidimensionally to the longitudinal direction in polymer matrix of PMMA, UDMA or bis-GMA. The improvement has been done to obtain the adequate flexural strength and higher torque. FRP wire shows the sufficient flexural

strength and a very good elastic recovery. The dependence of Young's modulus and flexural stress on fiber fraction obeys very well the rule of mixture. This FRP wire can cover the range of the strength corresponding to the conventional metal orthodontic wires from Ni-Ti used in the initial stage of orthodontic treatments to Co-Cr used in the last stage by changing the volume ratio of glass fibers with the same external diameter. FRP wire can satisfy both mechanical properties and estheticity, which is not possible for the conventional metal wire.

(3) Cytotoxicity due to ions and fine particles of Ti and other metals in vivo and in vitro

The removal of Ti plates for fixing jaw bone in 6 months after operation often reveals the slightly dark colored tissue in the circumferential soft tissue. The observation and analysis by optical microscopy, electron microscopy and XSAM revealed that the colored tissue contains the abraded fine particles of Ti, probably produced during plate fixation in operation.

The animal experiments to implant various sizes of Ti particles of 1-100 μ m and macroscopic cylindrical Ti implant in μ m order for 3 days to 8 months showed that the macroscopic size of Ti was encircled with fibrous connective tissue layer from early stage and there was no inflammation. As the size of particle becomes smaller, many phagocytic cells appear with fibrous connective tissue layer inside the particle inserted region and tissue showed inflammation. It takes more time to encircle the particle-contained tissue region and heal inflammation. For 1-3 μ m the inserted region is never encircled with fibrous connective tissue layer and inflammation continues.

The in vitro cell functional tests on cell survial rate, LDH(Lactate Hydrogenase CII) protein released at the breakdown of cell membrane and superoxided anion(O²⁻) sing human neutrophils showed that Ni solution has he cell disruption effect. The deformed and disrupted morphology of neutrophils was confirmed by SEM observation. Whilst Ti and V solution showed the increase of superoxide anion and negligible change in the others, which suggests the cell stimulation effect.

SEM observation confirmed that neutrophis are inflated with more complicated polyacicular morphology. One of the marking cytokines released at phagocytization, TNF- α , was not detected in any solution of Ni, V, Ti, the simulated body fluid(Hank's solution) mixed with 10mm paricles of Ti and with submicron size Ni particles. TNF- α was found only in the 1-3 μ m Ti particle mixed Hank's solution, which suggests that particles were phagocytized. SEM observation and EDS elemental analysis confirmed the phagocytosis of Ti particles by neutrophils.

The difference of cell reaction to 1-3 μ m and 10 μ m Ti particles suggests that the particles(1-3 μ m) smaller than cell size(about 5 μ m in neutrophils) induces cytotoxicity as a result of phagocytosis, while for particles larger than cell size(10 μ m) phagocytosis is not possible, resulting in the less clear cytotoxicity effect.

The study shows the cytotoxicity originating from physical size effect of particles other than biochemical toxicity effect, which is significant for the cases where the fine particles are produced during abrasion by long term usage of moving parts in the artificial bone joint.

(4) Biocompatibility test and biomedical application of carbon nanotubes(CNT) and other nano materials

Biocompatibility and cytotoxicity of carbon nanotubes(CNT), carbon nanorod, fullerene and other nano materials were investigated. Various type of CNT including nanorods and muti-wall CNTs(MWCNT) were used with the aim of the biomedical application and the pretreatment method of purification, solubilization, dispersion, surface modification were developed. Both applications of the monotubes as delivery systemof DNA, protein, saccharic tips and the sintered bulk as implant materials are under development.

(5) In situ observation of etching process of human teeth in acid agent by atomic force microscopy

Composite resin with fillers of ceramic powders in polymer matrix has

estheticity similar to natural teeth color and is widely used for treatments of caries in incisal teeth. Physical-mechanical anchoring effect plays an important part in binding force between teeth and composite resin. The pretreatment to make etching of teeth is generally done using acid agents for enhancement of binding. SEM is usually used for the evaluation of etching effect. It can observe, however, only the result after a certain etching time. To observe the sequence of etching process it is necessary to prepare the series of specimens treated with different etching time. Atomic force microscope is applied for the in-situ observation of etching process of human enamel and dentin in acid agents. The chronological change of surface morphology can be successively observed and quantitative analysis is done for different etching conditions.

(6) Fabrication of composite resin prostheses by laser lithography:

Laser lithography, one of the CAD/CAM systems to fabricate the polymer models by piling up the thin slices, which are photo-polymerized by scanning laser beam originally on the shallow depth of liquid epoxy monomer, was applied for the fabrication of dental prosthoses of photo-curing composite resin composed of silica fillers in the matrix of high strength UDMA resin. The full dental crown could be fabricated using the shape data pre-designed by computer with high accuracy due to the smaller polymmerization shrinkage than by conventional methods. Then the functionally graded dental core and post with gradually changing filler content from 70 to 0% from the head of core abutment toward the apex of post was successfully fabricated. The stress concentration at the pulp root inserted with the conventional dental post has often caused the fracture in the surrounding dentin by impact force on the tooth crown. The stress relaxation effect by application of the functionally graded dental post was confirmed by simulation using the photoelastic method and finite element method(FEM).

(7) Radiation effects on polymer resin:

Radiation effects by C⁺ion, γ-ray from Co⁶⁰ and electrons on one of the main

matrix polymer UDMA(urethane dimethacrylate) for dental composite resin were investigated with various mechanical tests and spectroscopies. C⁺ion radiation induced the large change in the structure sensitive properties of mechanical properties, Vickers hardness, flexural strength, abrasion resistance and little change in the non-structure sensitive properties of spectroscopies, FT-IR, Raman scattering, Fluorescence, NMR and thermal expansion coefficient. The results suggest that the mechanism of radiation effect is mostly due to the physical structure change such as lattice defects of vacancies, interstitials, depleted zone rather than the chemical effect of cross-linking by further progress of polymmerization of residual monomers.

(8) Evaluation of biocompatibility of refractory metals and their application

Refractory metals of IVA group(Ti, Zr, Hf), VA group(V, Nb, Ta) and VIIA group(Re) are investigated in their biocompatibility and other bioreactivities. Animal implantation tests show that the fraction of direct contact of newly formed bone to implant material without intervening of fibrous connective tissue at the interface and the amount of new bone vary depending on materials. The composites of these refractory metals are also made and the comparison and the composite effect is investigated.

(9) Surface treatment of dental and biomedical materials with sol-gel method Biocompatibility and adhesivity to tissue is important for dental materials. Various dental metals were coated by amorphous silica gels with sol-gel method. In some cases, biocompatibility were improved.

(10) Tissues and dental materials observation by XSAM

The scanning X-ray analytical microscope (XSAM) was applied for the analysis of the soft tissue of rat in which various metals including Fe, Cu, SUS, V, Co, Ni were implanted. The dissolution of implanted metals and inflammation of tissues were observed by elemental mapping image obtained by XSAM.

(11) Bonding property and cytotoxicity of dental zirconia ceramics (YPSZ)

Yttria partially stabilized zirconia (YPSZ) ceramic is suitable for dental and medical use because of it's high fracture toughness and chemical durability. The bonding properties of dental zirconia with various luting cements and surface treatments are investigating. The cytotoxicity dental zirconia ceramics compared to other dental ceramics was also evaluated.

(12) Dental Applications of Acoustic Emission Technique

Fracture toughness of dental materials including more detailed discussions using an acoustic emission technique. Acoustic emission (AE) is employed to evaluate the microscopic and macroscopic aspects of mechanical behavior of metal-, ceramics- and polymers- based materials and their composite materials.

(13) Grafting of Methyl Methacrylate onto Collagen Using Ferric Chloride-N-Phenylglycine

Graft polymerization of vinyl monomer onto human hard tissues has not been studied extensively, without tri-n-buthylborane initiated MMA-based materials. The purpose of this study was to grafting of MMA onto collagen using various ferric ions-N-phenylglycine as a redox initiator.

(14) Abrasion-resistant implant made of refractory metal nitrides and carbides

Surface-nitrided titanium(Ti(-N)) showed high corrosion resistance and nearly equivalent biocompatibility with Ti in soft and hard tissue in animal implantation test. Surface durability was evaluated by three static and dynamic mechanical tests; Vickers hardness test, Martens scratch test and for more practical viewpoint newly developed abrasion test using ultrasonic dental scaler which is used to remove calculus on teeth in dental clinics. Vickers hardness of Ti(-N) was 1300, ten times larger than Ti. Martens scratch test showed that the bonding of nitrided layer with 2µm thickness is coherent to matrix Ti and enough strong. Abraded volume by

ultrasonic scaler was increased with the load in Ti, while no trace was formed in Ti-(N), instead stainless tip of scaler was abraded. The test showed that abrasion would be negligibly small under the practical conditions of the load 50g in clinics. Ti-(N) with biocompatibility and surface abrasion resistance would be suitable as abrasion-resistant implant materials for the application to the artificial joint of implant and abuttment part of dental implant.

(15) Development of visible-light responsible photocatalysis and its application

The current photocatalysis of anatase TiO₂ mostly works only by ultraviolet light. To make applicable for medical use it is necessary to develop the visible-light reactive photocatalysis. Visible light sesitization was obtained by surface modification with caions of Au, Ag, Cu, Pt, Pd. Depigmentation with visible light around 470nm which is used for photopolymerization of composite resin restoration in dental clinics could be done with the Ag activated TiO₂ in contrast to very little effect in an untreated TiO₂. Antibacterial effect was also confirmed to streptococcus mutans, one of the most popular bacteria for caries. The application to bleaching of pigmented teeth was developed.

(16) Development of discrimination method of resin-restored teeth

In the health checkup in school mass of patients must be checked in the limited time. Due to the recent development of estheticity of composite resin it is now very difficult to recognize the resin-restored teeth and discern resin part from natural teeth. Total reflection spectroscopy and fluorescence spectroscopy were measured and images were taken with reflected light and fluorescence light using the filters to select the appropriate wave length. In the long wave length region for more than 600 nm the reflectivity of teeth is higher than that of composite resin. The image formed with filtered light, however, did not show the contrast enough to discern the resin part from tooth. For less than 400nm both teeth and resin showed the fluorescence emission with high and comparable intensity. For the light of 430-450 nm teeth emitted higher fluorescence and the relative difference is larger. The

images formed with fluorescence light for more than 500nm emitted by 430-450 nm light excitation showed the easily recognized contrast to discriminate resin from tooth.

Other activities:

Prof.WATARI promoted the Summer Seminer in the Hokkaido-Tohoku branch of Japanese Society of Dental Materials and Devices, held at Hotel Piano, Kiroro, on July 20th. Three special lectures about "Trends in Dental Alloys" and nine related subjects were presented.

The three-year research project on "Tissue Reaction and Biomedical Application of Nanotubes, Nanoparticles and Microparticles" was started as Research on Advanced Medical Technology under Health and Laybour Sciences Research Grants from the Ministry of Health, Laybour and Welfare of Japan. Leader: constitute ofProf.Fumio WATARI. Assigned Researchers:Dr.Mamoru OMORI (Institute for Materials Research, Tohoku University), Prof.Kazuyuki TOHJI(Department of Geoscience and Technology, Tohoku University), Prof. Toshiyuki HASHIDA (Fracture Research Institute, Graduate School of Engineering, Tohoku University), Prof. Yasunori TOTSUKA(Graduate School of Dental Medicine, Hokkaido University), Prof.Takao KAWASAKI(Graduate School of Dental Medicine, Hokkaido University), Prof.Kohichi HANEDA(Department of Information Technology and Electronics, Ishinomaki Senshu University), Prof.Fumio NOGATA(Department of Human and Information Systems, Tohoku University) and Collaborating Researchers. The first meeting was held at Hotel Piano, Kiroro, on Sep.9-10. target of project and problems in research development were discussed.

Prof.WATARI attended the 7th Int.Symp.on Functionally Graded Materials FGM2002 held at Beijing, China on Oct.15-19 and gave the invited talk "Development of functionally graded implant and dental post for bio-medical application". He visited Prof.CUI Fu-Zhai, Director of Biomaterials Laboratory, Department of Materials Science and Engineering, Tsinghua University, Beijing,

China and started the collaboration research on nano-biomaterials.

Dr. WON Dae-Hee, Department of Dental Materials, College of Dentistry, Chonbuk National University, KOREA stayed during March 1 - May 28 and was engaged in "the study of mechanical properties of titanium bonded by infra-red soldering and laser welding" as collaboration research.

Dr.ROSCA Iosif Daniel of University Polytechnica Bucharest, Bucharest, Romania joined on November 6 as the invited researcher of the Japan Society for Promotion of Science (JSPS) and started the collaboration research on the development of polymer biomaterials for two year period.

Dr. Tsukasa AKASAKA, specializing polymer chemistry, joined as research associate on December 1.

The international collaborations are continued with Institute of Dental Materials Science, Umea University, SWEDEN (Emerita Prof. Maud BERGMAN) on application of Ti, ZrO₂, amalgum for dentistry, and research on side effects, with Department of Dental Materials, Chonbuk National University, KOREA (Prof.Tae-Sung BAE) on evaluation of mechanical properties of laser-welded Ti, dental porcelain, and with Institute for Materials Science, Dresden Institute of Technology, GERMANY (Prof.W.POMPE) on the biocompatibility evaluation and application of collagen-hydroxyapatite composites.

The collaboration with Laboratory for Advanced Materials, Institute for Materials Research, Tohoku University (Dr.Mamoru OMORI) is also undergoing on the fabrication of new biomaterials including composite materials and functionally graded materials by applying a spark plasma system(SPS) as a method to enhance sintering. The research on the surface treatment of Ti by sol-gel method and evaluation of cytotoxicity is developed in cooperation with Department of Materials Science and Engineering, Muroran Institute of Technology(Prof.Kazuyoshi SHIMAKAGE, Assoc.Prof.Shinji HIRAI). The development of FRP esthetic orthodontic wire has continuously been done with Department of Industrial Chemistry, Chiba Institute of Technology(Associate Prof.Masahiro KOBAYASHI).

Presentations

The recent trend in the research of advanced dental materials; F.Watari, 174th meeting of JSPS 133th Committee, Sapporo, July 2002.

Stress Relaxation Effect of Functionally Graded Dental Post, Fumio WATARI, Shingo MATSUO, Noriyuki SATOH, Yasuo UEDA, Noboru OHATA, 14th Symposium on Functionally Graded Materials, Nagoya, Nov.19-20, 2002.

Development of functionally graded implant and dental post for bio-medical application; F.WATARI, H.KONDO, S.MATSUO, R.MIYAO, A.YOKOYAMA, M.OMORI, T.HIRAI, Y.TAMURA, M.UO, N.OHATA, T.KAWASAKI; 7th Int.Symp.on Functionally Graded Materials FGM2002,Beijing,China, Oct.15-19, 2002.

Tissue Reaction and Biomedical Application of Nanotubes, Nanoparticles and Microparticles; F.WATARI: 1st meeting as Research on Advanced Medical Technology under Health and Laybour Sciences Research Grants from the Ministry of Health, Laybour and Welfare of Japan, Kiroro, Sep.9-10, 2002.

Physical properties and spectroscopic measurements of dental UDMA resin irradiated by carbon ions and gamma ray; S.HAQUE, S.TAKINAMI, M.NAKAMURA, M.UO, F.WATARI: Joint Meeting of the Iron and Steel Society and the Japan Institute of Metals, Hokkaido Division, Sapporo, Jan., 2002.

Rapid analysis of intra oral metallic restoratives using X-ray scanning analytical microscope; M.Uo, T.Sugawara, S.Ohkawa, F.Watari; The Japanese Society of Dental Materials and Devices, Matsumoto, Sep. 2002.

Structual analysis of arabinogalactan from Japanese larch in Hokkaido; T.Akasaka, Y.Maekawa: The Japanese Society of Carbohydrate Research, Yokohama, Aug.,

2002.

Morphological observation and Raman analysis of tooth irradiated by Nd:YAG, Er:YAG and CO₂ lasers; M.K. Yamada, M.Uo, S.Ohkawa, Y.Nodasaka, F.Watari; 2002-year Meeting for Hokkaido Divisions of Three Associations (Electrochemistry, Corrosion, Surface Technology), Sapporo, Jan., 2002.

Morphological and spectroscopical effect of Nd:YAG, Er:YAG, CO₂ laser on tooth; M.K.Yamada, M.Uo, S.Ohkawa, F.Watari; 80th IADR(Int.Assoc.for Dent Res.), San Diego, Mar., 2002.

Quantitative analysis of tooth surface by SEM and CLSM after Nd:YAG, Er:YAG and CO₂ lasers irradiation; M.K. Yamada, M.Uo, S.Ohkawa, Y.Nodasaka, T.Kumazawa, H.Inoue, F.Watari; The Japanese Society for Dental Materials and Devices, Hokkaido Division, Akaigawa, July, 2002.

CLSM and SEM quantitative analysis of surface topography of human teeth irradiated by Nd:YAG, Er:YAG and CO₂ lasers; M.K. Yamada, M.Uo, S.Ohkawa, F. Watari, The 8th International Congress on lasers in Dentistry, Yokohama, July, 2002.

Morphological and quantitative analysis of teeth irradiated by Nd:YAG, Er:YAG and CO₂ lasers; M.K.Yamada, M.Uo, S.Ohkawa, F.Watari, The fourth international congress on dental materials, Honolulu, Hawaii, Oct., 2002.

Examination of photocatalytic ability of ion-decorated titanium dioxide with visible light responsibility; Y.Tanimura, R.Kumazawa, Y.Totsuka, M.Uo, S.Ohkawa, T.Sugawara, F.Watari; The Japanese Society of Dental Materials and Devices, Tokyo, Apr., 2002.

Current Activities and Presentations

Visible light responsible photocatalystic efficiency and antibacterial activity of ion-decorated titanium dioxide; Y.Tanimura, R.Kumazawa, Y.Totsuka, M.Uo, T.Sugawara, S.Ohkawa, F.Watari; 2002-year Meeting for Hokkaido Divisions of Three Associations (Electrochemistry, Corrosion, Surface Technology), Sapporo, Jan., 2002.

Evaluation of biocompatibility of titanium particles; K. Tamura, N. Takashi, Y. Totsuka, F. Watari; The Society for Artificial Organs, Sapporo, March 2002.

Cell Functional test of metallic particles and their size effect; K.Tamura, N.Takashi, Y.Totsuka, M.Uo, S.Ohkawa, T.Sugawara, F.Watari; The Japanese Society of Dental Materials and Devices, Matsumoto, Sep., 2002.

Dependence of time on the flexural action of orthodontic wires; S.Tanaka, S.Yamagata, M.Uga, N.Swa, J.Iida, M.Uo, S.Ohkawa, T.Sugawara, F.Watari; The Japanese Society of Dental Materials and Devices, Tokyo, Apr., 2002.

Size Dependence and Shape Effect of Particles on Cell Function; K.Tamura, Y.Totsuka, F.Watari; The Japanese Association for Dental Research, Sendai, Nov. 2002

The mechanical and histological evaluation of the functionally graded implant produced by spark plasma sintering method; H.Kondo, A.Yokoyama, M.Uo, F.Watari, T.Kawasaki: Society for Artifical Organs, Sapporo, March 2002.

Fabrication and evaluation of nitrided titanium/apatite functionally graded implants; H.Kondo, A.Yokoyama, Y.Tamura, T.Kawasaki, M.Uo, S.Ohkawa, T.Sugawara, F.Watari: The Japanese Society of Dental Materials and Devices, Matsumoto, Sep., 2002.

Effect of spark plasma sintering pressure on the properties of functionally graded

implant and its biocompatibility; R.Miyao, F.Watari, A.Yokoyama, Y.Tamura, H.Kondo, M.Uo, T.Kawasaki, M.Ohmori, A.Ohkubo, T.Hirai: Japan society of powder and powder metallurgy, Tokyo, Jun.2002.

Spectroscopic research for the visible differentiation of tooth from composite resin; K.Tani, H.Watari, M.Uo, S.Ohkawa, T.Sugawara, M.Morita; The Japanese Society of Dental Materials and Devices, Tokyo, Apr., 2002.

Evaluation of reflectance of tooth and composite resin: K.Tani, H.Watari, M.Uo, M.Morita; 2002-year Meeting for Hokkaido Divisions of Three Associations (Electrochemistry, Corrosion, Surface Technology), Sapporo, Jan., 2002.

Improved contraction of porcelain inlays by CIP method; C.Kawamoto, J.Konishi, F.Watari, H.Sano:81th IADR(Int.Assoc.for Dent Res.), San Diego, March, 2002.

Effect of particles on porcelain inlay processed with cold isostatic pressure method; J.Konishi, C,Kawamoto, H.Sano, F.Watari: Japanese Society of Dental Materials and Devices, Tokyo, April, 2002.

Sphericalized porcelain powder containing intermediate oxidatives for processing with CIP to simplify the making of dental porcelain; J.Konishi, C.Kawamoto, H.Sano, M.Uo, F.Watari: Joint Meeting of the Iron and Steel Society and the Japan Institute of Metals, Hokkaido Division, Sapporo, Jan., 2002.

Fabrication of Functionally Graded Composite Resin Post by Laser Lithography; S.Matsuo, F.Watari, N.Ohata, M.Uo, S.Ohkawa and T.Sugawara; IADR 80th General Session, San Diego, Mar., 2002.

LABORATORY OF ADVANCED MATERIALS CHEMISTRY

Prof. Dr. Hidetaka Konno
Tel.&Fax:+81-11-706-7114
E-mail:ko@eng.hokudai.ac.jp
Assoc. Prof. Dr. Hiroki Habazaki
Tel.&Fax:+81-11-706-6575
E-mail:habazaki@eng.hokudai.ac.jp
Instructor Mr. Akira Shimizu
Tel.:+81-11-706-6577
akira@eng.hokudai.ac.jp

Students

M. Endo, M. Uozumi, K. Yokoyama, T. Kinomura, S. Sato, A. Sudo, T. Matsuo, H. Tachibana, Y. Takahashi, D. Abe, A. Tamura

Equipments

DC magnetron sputtering: Shimadzu SP-2C X-ray diffractometer: Rigaku Geigerflex

Laser Raman Spectrometer: Jasco TRS-401 and Jobin Yvon T64000

FT-IR spectrometer: Jasco FT-IR350 Uv-vis spectrometer: Jasco V-550

EPMA: JEOL JSM-5410 equipped with Oxford WDX-400

TG/DTA: Seiko TG/DTA6300

TOC analyzer: Shimadzu TOC-5000A

Capillary Electrophoresis analyzer: Ohtsuka Electronics CAPI-3100

The research activities of the laboratory are directed toward (1) formation and characterization of carbon-based composites, carbides, and double oxides

with unusual valence state ions (2) formation of dielectric layers by anodizing of valve metal alloys and (3) electrochemical and biochemical water treatments.

Current research topics are in the following:

(1) Formation and characterization of composite materials of carbon, ceramics and metals

Various carbon composites were formed by carbonization of 1) polyimide films containing metal complexes, 2) powder mixtures of organic polymer and ceramics and 3) chelate resins complexed with metal ions. Basic researches on the structure, composition, electric and magnetic properties of the composites are in progress by using XRD, TEM, SEM, Raman spectroscopy, SQUID, EIS and others.

(2) Development of a new formation process of B/C composites and B₄C carbide

New precursors were found for production of title materials. They were prepared by chemical processes using the combinations of (a) sugars, polyhydric alcohols or the compounds containing N-glucamine functional groups and (b) boric acid or organoboranes. Carbonization of these precursors provided the B/C composites with high boron concentration and B₄C. Preliminary characterization revealed that the composites show good oxidation resistance in a pure oxygen atmosphere.

(3) Synthesis and characterization of rare earth-chromium(V) compounds

Unusual chemical state compounds, RECrO₄ (RE=rare earth elements) were synthesized and their structures including atomic positions, composition, vibrational structures, electric properties, electron configurations were investigated in detail. Reversible structural transformation of these compounds, caused by reaction with methanol and oxidation in air, has been demonstrated.

(4) Preparation of carbon nanorods and nanotubes using porous anodic alumina template

Porous anodic alumina has been used as a template to prepare carbon nanorods and nanotubes. Instead of usual CVD process we have prepared these nanocarbon materials simply by heating a mixture of the template and organic polymers, such as polyvinylalcohol and polyvinylchloride, which melt during carbonization process.

(5) Electrochemical wastewater treatment using oxide anodes

Various oxide anodes have been prepared by thermal decomposition of precursor salts on titanium substrate and anodic deposition. Using these anodes electrochemical decomposition of organic pollutants such as phenol, which are not easily decomposed by other methods, in wastewater has been examined to clarify the suitable electrochemical conditions and to develop effective anodes for their anodic decomposition.

(6) Formation of barrier-type amorphous anodic films on titanium and niobium alloys

Alloying of titanium with other valve metals is found to result in the formation of uniform amorphous anodic films to relatively high voltages in neutral and acid electrolytes, in contrast to an amorphous-to-crystalline transition of anodic films on titanium at low voltages. Such anodic films formed on the titanium alloys are possible candidates of new dielectric materials for electrolytic capacitors. The positive effects of nitrogen addition to niobium on the dielectric properties and thermal stability of its anodic film for capacitor applications has been found recently.

(7) Tailoring of novel oxidation- and sulfidation-resistant materials at high temperatures

Since niobium has exceptionally high sulfidation resistance and aluminum and chromium are most effective elements in enhancing the oxidation resistance of metals, Nb-Al-Cr ternary alloys have been prepared by sputter deposition, and their sulfidation and oxidation behavior has been examined. These alloys are found to possess high oxidation resistance comparable to typical chromia formers as well as high sulfidation resistance.

Other activities

Professor Konno attended International Conference on Carbon in 2002 (CARBON 2002) held at Beijin, China, in September and presented three papers and served as a chairman. After the conference he was invited from Fudan University, Shanghai, China, and gave a lecture on "Anodic Oxide Films for High Performance Capacitors."

Associate Professor Habazaki attended ISE Annual Meeting held at Dusseldolf, Germany in September and presented two papers entitled "Strecture-composition relationship of anodic films on Ti-Zr alloys" and "Formation and dielectric properties of anodic oxide films on NbNx. He also attended International Symposium on GD OES for Surface Analysis held at Yokohama in November and presented a paper entitled "GDOES analysis of anodic oxide films on NbN_x" and served as a vice-chairman of this Symposium.

Presentations

Structural Modification of Anodic Films on Titanium by Alloying; M. Uozumi, H. Habazaki and H. Konno: The joint Meeting of Hokkaido Secs. of ECSJ, SFSJ and JSCE, Sapporo, Jan, 2002.

Electrochemical Decomposition of Phenol Using Tungsten Oxide Anodes; Y. Hayashi, H. Habazaki and H. Konno: The joint Meeting of Hokkaido Secs. of ECSJ, SFSJ and JSCE, Sapporo, Jan, 2002.

Anisotropy of Electrical Conductivity of Carbon Films Prepared From Polyimide Film; A. Yoneda, H. Konno, H. Habazaki: The Winter Joint Meeting of Hokkaido Secs. of Chem. Soc. Jpn. And Jpn. Soc. Anal. Chem., Sapporo, Feb., 2002.

Low-Temperature Synthesis of Boron Carbide From Sugar-Boric Acid Aqueous Solutions; A. Sudo, H. Konno and H. Habazaki: The Winter Joint Meeting of Hokkaido Secs. of Chem. Soc. Jpn. And Jpn. Soc. Anal. Chem., Sapporo, Feb., 2002.

Formation of Anodic Oxide Films on Valve Metal Alloys; H. Habazaki, M. Uozumi, T. Matsuo, H. Konno, S. Nagata, K. Shimizu, K. Takayama and Y. Oda: 105th Meeting of the Surface Finishing Society of Japan, Hitachi, Mar. 2002.

Analysis of Ni double layers electrodeposited on ZDC Using rf-GDOES, EPMA, SAM and cross-sectional SEM and TEM; Y. Kasahara, K. Shimizu ahd H. Habazaki: 105th Meeting of the Surface Finishing Society of Japan, Hitachi, Mar. 2002.

Mobility of Electrolyte Anion Species in Amorphous Anodic Titania; H. Habazaki, H. Konno, S. Nagata: 105th Meeting of the Surface Finishing Society of Japan,

Hitachi, Mar. 2002.

High Temperature Corrosion of Sputter-Deposited Nb-Al-Cr alloys in SO₂-O₂ Atmospheres; K. Yokoyama, H. Habazaki and H. Konno: 130th Meeting of the Japan Institute of Metals, Tokyo, Mar., 2002.

Formation of Al(III)-molybdate Composite Films on Steel and Zinc-plated Steel by Chemical Conversion; H. Konno, K. Narumi, H. Habazaki: The 69th Annual Meeting of the Electrochem. Soc. Japan, Sendai, April, 2002.

Synthesis of B₄C Crystals from Saccharides and Boric Acid; H. Konno, A. Sudoh, H. Habazaki: The 69th Annual Meeting of the Electrochem. Soc. Japan, Sendai, April, 2002.

Synthesis of β-SiC Fine Powder from Silicone Polymerized in Exfoliated Graphite; H. Konno, T. Kinomura, M. Aramata: The 69th Annual Meeting of the Electrochem. Soc. Japan, Sendai, April, 2002.

Reversible Structure Change of Zircon-type Nd^{III}Cr^VO₄ by Redox Reaction and the Mechanism; H. Konno, Y. Aoki: The 69th Annual Meeting of the Electrochem. Soc. Japan, Sendai, April, 2002.

Effect of Carbon Fiber on the Removal of Dissolved Mn(II) Ions by the Fungus Isolated in Hokkaido; H. Konno, M. Endo, K. Sasaki: 261st Meeting of JSPS 117 Committee, Tokyo, April, 2002.

Graphitization of Polyimide Films Studied by Positron Annhilation Spectroscopy; H. Konno, K. Süvegh, A. Vértes: 63rd Annual Sympo. Japan Soc. Anal. Chem., May 2002.

Current Activities and Presentations

Application of Scanning Auger Microprobe for Corrosion Studies; K. Shimizu, H. Habazaki: Materials and Environments 2002, Kawasaki, May 2002.

Compositional Dependence of Structure and Dielectric Properties of Anodic Films on Ti-Zr Alloys; M. Uozumi, H. Habazaki and H. Konno: The Summer Joint Meeting of Hokkaido Secs. of Chem. Soc. Jpn. And Jpn. Soc. Anal. Chem., Asahikawa, Jul., 2002.

Formation and Dielectric Properties of Anodic Films on Nitrogen-Doped Niobium; T. Matsuo, H. Habazaki, H. Konno, S. Nagata, K. Takayama, Y. Oda: The Summer Joint Meeting of Hokkaido Secs. of Chem. Soc. Jpn. And Jpn. Soc. Anal. Chem., Asahikawa, Jul., 2002.

Synthesis of B₄C Micro-crystals from Saccharides and Boric Acid at Moderate Temperatures; H. Konno, A. Sudoh, H. Habazaki: CARBON2002, Beijin, September 2002.

Anisotropy of Electric Conductivity of Carbon and Graphite Films Derived from Kapton-type Polyimide; H. Konno, A. Yoneda, H. Habazaki: CARBON2002, Beijin, September 2002.

Effect of a Trace Amount of Ni and Fe on the Carbonization of Polyimide Films; H. Konno, A. Yoneda, H. Habazaki, M. Inagaki: CARBON2002, Beijin, September 2002.

Morphological Characterization of Jarosite Minerals Formed by Bioremediation; K. Sasaki, T. Sakimoto, M. Endo, H. Konno: 2002 Autumn Meeting of MMIJ, Kumamoto, September 2002.

Effect of Nitrogen Addition on Formation and Dielectric Properties of Anodic

Oxide Films on Niobium; T. Matsuo, H. Habazaki, H. Konno, S. Nagata, K. Matsumoto, K. Takayama, Y. Oda: Fall Meeting of the Electrochemical Society of Japan, Atsugi, Sep., 2002.

Strecture-composition relationship of anodic films on Ti-Zr alloys; H. Habazaki, M. Uozumi, H. Konno, K. Shimizu and S. Nagata: 53rd Annual Meeting of the International Society of Electrochemistry, Dusseldolf, Sep., 2002.

Formation and dielectric properties of anodic oxide films on NbNx, H. Habazaki, T. Matsuo, H. Konno, K. Shimizu, S. Nagata, K. Takayama, Y. Oda, 53rd Annual Meeting of the International Society of Electrochemistry, Dusseldolf, Sep., 2002.

GDOES analysis of anodic oxide films on NbN_x; H. Habazaki, T. Matsuo, H. Konno, K. Shimizu, P. Skeldon and G.E. Thompson: International Symposium on GD OES for Surface Analysis, Yokohama, Nov., 2002.

Acceleration of Water Treatment with Manganese-oxidizing Fungus by Carbon Fiber; M. Endo, K. Sasaki, H. Konno: 29th Meeting of the Carbon Society of Japan, Osaka, December, 2002.

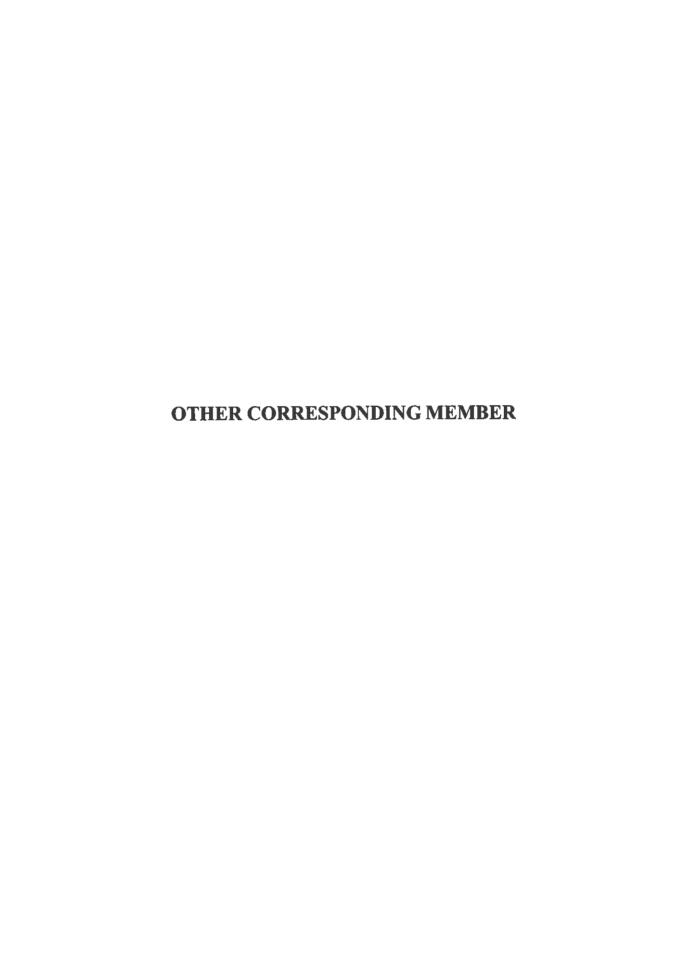
Formation of β-SiC Fine Powder from Exfoliated Graphite and Silicone; T. Kinomura, H. Konno, M. Aramata: 29th Meeting of the Carbon Society of Japan, Osaka, December, 2002.

Synthesis of Boron Carbide Cellulose and Boric Acid; A. Sudoh, H. Konno, H. Habazaki: 29th Meeting of the Carbon Society of Japan, Osaka, December, 2002.

Formation of Carbon Composites Containing Large Amounts of Copper from Chelate; Y. Takahashi, R. Matsuura, H. Konno, H. Habazaki: 29th Meeting of the Carbon Society of Japan, Osaka, December, 2002.

Current Activities and Presentations

Preparation Process of Carbon Fibers Intercalation Compounds through Electrochemical Treatment and Their Exfoliation; M. Toyoda, H. Konno, M. Inagaki: 29th Meeting of the Carbon Society of Japan, Osaka, December, 2002.



Assoc. Prof. Dr. Hiroki Tamura

Tel.: +81-11-706-6741, Fax : +81-11-706-6740 Email: h-tamura@eng.hokudai.ac.jp

Presentations

Synthesis of Hydrotalcite - ATP Intercalates; M. Ito, H. Tamura, and S. Kikkawa: The 81st Spring Annual Meeting of Chem. Soc. Jpn., Tokyo, Mar., 2002. Cation Exchange Properties of Tetratitanic Acid with Protons in Interlayer Nanospaces; H. Tamura, K. Nakamura, and S. Kikkawa: The 224th ACS National Meeting, Boston, USA, Aug., 2002.

Synthesis of Hydrotalcite - ATP Intercalates by Anion Exchange; H. Tamura, M. Ito, and S. Kikkawa: The 18th Ion Exchange Meeting, Chiba, Oct., 2002.

Properties of Protective Oxides on Metals -Solubility, Ion Permeability, and Electron Conductivity-; H. Tamura: The 144th Autumn Annual Meeting of ISIJ -International Session for Galvanized Steels for Saving Environment and Resources-, Osaka, Nov., 2002.

Synthesis of Layered Manganese Dioxide and Its Interlayer Modification; K. Nakamura, H. Tamura, and S. Kikkawa: The 13th Symposium of Reactivity of Solids, Osaka, Nov., 2002.

			я	





Corrosion of Tin Alloys in Sulfuric and Nitric Acids

M. Mori, K. Miura, T. Sasaki, and T. Ohtsuka

Corrosion Science, 44, 887-898 (2002).

To obtain a fundamental understanding of the corrosion behavior of lead-free solder, the corrosion behavior of tin-based eutectic alloys in sulfuric and nitric acids saturated with oxygen was investigated. The presence of bismuth in a Sn-Bi alloy (43Sn-57Bi (wt%)) slightly accelerated the preferential dissolution of tin instead of dissolving itself in 0.05 M H₂SO₄ and greatly accelerated in 0.1 M HNO₃ compared with that of pure tin. In both acids, dissolution of both tin and zinc from a Sn-Zn alloy (91Sn-9Zn (wt%)) occurred depending on the ratio of composition, and dissolution of tin from a Sn-Ag alloy (96.5Sn-3.5Ag (wt%)) was accelerated. Dipping test in H₂SO₄ and HNO₃ of pH 4 showed that dissolution of only zinc and lead occurred, suggesting that the tin-based alloys investigated in this study are preferable to substitutes for lead solders in terms of corrosion.

Improvement of Corrosion Property and Structual Change in 304 Stainless Steel by means of Ion-Mixing

Y. Matsumoto, M. Takeda, T. Suda, S. Watanabe, S. Ohnuki, T. Ohtsuka, and K. Ikezawa

Materials Transaction, 43, 638-640 (2002).

High energy ion-beam mixing was applied for the surface modification of austenitic stainless steel, followed by electrochemical characterization and microstructual observation. The co-mixing of silicon and chromium resisted the passivation current to 1/1000 relative to the un-modified condition. The corrosion resistance improved remarlably. Micro structural observation revealed that the enhanced diffusion and induced amorphous structure introduced by the co-mixing of silicon and chromium, which played a very important role in the improvement of electrochemical behavior at surface.

Double-Pulse Technique As An Electrochemical Tool for Controlling The Preparation of Metallic Nanoparticles

M. Ueda, H. Dietz, A. Anders, H. Kneppe, A. Meixner, and W. Plieth

Electrochimica Acta, 48, 377-386 (2002)

Various structures of silver nanoparticles were generated by means of the double-pulse technique. The interaction of the pulse parameters has been modeled to demonstrate that the electrodeposition of nanoparticles can be variably controlled. The results derived showed how to create nanoparticle structures with respect to size, density and monodispersity according to the application goal.

Evaluation of Corrosion Behavior of Iron by Scanning Electrochemical Microscopy

K. Fushimi and M. Seo

Materia Japan, 41, 856-857 (2002).

Heterogeneity of electrochemical activity on electrode surface can be detected with scanning electrochemical microscopy (SECM). The principle, characteristic and performance of SECM were described and the results of application of SECM to the passivity and localized corrosion of polycrystalline iron were introduced as typical examples. The probe current image of the SECM revealed that the thickness of passive film on iron depended on the substrate grain orientation. A local breakdown of the passive film could be induced by chloride ions which were generated locally by cathodic polarization of an Ag/AgCl microelectrode used as a probe electrode. The resistance for local breakdown of the passive film also depended on the substrate grain orientation, i.e., the film thickness. (Japanese)

Application of AC Resistmetry to Localized Corrosion on Iron

K. Azumi, K. Iokibe, T. Ueno, and M. Seo

Corrosion Science, 44, 1329-1341 (2002).

The electric resistance of an iron wire electrode was traced during a potential sweep in a neutral borate buffer solution. The dissolution depth calculated from resistance change due to iron dissolution in the active potential region was in a good agreement with that calculated from the electric charge. Using a wire electrode with a diameter of 100 µm, the resolution of the dissolution depth was in the order of nm. When Cl ions were added to induce pitting, resistance increased more rapidly than that predicted from uniform dissolution. From comparison of resistance change, electric charge of iron dissolution, and surface observations using an scanning electron microscope and optical microscope, the degree of nonuniform dissolution was evaluated.

Crevice Corrosion of Types of 304L and 316L Stainless Steel in Nitric Acid Solutions

Y. Arai, K. Mabuchi, T. Honda, S. Shouji, T. Yokosuka and H. Takahashi

Zairyo-to-Kankyo, 51, 165 - 172 (2002).

Crevice corrosion of 304L- and 316L-stainless steel has been examined for 7200 or 1800ks in nitric acid solutions with/without RuNO(NO)₃, by measuring the mass loss of the specimen, the amounts of metal ions dissolved, and the galvanic current.

Specimen surface at/around the crevice corroded more vigorously than that without the crevice, and the tendencies became more remarkable at higher HNO₃ concentrations, higher temperatures, and with RuNO(NO)₃. Current was observed by connecting the specimens with/without crevice through a galvanometer, indicating an anodic reaction on the specimen without crevice and a cathodic reaction on the specimen with crevice. The sensitivity for the crevice corrosion was higher on 316L than on 304L stainless steel.

Mechanisms on the crevice corrosion of stainless steels in HNO₃ solutions is discussed in terms of a catalytic action of Fe³⁺ ions accumulated on the surface at the crevice. (Japanese)

Localized Corrosion of Zn-Al Alloy Coated Steels by Photon Rupture Method - Effect of Chloride lons -

M. Sakairi, K. Itabashi and H. Takahashi

Proc of Japan-China Joint Seminar on Marin Corrosion, 58-65, (2002).

Electrochemical analysis of abruptly destroyed passive oxide films on the coated layer is important to understand the initial stage of localized corrosion of coated steels. A photon rupture, a focused one pulse of laser beam irradiation, method has been developed since it enables the oxide film stripping at extremely high rate without any contamination from removable tool. In the present investigation, Zn - 55mass%Al alloy and Al coated steel specimens covered with protective films were irradiated with a focused ones pulse of pulsed Nd - YAG laser beam at a constant potential in solutions with/without chloride ions to monitor the current transient. Irradiation with a pulsed laser in solutions causes abrupt removal of the protective film on the specimens at the laser-irradiated area. Without chloride ions, oxide films were reformed in the solutions at - 0.5 to 1 V after removal of the anodic oxide film. However, in chloride ion containing solutions, pitting corrosion of coated layers occurs at high potentials, while film reformation occurs at low potentials. It was also found that chloride ions enhance dissolution of aluminum and zinc at the very initial period after laser irradiation.

Luminescence from Band-gap Photo-excitation of Titanium Anodic Oxide

M. Ueda and T. Ohtsuka

Corrosion Science, 44, 1633-1638 (2002).

Luminescence light from the anodic thin oxide films formed on titanium in neutral phosphate solution was measured by photo-excitation of ultra-violet light irradiation with 3.82 eV energy. The luminescence light is observed with a peak of about 3 eV energy that corresponds to the band-gap energy of the n-type semiconductive TiO₂ oxide. It can therefore be presumed that the luminescence is induced by de-excitation or recombination between electrons in the conduction band and holes in the balance band. The peak wavelength of the luminescence light changes with the formation potential of the oxide film from 409 nm at 1 V to 425 nm at 6 V. The shift of the peak may reflect an amorphous-crystaline transition with increase of potential.

Electrochemo-mechanical Properties of Passive Metal Surfaces

M. Seo, K. Ueno and J. –D. Kim

Proc. 15 th International Corrosion Congress, CD-ROM, pdf. No.5 (2002).

The changes in stress of the iron and titanium surfaces passivated or anodically oxidized in pH 8.4 borate solution were measured by using a bending beam method to evaluate the electrochemo-mechanical properties of the passive surfaces. The stress of the iron surface changed to the tensile direction in the pre-passive potential region and then changed gradually to the compressive direction with increasing potential in the passive potential region, while the stress of the titanium surface changed always to the compressive direction during anodic oxidation. The tensile stress of the iron surface in the pre-passive potential region was ascribed to dehydration of the pre-passive film for transition to the compact passive film. The compressive stress in anodic oxide film on titanium due to electrostriction could be obtained experimentally, which was in the same order of magnitude as that calculated and was only few % of the total compressive level in the anodic oxide film. The reversible changes in stress of the titanium surface to the compressive and tensile directions were observed during cyclic potential steps between - 0.5 V and 0.5 V (RHE) after 1h-anodic oxidation, which were explained in terms of volume expansion due to hydrogen absorption into the anodic oxide film at - 05 V (RHE) and volume shrinkage due to hydrogen removal from the anodic oxide film at 0.5 V (RHE).

Mechanical Properties of Amorphous Anodic Alumina and Tantala Films Using Nanoindentation

G. Alcala, P. Skeldon, G.E. Thompson, A.B. Mann, H. Habazaki and K. Shimizu

Nanotechnology, 13, 451-455 (2002)

The hardness and Young's modulus of barrier-type, amorphous anodic oxides have been determined by nanoindentation. The procedure used shallow indents, of 55 nm depth, with alumina, tantala and alumina/tantala 'mixed oxide' films of about 500 nm thickness. The results revealed respective hardnesses of approximately 7.0, 5.3 and 6.5 GPa, and respective Young's moduli of approximately 122, 140 and 130 GPa. Thus, the hardness and Young's modulus followed opposite trends, with alumina having the highest hardness and lowest modulus, and the 'mixed oxide' having intermediate properties. The hardness and Young's modulus of amorphous alumina are factors of about 3.1- 3.7 times lower than those of crystalline aluminas.

Enrichment Behaviour of Gallium in Heat and Surface Treatments of Al-Ga Foils

Z. Ashitaka, P. Skeldon, G.E. Thompson, K. Shimizu and H. Habazaki

Corrosion Science, 44, 2725-2735 (2002)

The behaviour of gallium is examined after heat and surface treatments of aluminium foils containing either 120 or 1300 ppm gallium, with low enrichments of gallium at the surfaces arising from foil manufacture. Vacuum heat treatment at 823 K for 20 ks caused negligible additional enrichment, probably associated with the high solubility of gallium in aluminium. Subsequent alkaline etching in 0.25 M sodium hydroxide for 60 s at 348 K increased significantly enrichments, to about 3.2×10^{14} and 3.6×10^{15} Ga atoms cm⁻² for the foils containing 120 and 1300 ppm gallium respectively. The enrichments were probably located in both the metal and the overlying etching products. In contrast, electropolishing in perchloric acid / ethanol eliminated pre-existing enrichments, probably due to activation of the foil, with no enrichment developing during the electropolishing procedure. Barrier-type anodic films formed on the alkaline-etched foils contained gallium species, with increased concentrations at the film surface. Gallium enriched the metal region immediately beneath the anodic film during anodizing and led eventually to detachment of the growing film from the etched foil, followed by growth of a second film beneath the detached film. The combined amounts of gallium in the anodic film and enriched metal layer were similar to the levels at the surface regions of the etched foils. The anodic films formed on the electropolished foils, with no preexisting enrichment, were free of gallium species and remained attached to the foils, since insufficient gallium could enrich in the metal beneath the anodic film during the relatively short period of anodizing.

Formation of Anodic Films on Magnesium Alloys in an Alkaline Phosphate Electrolyte

F.A. Bonilla, A. Berkani, Y. Liu, P. Skeldon, G.E. Thompson, H. Habazaki, K. Shimizu, C. John and K. Stevens

Journal of the Electrochemical Society, 149, B4-B13 (2002)

The development of anodic films at a constant current density of 10 mA cm⁻² has been studied for Mg-W alloys, containing 0.4 and 1.0 atom % W, in 3 M ammonium hydroxide/0.05 M ammonium phosphate electrolyte at 293 K. The structure, morphology, and composition of the films were determined by X-ray diffraction, scanning electron microscopy, atomic force microscopy, glow discharge optical emission spectroscopy, Rutherford backscattering spectroscopy, and nuclear reaction analysis. During anodizing to about 50 V, a relatively smooth film develops. Cross-sectional atomic force microscopy suggests the film may be finely porous. With an increase in voltage, the film transforms gradually to a coarse, porous morphology due to dielectric breakdown. The transformation coincides with a reduction in slope of the voltage-time response. Significant regions of both types of film morphology coexist during anodizing to 150 V. With further anodizing, a porous film, developed in the presence of sparking above about 270 V. eventually covers all of the macroscopic surface. Magnesium, phosphorus, oxygen, hydrogen, and nitrogen species are present throughout the film thickness at the resolution of the measurements. However, the films are initially free of tungsten species due to enrichment of tungsten in the alloy. The O: Mg atomic ratio is in the range 1.7 to 2.1, reducing with an increase in voltage for films formed up to 220 V, consistent with films composed primarily of hydroxide or oxyhydroxide. The P:O atomic ratio increases with an increase in voltage, starting at about 0.03 for voltages below 50 V and reaching 0.29 at 330 V. The films form at a reduced efficiency, typically about 40-50%.

Enrichment of Alloying Elements in Anodized Magnesium Alloys

F.A. Bonilla, A. Berkani, P. Skeldon, G.E. Thompson, H. Habazaki, K. Shimizu, C. John and K. Stevens

Corrosion Science, 44, 1941-1948 (2002)

The possibility of enrichment of alloying elements in magnesium alloys as a consequence of growth of an anodic film has been investigated for sputtering-deposited Mg-0.4 at.% W and Mg-1.0 at.% W alloys. The alloys were anodized at 10 mA cm⁻² to various voltages, up to 150 V, in 3 M ammonium hydroxide/0.05 M ammonium phosphate electrolyte at 293 K. The alloys revealed enrichments of tungsten to at least 1.7 x 10¹⁵ and 2.9 x 10¹⁵ W atoms cm⁻² for the Mg-0.4 at.% W and Mg-1.0 at.% W alloys respectively. The enrichment behaviour appears to be similar to that in dilute aluminium alloys, which occurs for alloying elements with oxides having Gibbs free energies per equivalent for formation exceeding that for formation of alumina.

Behavior of Impurity and Minor Alloying Elements During Surface Treatments of Aluminum

C.E. Caicedo-Martinez, E. Koroleva, P. Skeldon, G.E. Thompson, G. Hoellrigl, P. Bailey, T.C.Q. Noakes, H. Habazaki and K. Shimizu

Journal of the Electrochemical Society, 149, B139-B145 (2002)

The behavior of impurity and minor elements during electropolishing, chemical polishing, and anodizing treatments is examined for 99.99% Al and Al-0.2 atom % Mn alloy containing iron, copper, and silicon impurities in the parts per million range. Copper is enriched strongly, to at least 2-4 x 10¹⁴ copper atoms cm⁻², during the two polishing treatments. Assuming that the copper is located in a metal layer of thickness 1 nm, just beneath the surface film, the enrichment corresponds to an average concentration of about 5 atom % copper. In contrast, iron and silicon impurities were not enriched significantly by the various treatments. Manganese was enriched in the Al-0.2 atom % Mn alloy to about 7 x 10¹⁴ atoms cm⁻². Manganese appeared to interact with copper impurity in the alloy to reduce the level of copper enrichment. The factors determining the degree of enrichment include the Gibbs free energies per equivalent for formation of the various impurity and alloying element oxides, interactions between coenriching elements, and the location of the particular atoms in the metal, especially the proportions of the atoms in solid solution, in fine particulates, and segregated at cellular and grain boundaries.

Surface Nanotextures on Aluminium

C.E. Caicedo-Martinez, E.V. Koroleva, G.E. Thompson, P. Skeldon, K. Shimizu, H. Habazaki and G. Hoellrigl

Surface and Interface Analysis, 34, 405-408 (2002)

Chemical polishing and electropolishing of aluminium result in fine cellular textures of nanometre dimensions, which play a role in the electrochemical behaviour of aluminium and its response to further treatment processes such as conversion coating and anodizing. Concerning the latter, the surface texture is highlighted by porous anodic film growth for protection of the substrate. The influence of residual impurities and low additions of alloying elements on the development of the textures is investigated here for superpure aluminium (99.99%) and an Al-0.4wt.%Mn alloy, respectively. Complementary analytical approaches, including atomic force microscopy and transmission electron microscopy, disclose scalloped cellular textures comprising adjacent peaks and troughs, with a dependence on the grain orientation of the aluminium substrate. In addition to texture development, enrichment of copper impurity in the alloy occurs adjacent to the alloy/oxide film interface, as revealed by in-depth elemental profiles generated by r.f. glow discharge optical emission spectroscopy. The absence of similar enrichments of iron and silicon in the alloy suggests that these elements are distributed mainly as fine segregates in the aluminium, unlike copper, which is in solid solution. At low alloying levels, manganese reveals limited enrichment and is also probably present mainly as segregates. The origin of the textures and their dependence on grain orientation are thus considered to be related to the presence and location of relatively high- melting-point elemental impurities in the alloy and their local electrochemical responses relative to the adjacent alloy surface.

Characterization of Electrodeposited WO₃ Films and its Application to Electrochemical Wastewater Treatment

H. Habazaki, Y. Hayashi and H. Konno

Electrochimica Acta, 47, 4181-4188 (2002)

WO₃ films have been prepared on to IrO₂-coated Ti substrate by cathodic deposition, and as-deposited and annealed films have been characterized using XRD, TEM, Raman and FT-IR spectroscopy. The as-deposited film consists of nanocrystalline, orthorhombic WO₃·H₂O and this phase transforms to amorphous WO₃ by annealing at 250°C and to monoclinic WO₃ by annealing at and above 350°C. The as-deposited and annealed films have been used as anodes for electrochemical decomposition of phenol in aqueous solutions with and without chloride ions. The monoclinic WO₃ anodes prepared by annealing at 350 and 400°C show relatively high electrochemical activity in the chloride-containing solution. In addition, the anodes possess high chemical and physical stabilities: very low dissolution rate of WO₃ during the electrolysis and good adhesion to the substrate. Thus, WO₃ anodes may be promising materials for anodic oxidation of bio-refractory organics in wastewater, although further improvement of electrochemical activity is needed for more effective decrease in total organic carbons in wastewater.

Ionic Mobilities in Amorphous Anodic Titania

H. Habazaki, K. Shimizu, S. Nagata, P. Skeldon, G.E. Thompson and G.C. Wood

Journal of the Electrochemical Society, 149, B70-B74 (2002)

The mobilities of various electrolyte-derived species in amorphous anodic titania have been determined, with stabilization of the oxide structure by incorporation of silicon species from a sputter-deposited Ti-6 atom% Si alloy. From comparison of the distributions of silicon marker species and electrolyte-derived species in films formed at high current efficiency, boron, chromium, molybdenum, and tungsten species migrate outward more slowly than do Ti⁴⁺ ions. Their migration rates, relative to that of Ti⁴⁺ ions, correlate well with the energies of the respective metal-oxygen bonds. Further, chromium species incorporated into the film from chromate electrolyte are mainly present in the trivalent state, indicating reduction of Cr⁶⁺ ions to Cr³⁺ ions in the growing anodic oxide. This reduction of chromium species can be explained by considering the influences of Cr³⁺ and Cr⁶⁺ ions on the band structure of titania.

Ionic Transport in Amorphous Anodic Titania Stabilised by Incorporation of Silicon Species

H. Habazaki, K. Shimizu, S. Nagata, P. Skeldon, G.E. Thompson and G.C. Wood

Corrosion Science, 44, 1047-1055 (2002)

Incorporation of silicon species from an alloy substrate into anodic titania is shown to stabilise the amorphous structure of the film, facilitating investigation of the ionic transport processes in amorphous titania grown at high efficiency. Thus, an amorphous anodic film developed on a sputtering-deposited Ti-6 at.% Si alloy formed to 100 V in phosphoric acid electrolyte in contrast to a partially crystalline film developed on relatively pure titanium at <20 V. Silicon species, which are immobile and act as marker species in the growing film, are present in the inner 58% of the film thickness. Evidently, the film material forms simultaneously at the film/electrolyte and alloy/film interfaces by co-operative transport of cations and anions, as is usual in amorphous anodic oxides. The phosphate anions incorporated from the electrolyte migrate inward at 0.34 times the rate of O²⁻ ions and hence are present in the outer 62% of the film thickness.

Materials for Global Carbon Dioxide Recycling

K. Hashimoto, M. Yamasaki, S. Meguro, T. Sasaki, H. Katagiri, K. Izumiya, N. Kumagai, H. Habazaki, E. Akiyama and K. Asami

Corrosion Science, 44, 371-386 (2002)

CO₂ emissions, which induce global warming, increase with the development of economic activity. It is impossible to decrease the CO₂ emissions by suppression of the economic activity. Global CO₂ recycling can solve this problem. The global CO₂ recycling consists of three district: The electricity is generated by solar cells on deserts. At desert coasts, the electricity is used for H₂ production by seawater electrolysis and H₂ is used for CH₄ production by the reaction with CO₂. CH₄ which is the main component of liquefied natural gas is liquefied and transported to energy consuming districts where CO₂ is recovered, liquefied and transported to the desert coasts. A CO₂ recycling plant for substantiation of our idea has been built on the roof of the Institute for Materials Research in 1996. Key materials necessary for the global CO₂ recycling are the anode and cathode for seawater electrolysis and the catalyst for CO₂ conversion. All of them have been tailored by us. They have very high activity and selectivity for necessary reactions in addition to excellent durability. A pilot plant consisting of minimum units in an industrial scale is going to be built in three years.

Ionic Transport in Anodically Oxidized AI/W Layers

L. Iglesias-Rubianes, P. Skeldon, G.E. Thompson, H. Habazaki and K. Shimizu

Journal of the Electrochemical Society, 149, B23-B26 (2002)

The growth of an anodic oxide film on a specimen consisting of a layer of aluminum deposited upon a layer of tungsten was examined by transmission electron microscopy. The findings reveal initial growth of anodic alumina, followed by penetration of the alumina by fingers of tungsten oxide once the metal/film interface reaches the tungsten layer. The fingers are approximately cylindrical or lanceolate, with width in the range 1-15 nm and aspect ratios up to about 40. The current flows preferentially to regions of tungsten oxide rather than the alumina due to the lower electric field for growth of the former oxide. The penetration of the alumina is assisted by the relatively high Pilling-Bedworth ratio for W/WO₃ and the inherent plasticity in amorphous anodic oxides. The tungsten oxide of the fingers appears to be of higher density than that formed at the metal/film interface after the aluminum has been fully oxidized, which may be due to the penetration of the alumina layer by a displacement process.

Transient Anodic Oxidation of an Al-W Alloy: Effects of Current Ratio

L. Iglesias-Rubianes, P. Skeldon, T.E. Thompson, H. Habazaki and K. Shimizu

Corrosion Science, 44, 751-760 (2002)

Previous experiments involving stepped changes in current during anodizing of aluminium alloys have disclosed subtle transient and long-term influences of current density on film growth. The present work employs a current reduction of a factor of 10⁴, much larger than that in earlier work, to investigate the phenomena further. The findings from transmission electron microscopy of film sections disclose that the step in current leads to generation of fine light bands of film material, each about 6 nm thick, at the alloy/film and film/electrolyte interfaces. Further, the film material formed at the alloy/film interface following the step in current is generally of lighter appearance than that formed previously. The lighter film material probably contains relatively less tungsten species, and/or is of reduced density, compared with adjacent material. The greater reduction in current, compared with that of previous studies, appears to accentuate the alterations in composition and/or density of film material.

Molybdate/Al(III) Composite Films on Steel and Zinc-Plated Steel by Chemical Conversion

H. Konno, K. Narumi and H. Habazaki

Corrosion Science, 44, 1889-1900 (2002)

A molybdate(VI)-Al(III) chemical conversion process was developed as an alternative to the chromate processes. Steel and zine-plated steel specimens were treated in the solutions of 0.16 mol I⁻¹ ammonium alum (AlNH₄(SO₄)₂ 12H₂O) with small amounts of ammonium molybdate(VI) (0.002-0.016 mol I⁻¹ (NH₄)₆Mo₇O₂₄ 4H₂O) at 60°C for 10-30 min in an ultrasonic rinsing apparatus. The formed films were composed of oxyhydroxides containing Mo(V,VI), Al(III), Fe(II,III) and sulfate ions (and Zn(II) ions in the case of zinc-plated steel), and showed good corrosion resistance in an aerated 0.5 mol I⁻¹ NaCl-0.15 mol I⁻¹ H₃BO₃ solution (pH = 7). The films macerated during the corrosion test, but they did not detach and functioned as a protective layer. This process may be useful in forming undercoats for paints and polymer coatings on steel and zinc-plated steel.

Detachment of Alumina Films from Aluminium by 100 keV H⁺ lons

Y. Liu, M. Alexander, E. Koroleva, P. Skeldon, G.E. Thompson, P. Bailey, T.C.Q. Noakes, K. Shimizu and H. Habazaki

Surface and Interface Analysis, 33, 318-321 (2002)

Irradiation of aluminium covered by anodic oxide films 3-14 nm thick using 100 keV H⁺ ions is shown to result in detachment of the oxide film. A dose of 6.6 x 10¹⁶ H⁺ ions cm⁻² on a 6.5 nm thick film causes the removal of large pieces of oxide with dimensions at least 15 µm. Atomic force microscopy analysis shows that the location of the failure is within ~1 nm of the metal/oxide interface. The large aspect ratio (width to thickness) of the detached pieces is thus similar to 2000:1 and indicates that there is a disruption of the oxide bonding over large areas. The bombardment also results in the formation of blisters with diameters up to several hundred nanometres in the oxide, accompanied by shallow depressions, similar to 5 nm deep in the underlying metal. The detachment is suggested to be associated with either condensation of vacancies generated in the metal by the H⁺ ions or accumulation of hydrogen atoms deposited in the metal by the ion beam in the region of the metal/oxide interface. Although the beam energy and dose were expected to cause some disruption in the implanted material, the complete detachment of large areas of oxide was not anticipated. In fact, this appears to be the first time such gross detachment of an anodic film by H+ ion irradiation has been reported.

Anodic Film Growth on an Al-21at.%Mg Alloy

Y. Liu, P. Skeldon, G.E. Thompson, H. Habazaki and K. Shimizu

Corrosion Science, 44, 1133-1142 (2002)

As a contribution towards the understanding of the electrochemical behaviour of magnesium-containing second phase particles in aluminium alloys, the formation of barrier-type anodic films on sputtering-deposited Al-21 at.% Mg is examined by analytical transmission electron microscopy. Amorphous anodic films of uniform thickness develop on the alloy in ammonium pentaborate electrolyte of pH 8.3 at current densities between 0.1 and 100 mA cm⁻². The films contain incorporated magnesium species that reduce the electric field required for film growth. The magnesium species migrate through the film about three times faster than Al³⁺ ions and are lost to the electrolyte on reaching the surface of the film, leading to a reduced efficiency of growth of about 92%. Further, the growing films can detach from the alloy, particularly at relatively low current density. In strongly alkaline conditions, the comparatively rapid transport of magnesium species and the stability of the resulting magnesium-rich surface regions of the film permits highly efficient film growth in sodium hydroxide solution of pH 13.

Porous Tantala and Alumina Films from Non-Thickness Limited Anodising in Phosphate/Glycerol Electrolyte

Q. Lu, G. Alcala, P. Skeldon, G.E. Thompson, M.J. Graham, D. Masheder, K. Shimizu and H. Habazaki

Electrochimica Acta, 48, 37-42 (2002)

The present study demonstrates that the phenomenon of non-thickness limited (NTL) growth of anodic films in a phosphate/glycerol electrolyte at 453 K on tantalum and aluminium is due to the formation of porous films. For both tantala and alumina films, the resultant morphology comprises cells of material orientated approximately normal to the metal/film interface, with each cell containing a central pore of typical diameter in the range 3-15 nm and a barrier layer of film material at the base of the pore. The total porosity is about 5%. The hardness of NTL tantala films, determined by nanoindentation, was 5.1 GPa, reasonably similar to that of conventional anodic tantala.

Anodic Film Growth on Tantalum in Dilute Phosphoric Acid Solution at 20 and 85°C

Q. Lu, S. Mato, P. Skeldon, G.E. Thompson, D. Masheder, H. Habazaki and K. Shimizu

Electrochimica Acta, 47, 2761-2767 (2002)

The effects of current density and temperature on the anodic films formed on tantalum in dilute H₃PO₄ (0.06 wt%) solution have been studied by transmission electron microscopy, using ultramicrotomed sections, and Rutherford backscattering spectroscopy. Two-layered films have been identified, comprising an inner relatively pure Ta₂O₅ layer, adjacent to the metal/film interface, and an outer layer containing incorporated PO₄³⁻ anions. The total amount and depth of incorporated phosphorus species increase with increasing current density and decreasing temperature, in correspondence with the enhancement of the electric field. The formation conditions for the films include those relevant to the commercial anodising of tantalum for capacitors for which the extent of phosphorus incorporation is shown to be comparatively low.

Transmission Electron Microscopy of Non-Thickness-Limited Anodic Films on Tantalum

Q. Lu, P. Skeldon, G.E. Thompson, M.J. Graham, D. Masheder, H. Habazaki and K. Shimizu

Journal of the Electrochemical Society, 149, B531-B533 (2002)

Non-thickness-limited (NTL) growth of anodic films on tantalum is a remarkable recently reported phenomenon whereby anodic films can be formed on tantalum to high thickness due to a change in the film growth mechanism from the usual high-field type of process. The present work employs transmission electron microscopy to reveal the structure, composition, and morphology of an NTL-type film formed by anodizing tantalum at 1 A m⁻² in 10 wt % dibasic potassium phosphate/glycerol electrolyte at 453 K. A relatively compact, amorphous layer of NTL-type film material, composed of essentially tantala, was formed above an inner layer of usual high-field-type tantala under the selected conditions of anodizing and drying of the electrolyte. The field for growth of NTL-type film material is less than or equal to10 MV m⁻¹, compared with ~400 MV m⁻¹ for high-field growth. Thus, the thickness of the inner layer is approximately equal to the product of the formation ratio for usual anodic tantala and the final anodizing voltage.

Anodically Deposited Manganese Molybdenum Tungsten Oxide Anodes forOxygen Evolution inSeawater Electrolysis

T. Matsui, H. Habazaki, A. Kawashima, K. Asami, N. Kumagai and K. Hashimoto

Journal of Applied Electrochemistry, 32, 993-1000 (2002)

Ternary manganese molybdenum tungsten oxides were anodically deposited on to IrO₂-coated titanium substrates at current densities of 60-600 A m⁻² in 0.4 M MnSO₄ solutions containing 0.003 M Na₂MoO₄ and 0.003 M Na₂WO₄ at pH 0-1.5 and at 30- 90°C. The effect of anodic deposition conditions on the activity. selectivity and durability of the anodes for oxygen evolution in 0.5 M NaCl solution was investigated. Most of the oxide anodes prepared initially gave an oxygen evolution efficiency of almost 100%. When the anodic deposition was performed at temperatures lower than 90°C gradual oxidative dissolution occurred during the electrolysis in the NaCl solution, due to formation of poorly crystalline oxides. In contrast, the oxide deposited at 90°C revealed no obvious dissolution during electrolysis for more than 1500 h. The oxygen evolution efficiency, however, decreased gradually with time of electrolysis because of partial detachment of the deposited oxide. The anodic deposition in electrolytes at lower pH and at higher current density resulted in the formation of oxides with better adhesion to the substrate, resulting in improved anode durability. The durability was further improved by repeated anodic deposition with the oxide surface washed during intervals.

Radio Frequency GDOES Depth Profiling Analysis of a B-Doped Diamond Film Deposited onto Si by Microwave Plasma CVD

K. Shimizu, Y. Einaga, K. Ohnishi, A. Fujishima, H. Habazaki, P. Skeldon and G.E. Thompson

Surface and Interface Analysis, 33, 35-40 (2002)

Analysis of a boron-doped diamond film, similar to 13 µm thick, deposited onto a mirror-finished n-Si(100) substrate using microwave plasma chemical vapour deposition (CVD), demonstrates the suitability of radio frequency glow discharge optical emission spectroscopy (rf-GDOES) for rapid depth profiling analysis. The distributions of boron and hydrogen are revealed clearly. Interestingly, the sputtering of the diamond film is accompanied by smoothing of the initial rough, faceted surface, implying that the ridges sputter more rapidly than the valleys during analysis.

Radio Frequency Glow Discharge Optical Emission Spectroscopy - Depth Profiling Analysis of Thin Anodic Alumina Films as Potential Reference Materials

K. Shimizu, H. Habazaki, P. Skeldon, G.E. Thompson and R.K. Marcus

Spectroscopy, **17**(10), 14-23 (2002)

The need for reference materials that can be applied in the area of thin (<10 μ m) films analysis has long been realized but is still, in general, under-addressed. Alumina films of single-micrometer thickness, having either fine distributions of impurities or delta function impurity marker layers, can be prepared routinely by anodic oxidation of electropolished aluminum specimens in appropriate electrolytes. Selected films were examined by transmission electron microscopy (TEM) and analyzed by radio frequency glow discharge optical emission spectroscopy (rf-GD-OES), providing very rapid, yet high-resolution, depth-resolved analysis of these electrically insulating materials.

Role of Metal Ion Impurities in Generation of Oxygen Gas Within Anodic Alumina

K. Shimizu, H. Habazaki, P. Skeldon, G.E. Thompson and G.C. Wood

Electrochimica Acta, 47, 1225-1228 (2002)

The generation of oxygen gas within an amorphous anodic alumina film is reported. The film was formed by anodizing aluminum, which was first electropolished and then chemically polished in CrO_3 - H_3PO_4 solution, in sodium tungstate electrolyte. The procedure results in incorporation of mobile Cr^{3+} species, from the chemical polishing film, and mobile W^{6+} species, from the electrolyte, into the amorphous structure. The tungsten species are present in the outer 27% of the film thickness, while Cr^{6+} species occupy a thin layer within the tungsten-containing region. Above the Cr^{3+} containing layer, a band develops that contains oxygen bubbles of a few nanometres size. The oxygen is generated by oxidation of O^{2-} ions of the alumina. A mechanism of oxygen generation within the alumina is proposed based on the electronic band structure of the oxide, modified by the Cr^{3+} and W^{6+} species and on the ionic transport processes during oxide growth.

Oxygen Evolution Within Barrier Oxide Films

E. Zhuravlyova, L. Iglesias-Rubianes, A. Pakes, P. Skeldon, G.E. Thompson, X. Zhou, T. Quance, M.J. Graham, H. Habazaki and K. Shimizu

Corrosion Science, 44, 2153-2159 (2002)

Using residual gas analysis, with scraping of oxide films, it is demonstrated that oxygen gas can be generated within anodic films on Al-Cu alloys and InP. The oxygen is produced by oxidation of O² ions of the film material, and is present in numerous bubbles in the bulk film. The generation of oxygen is suggested to be related to the electron energy levels of the film material, which in the case of alumina films are modified by the incorporation of copper species and, from previous work, other non-valve metal species. Oxygen is also present in low amounts in alumina films nominally free of the latter species; the oxygen may be located either in the bulk oxide or at flaws.

Visible Light Responsibility of Titanium Dioxide Photocatalyst by Metal Ion Decoration and Basic Research into Its Dental Application

Y. Tanimura, F. Watari, M. Uo, and Y. Totsuka

The Journal of Japanese Society of Dental Materials and Devices, 21 (2002)

Although titanium dioxide photocatalyst is usually initiated only by ultraviolet in radiation, visible light responsiveness after metal ion processing was investigated by examination of the decomposition of methylene blue pigment and optimal processing conditions were studied. The photocatalyst effect depended on metal ion/TiO₂ ratio during treatment with metal ion solution. Using a 0.3µm powder, the optimal catalyst efficiency under visible light was obtained with a Ag/TiO₂ ratio of 30µg/g. An antibacterial effect on Streptococcus mutans was clearly confirmed on titanium dioxide film formed by sol-gel method on a glass plate and decorated with metal ion. Dentition bleaching was also successfully carried out. Thus visible light responsiveness and an increase in catalyst efficiency were obtained, enabling antibacterial activity and dentition bleaching. These findings suggest the applicability of photocatalyst in dental practice.

Therefore, the order of toxicity of these elements in same concentration was estimated as Ni, Cu and Fe. For Ag, Ti, Ni-Ti, SUS304 and SUS316 implants, significant distribution and severe tissue damage was not observed. The XSAM was useful for the study of dissolution and distribution property of highly toxic and chemically unstable metal implants in the soft tissue.

Modeling the Kinetics of Lithium Ion Incorporation into Tunnel Vacancies of Spinel-Type Manganese Dioxide λ -MnO₂ from Aqueous Solutions

Akio Tanaka, Hiroki Tamura, and Shinichi Kikkawa

Electrochemistry, 70, 622-629 (2002).

Spinel-type manganese dioxide, \(\lambda \cdot MnO_2 \), has a three dimensional network of tunnels connecting vacant sites in the oxide lattice. This oxide can preferentially incorporate lithium ions into the lattice vacancies since lithium ions fit the tunnels in size. With the incorporation, the lattice Mn(IV) reduces to Mn(III) maintaining electric neutrality. The rate of incorporation decreased with time, suggesting inhibition of the reaction due to reaction products as pre-formed Mn(III) in the oxide decreased the incorporation rate. The incorporation rate increased with increasing pH, temperature, the mass concentration and specific surface area of the λ -MnO₂ samples, and the amount of a radical scavenger added. A kinetic model is proposed by considering the following reaction processes: (1) an Mn(IV)-vacancy pair on the oxide surface oxidizes a hydroxide ion in solution and forms a free vacancy, lattice Mn(III), and a hydroxyl radical. A part of the products reacts backward because the reaction products do not satisfy electric neutrality; (2) the free vacancy remaining takes up the lithium ion from the solution to reestablish electric neutrality; (3) the formed Mn(III) reduces the Mn(IV)-vacancy pair in the oxide bulk and the lithium ion transfers to the bulk through the tunnel, regenerating the Mn(IV)-vacancy pair on the surface; and (4) the hydroxyl radical decomposes to oxygen and water. The steps (1) and (2) were assumed to be rate determining, and the rate equation was derived. The model rate equation reproduced the observed results, and the lithium ion incorporation properties of λ-MnO₂ could be evaluated with the model parameters. (Japanese)

Ion-Exchange Properties of Tetratitanic Acid with a Layer Structure for Alkali Metal Ions

Hiroki Tamura, Kyosuke Nakamura, and Shinichi Kikkawa

Electrochemistry, 70, 530-535 (2002).

Tetratitanic acid, H₂Ti₄O₉ • H₂O, has a layer structure composed of the TiO₆ octahedra sheets containing two protons and one water molecule per tetratitanate unit. The protons are exchanged with cations in bulk solution, and the amount of alkali metal ions incorporated into the interlayer was measured as a function of pH. With increasing pH, the amount increased, but the effect of pH on the extent of incorporation was far smaller than that expected from the mass action law. This behavior was modeled with the Frumkin equation where suppressive interactions between adsorbed ions owing to either electrostatic repulsion or steric hindrance are taken into account. The measured data were fitted with the model equation and the ion adsorption abilities of tetratitanic acid, adsorption affinities of sodium and potassium ions, and suppressive interaction properties of adsorbed ions were evaluated with model parameters. The molecular form of the exchanging protons and the mechanism of exchange with cations are discussed. (Japanese)

Ion Complexation at Oxide-Solution Interfaces

H. Tamura

Encyclopedia of Surface and Colloid Science, Marcel Dekker, Inc., 2856-2875 (2002).

A surface complexation model with general lateral interactions between interface species is described. This model considers the surface complexation to be an ion exchange between cations and surface hydroxyl protons or between anions and surface hydroxyl ions. For monovalent ions, 1:1 exchange reactions occur and the ions are adsorbed non-specifically to form electrical double layers. For divalent transition metal ions, 1:1 and 1:2 exchange reactions occur simultaneously, the ions are adsorbed specifically, and the 1:1 exchange causes a surface charge. The material balance equations were derived based on the reaction stoichiometry. The equilibrium conditions for surface complexation were derived according to the Frumkin equation. The Frumkin equation expresses the deviation from the mass action law due to electrical, geometrical, and other interactions at the interface by a linear increase in the Gibbs free energy change with respect to the surface coverage. The model fits and reproduces the observed charge and ion adsorption behaviors of metal oxides. With the numerical values of the model parameters, the densities of the respective surface species can be calculated and the properties of the ions and oxides evaluated.

Potential Modulation Reflectance of manganese Holgenated Tetrphenylporphyrin Derivatives Assembled on Gold Electrodes

T. Yamada, M. Nango, and T. Ohtsuka

J. Electroanal. Chem., 528. 93-102 (2002).

Electron transfer from/to redox manganese porphyrin self-assembled monolayers (SAMs) on gold electrodes in DMSO solution was investigated by potential-modulation reflectance, i.e. electroreflectance (ER) with cyclic voltammetry and ac impedance. The ER voltammogram reveals more clearly the redox waves of Mn(III)/Mn(II) in the porphyrin monolayers than the cyclic voltammogram(CV). The standard rate constants pf electron transfer, i.e. turn-over number of the redox reaction at the formal potential was evaluated from complex plane plots of ER of the manganese redox couples. On the complex plane plot of the ER, the rate constant can be determined from a characteristic frequency of the ac response. The rate constant thus obtained were complared with the values evaluated from the impedance data and further compared with the values calculated by Sagara's treatment from the relationship between the phase retardation and the frequency of the complex ER data. Fairly good agreement was obtained between the rate constants from the three evaluations. The ER response is found to be comparable to the complex capacitance defined as (dQ/dE) for the circuit involving the redox couple. It was found that the rate constants increase with a decrease in a distance between the electrode substrate and the redox manganese porphyrin and depend on the species bound to phenyl groups around the porphyrin unit in the order of Cl>H>F.

Hydrogen Generation from a Single Crystal Magnetite Coupled Galvanically with a Carbon Steel in Sulfate Solution

K. Fushimi, T. Yamamuro and M. Seo

Corrosion Science, 44, 611-623 (2002).

A galvanic coupling with a single crystal magnetite accelerated the corrosion of a carbon steel in sulfate solutions. A scanning electrochemical microscopic investigation revealed that the hydrogen generation on the magnetite as well as the reduction of the magnetite itself was contributed to a galvanic corrosion of the carbon steel. The estimated current efficiency for the hydrogen generation on the magnetite was about 50% in pH 5.8 sulfate solution. Moreover, the distribution of hydrogen generated above the magnetite surface was observed with the probe current image.

Effects of Dichromate Treatment on Mechanical Properties of Passivated Single Crystal Iron (100) and (110) Surfaces

M. Chiba and M. Seo

Corrosion Science, 44, 2379-2391 (2002).

An *in-situ* nanoindentation technique combined with an AFM was applied to evaluate the effects of dichromate treatment on the mechanical properties of the single crystal iron (100) and (110) surfaces passivated in pH 8.4 borate solution. The dichromate treatment was performed with natural immersion of the iron specimens in 5 x 10^{-2} M K₂Cr₂O₇ solution for 24 h prior to passivation at 0.25 V (SHE) for 1 h. The hardness, H and the works (elastic work, W_e , plastic work, W_p , and total work, $W_t = W_e + W_p$) made during nanoindentation were obtained from the measured load-depth curves.

The values of H and $W_{\rm e}$ / $W_{\rm t}$ at the indentation depth larger than 30 nm for the passivated single crystal iron surfaces were increased by the dichromate treatment. The increases in H and $W_{\rm e}$ / $W_{\rm t}$ due to the dichromate treatment were attributed to the promotion of repassivation at the sites of passive film ruptured during nanoindentation process.

Scanning Electrochemical Microscopic Study of Detecting Non-homogeneity in Surface Reactions of Metals

K. Fushimi and M. Seo

ISIJ International, 42, 1326-1333 (2002).

Scanning electrochemical microscopy (SECM) is powerful to investigate non-homogeneity surface reaction in solution. It is useful for evaluating the distribution of electrochemical reactions taking place on the electrode surface such as corrosion reaction, redox reaction on passive film and so on. The heterogeneous electrochemical reaction on polycrystalline iron and titanium and single crystal magnetite electrode surfaces were discussed. SECM can be also employed for inducing locally a certain surface electrochemical reaction on the specimen by operating a probe electrode as liquid-phase ion gun (LPIG). The application of LPIG to the passive film formed on iron for inducing the local film breakdown has revealed the details of its local breakdown process.

Monitoring of Hydrogen Absorption into Titanium using Resistmetry

K. Azumi, Y. Asada, T. Ueno, M. Seo and T. Mizumo

J. Electrochem. Soc., 149[9], B422-427 (2002).

Hydrogen absorption into Ti electrodes during electrochemical cathodic polarization was monitored by using resistmetry. Electric resistance of Ti increased with H absorption due to growth of a hydride layer from the surface toward the inside. The growth rate of the hydride layer was estimated from resistance data and was found to depend on the polarization current density, existence of a pre-formed anodic oxide film, and shape of the specimen. For example, pre-formation of an anodic oxide film at a potential higher than the breakdown potential, rather, promotes hydrogen penetration. In the case of a thin wire electrode, the hydride layer grew in a non-uniform manner because the volume expansion induced cracking on the surface. Therefore, the average thickness of the hydride layer was estimated from the change in resistance.

Effects of Iron(III) Ions on Corrosion of Stainless Steel in Concentrated Nitric Acid Solutions at High Temperature

Y. Arai, K. Mabuchi, T. Honda, and H Takahashi

Zairyo-to-Kankyo, 51, 23 - 29 (2002).

Effects of Fe(III) ions on corrosion of stainless steel were examined in highly concentrated HNO₃ solutions at high temperature, using mass loss measurements, electrochemical measurements, and quantitative analysis of NO_X evolved during immersion.

Addition of Fe(NO₃)₃ into HNO₃ caused the immersion potential of stainless steel to become nobler gradually from passive to trans-passive potential regions during immersion experiments. The average corrosion rate of stainless steel during 360ks immersion increased with increasing Fe(III) concentration. Quantitative analysis of NO_X evolved during immersion suggested that Fe(III) ions adsorbed on the specimen surface act as catalytic centers in the reduction of HNO₃. (Japanese)

Formation of Anodic Oxide Films on Aluminum in Diluted KOH Solutions

H. Shimada, M. Sakairi, and H. Takahashi

J. Surface Finishing Soc. Jpn., 53, 134 - 141 (2002).

Aluminum was anodized in diluted KOH solutions galvanostatically to examine the effect of KOH-concentration on the growth and breakdown of anodic oxide films. Time-variations in the anode potential, E_a, the amount of dissolved Al³⁺ ions, and electroluminescence intensity were measured during anodizing, and the film structure was observed by transmission electron microscopy and scanning electron microscopy.

At 5 x 10^{-5} and 5 x 10^{-4} M, E_a increased with time linearly at the initial stage, and the rate of increase in E_a decreased at 400 V. The slow increase in E_a stopped at about 600 V, and beyond the potential E_a increased at a high rate until the film breakdown started at 1600 V and 1100 V in 5 x 10^{-5} and 5 x 10^{-4} M solution, respectively. In both solutions, the growth of the oxide film was accompanied by the formation and growth of relatively large voids between 400 V and 600 V, and beyond 600 V small numerous voids developed on the entire surface. The film growth can be explained by the local oxide dissolution and precipitation of hydroxide.

At 5×10^{-3} M, E_a remained zero for the initial 1500 s of anodizing, and then increased linearly with time before film breakdown started at 600 V. The anodic oxide films consisted of two layers: an outer porous layer and an inner dense layer. (Japanese)

Increase in Breakdown Potential of Anodic Oxide Film on Aluminum by Pore-Filling Method

H. Shimada, M. Sakairi and H. Takahashi

J. Surface Finishing Soc. Jpn., **53**, 142 - 148 (2002).

Aluminum covered with porous anodic oxide films was re-anodized in 0.5 M-H₃BO₃ and 5 x 10⁻⁵M-KOH solutions to examine the formation and breakdown of the oxide film.

In H₃BO₃-solution, the pores were filled with new oxide during re-anodizing, resulting in the uniform thickening of the barrier layer until film breakdown started. The breakdown potential of the film formed by the "pore-filling" method was 200 V higher at maximum than that formed by anodizing after electropolishing.

In KOH solution, the pore-filling with new oxide was accompanied by local dissolution of oxide film, leading to the formation of rough interphase between oxide film and the substrate. The film breakdown potential of the film formed by the "pore-filling" was as high as that of the oxide film formed after electropolishing.

Effects of the structure of porous anodic oxide films on the film breakdown potential during re-anodizing in H₃BO₃ solution are discussed. (Japanese)

Repairing of Anodic Oxide Films on AI - Zn Alloy Coated Steel After Removal with Photon Rupture in Solutions

M. Sakairi, K. Itabashi and H. Takahashi

Corrosion Sci. and Tec., 31, 426-431, (2002).

Analysis of abrupt destroyed of passive oxide films on Al- Zn alloy layer coated on steel and its repair is important to understand the localized corrosion of steel. In the present investigation, anodic oxide films formed on Al - Zn coated steel specimens were removed by photon rupture method (one pulse of focused pulsed Nd - YAG laser beam irradiation) at a constant potential in a sodium borate solution, pH = 9.2, with / without chloride ions to monitor the current transient. Irradiation with a pulsed laser in solutions causes abrupt removal of the anodic oxide film on the specimen at the laser-irradiated area. Without chloride ions, oxide films were reformed in the sodium borate solution at - 0.5 to 1 V after removal of the anodic oxide film. However, in chloride ion containing solutions, pitting corrosion of Zn - 55 mass % Al coated layers occurs at high potentials, while film reformation occurs at low potentials. It was also found that chloride ions enhance dissolution of aluminum and zinc at the very initial period after laser irradiation.

Anodizing of Aluminum Covered with SiO₂ by Sol-Gel Coating. -Formation Mechanism of Composite Oxide Films with High Potential Sustainability-

K. Watanabe, M. Sakairi, H. Takahashi, S. Hirai, and S. Nagata

Proc. Corros. Symp., ECS / ISE Meeting in San Francisco 146-153 (2002).

Aluminum specimens were covered with SiO₂ film by a sol-gel coating and then anodized galvanostatically in diluted borate solution. Time-variations in the anode potential during anodizing were monitored, and the structure and dielectric properties of anodic oxide films were examined by TEM-EDX, RBS, and electrochemical impedance measurements.

It was found that anodizing of aluminum coated with SiO₂ films leads to the formation of anodic oxide films, which consist of an outer Al-Si composite oxide layer and an inner Al₂O₃ layer, at the interface between the SiO₂ film and the metal substrate. The breakdown potential of anodic oxide films formed on specimens with SiO₂-coating was about 100 V larger than without SiO₂-coating.

Conversion of Al₂O₃ to Al-Si composite oxide at the interface between the inner and outer layers is discussed in terms of inward transport of Si-bearing anions across the outer layer.

Scanning Confocal Laser Microscopy of the Surface of Anodized Al5052 Alloy

S.-M. Moon, M. Sakairi, and H. Takahashi

Proc. Corros. Symp., ECS / ISE Meeting in San Francisco 91-98 (2002).

The surface morphology of Al5052 alloy anodized in sulfuric acid solution was investigated using a confocal scanning laser microscopy (CSLM). The incident laser beam appeared to be reflected partially by the outer oxide surface, by the defects in the oxide surface, by the defects in the oxide film and / or by the inner oxide / metal interface. This allows us to obtain the CSLM images of the surface, defects in the oxide film were observed on the CSLM images: dark spots and bright spots. The dark and bright spots were attributed to the irregular pore structure or holes in the oxide film left after the preferential dissolution of magnesium and iron-rich region in the oxide film, respectively.

Effect of Mg and Si on the Microstructure and Corrosion Behavior of Zn-Al Hot Dip Coatings on Low Carbon Steel

J. Tanaka, K. Ono, S. Hayashi, K. Ohsasa and T. Narita

ISIJ International, 42, 80-85 (2002)

Coatings formed on a low carbon steel by a two step hot dipping, primarily in a Zn bath and secondarily in a Zn-6Al bath with or without 0.5mass%Mg and 0.1 mass %Si addition. The effects of the Mg and Si addition on the surface morphologies, microstructures, and corrosion characteristics of the coatings were investigated using a scanning electron microscope, a laser scanning microscope, and an electron probe microprobe analyzer. The coating formed in the Zn-6Al bath showed flaws as pores and cracks in the outer adhered layer, while there were few flaws in the Zn-6Al-0.5Mg-0.1Si bath coating. The Zn-6Al-0.5Mg-0.1Si coating has a lamellae structure developed well in the outer adhered layer and the initially formed α-Al was finer than that of the Zn-6Al coating. Corrosion in a 5%NaCl solution commenced from the α -Al phase at a very early stage and the Zn phase corroded preferentially. The Zn-6Al-0.5Mg-0.1Si coating corroded slowly and relatively homogeneously, while the Zn-6Al coating degraded locally due to a preferential corrosion along flaws. The Zn-6Al-0.5Mg-0.1Si coating incorporates Mg and Si in the outer adhered layer and Si in the inner alloy layer, making the Zn-6Al-0.5Mg-0.1Si coating more anti-corrosive.

Effect of Carbon Content on the Reaction Behavior of Hot Dipped Carbon Steel in Molten Zn-6mass%Al Bath

J. Tanaka, K. Ono, S. Hayashi, K. Ohsasa and T. Narita

Hyomen Gijutsu, 53,129-133 (2002)

The phases and microstructure of the alloy layer formed during hot dipping of carbon steels in molten Zn-Al bath were investigated. Pure iron, 0.2%C and 0.82%C steels and 2.45%C cast iron were used. A plate shape specimen of 300µm in thickness was firstly hot dipped in a molten Zn bath for 3s and then hot dipped in a molten Zn-6mass%Al alloy bath for certain times, and quenched with water. The microstructure of the quenched specimen was observed by using a SEM, and change in thickness of the specimen was measured by using a laser microscope. The pure iron specimen was entirely changed to an intermetallic compound of Fe₂Al₅(Zn) phase after 1.2ks hot dipping. The thickness of 0.2%C steel specimen was decreased linearly with the dipping time after an early non-reaction period. and 2/3 of the specimen was changed to the Fe₂Al₃(Zn) phase after 3.6ks hot dipping. It was observed that primarily precipitated ferrite phase preferentially reacted and pearlite structure scarcely reacted. The reacted thickness of the 0.82%C steel and cast iron specimens were only several µm after 86.4Ks hot dipping. In the cast iron specimen, cementite reacted with Al and an Al₃C₄ phase was formed. The growth of the alloy layer was restricted by the Al₃C₄ phase. A heat-treated 0.2%C steel specimen with sorbite structure also exhibited the same low reaction behavior as the 0.82%C steel due to homogenized ferrite+cementite structure. (Japanese)

Effect of Spark Plasma Sintering Pressure on the Properties of Functionally Graded Implant and its Biocompatibility

F.Watari, H.Kondo, R.Miyao, M.Omori, A.Okubo, T.Hirai, A.Yokoyama, M.Uo, Y.Tamura and T.Kawasaki

Journal of the Japan Society of Powder and Powder Metallurgy, 47, 1226-33 (2002)

The coexistence of Ti and hydroxyapatite(HAP) makes HAP decomposed at the sintering process heated at more than 1000°C in vacuum or Ar atmosphere. Spark plasma sintering(SPS) method could make the stable functionally graded materials(FGM) with the gradual change of concentration in the longitudinal direction from pure Ti to 100%HAP(Ti/100HAP) at the sintering temperature as low as 850°C. However, sintering is insufficient. To increase the degree of sintering the dependence of mechanical properties on sintering pressure during was investigated. By increase of sintering pressure from 40 to 80 MPa compression strength was increased from 48 to 88MPa, and flexural strength from 6 to 36MPa. Brinel hardness decreased monotonically from Ti region to HAP inside FGM This decreasing gradience inside implant contributes to stress relaxation in the implanted region of bone where the compatibility with tissue is essential in biomechanical properties. Animal implantation tests in hard tissue showed that the tissue reacted gradiently in response to the graded composition of FGM implant. The maturation of new bone occurred from the earlier stage in the Functionally graded implants could thus satisfy the HAP rich region. biocompatibility in both mechanical properties and biochemical affinity to osteogenesis.

Structual Analysis of Arabinogalactan from Japanese Larch in Hokkaido and Chemical Functionalization of Arabinogalactans

T.Akasaka, Y.Maekawa and S-I.Nishimura

Cellulose Commun. 9(1),13-17(2002)

Larch arabinogalactan (arabinogalactan was arreviated as AG hereafter) has several unique properties, including high water-solubility and produces low-viscosity solution. In general, it is a highly branched polysaccharide consisting of a galactan backbone with side-chaines of galactose and arabinose sugars. The present paper describes structural analysis of AG isolated from Japanese larch in Hokkaido. It is similar in structure to arabino-3,6-galactan from Western larch, but compositional and alkaline degradation analyses of AGs indicated a little difference in the ratio of arabinose/galactose and in the length of side-chaines. Subsequently chemical functionalization of AGs is reviewed.

Effects of Ti ions and Particles on neutrophil Function and Morphology

R.Kumazawa, F.Watari, N.Takashi, Y.Tanimura, M.Uo and Y.Totsuka

Biomaterials, 23, 3757-64 (2002)

We compared the cytotoxicity of soluble and particulate titanium (Ti),vanadium (V) and nickel (Ni) by biochemical functional analysis and by microscopic morphology with micro-area elemental analysis in vitro using human neutrophils as probes and in vivo in animals. The biochemical analyses of LDH, superoxide anion, TNF-a and scanning electron microscopy (SEM) showed that Ni in solution destroys the cell membrane of neutrophils, whereas Ti and V in solution stimulate neutrophils and increase the quantity of released superoxide anions. Fine Ti particles (1-3µm), which smaller than neutrophils (about 5µm), were phagocytized by the cells and the results were similar in vivo. These results showed that the cytotoxic effect of Ti particles is size dependent, and that they must be smaller than that of cells. The present study demonstrated that the biochemical functional tests are useful for evaluating the biocompatibility of materials.

Effects of Particle Size on Cell Function and Morphology in Ti and Ni

K. Tamura, N. Takashi, R. Kumazawa, F. Watari and Y. Tostuka

Materials Transactions JIM 12, 3052-3057 (2002)

The dependence of cytotoxicity on particles size in titanium (Ti) and nickel (Ni) was investigated by biochemical functional analysis and by microscopic observation of cellular morphology, in vitro using human neutrophils as probes and in vivo in animal implantation test. The biochemical analyses of cell survival rate, LDH, superoxide anion, cytokines of tumor necrosis factor-alpha (TNF- α), interleukin-1 beta (IL-1 β) and observation by scanning electron microscopy (SEM) showed that Ti fine particles (2 μ m) stimulate neutrophils and increases the quantity of released superoxide anions, whereas Ni particles deform or disrupt the cell membrane of neutrophils. The 2 μ m Ti particles, smaller than neutrophils of about 5-10 μ m, were phagocytized by cells in vivo and the results were similar in vitro, which lead to the remarkable release of TNF- α . These results showed that there is the size-dependent cytotoxic effect in Ti fine particles and the effect is the most pronounced when they are smaller than cells. On the other hand, Ni particles caused the disruption of neutrophils in vitro and necrosis of tissue in vivo mainly through ions produced by their dissolution.

Surface Properties and Biocompatibility of Nitrided Titanium for Abrasion Resistant Implant Materials

Y.Tamura, A.Yokoyama, F.Watari and T.Kawasaki

Materials Transactions, 43(12), 3043-51 (2002)

Corrosion, other related properties and biocompatibility of surface nitrided titanium were investigated to examine its possible use as an abrasion resistant implant material. The nitrided layer about 2 _m thick composed of TiN and Ti₂N was formed on titanium by a gas nitriding method. The dissolved amount of titanium ion in SBF was as low as the detection limit of ICP, and that in the 1% lactic acid showed no significant difference from titanium. The tissue reaction of the cylindrical implant in soft tissue of rats showed no inflammation, and fine particles of 1 _m induced phagocytosis, which was similar to titanium. The implantation in the femor showed the new bone formed in direct contact with implants. All the results suggested that the wettability, corrosion resistance, S.mutans adhesion and biocompatibility were nearly equivalent to those of titanium. The surface of nitrided titanium was promising, with biocompatibility comparable with titanium, as an implant material such as for an abutment part of a dental implant, which requires high abrasion resistance.

Mechanical Properties of Surface Nitrided Titanium for Abrasion Resistant Implant Materials

Y.Tamura, A.Yokoyama, F.Watari, M.Uo and T.Kawasaki

Dental Materials Journal, 21(4), 355-72 (2002)

In order to verify its application for abrasion-resistant implant materials such as abutment in dental implants and artificial joints, mechanical properties of surface nitrided titanium were evaluated by three different tests, the Vickers hardness test, Martens scratch test and ultrasonic scaler abrasion test. The Vickers hardness of a nitrided layer of 2_m in the thickness was 1300, about ten times higher than that of pure titanium. The Martens scratch test showed high bonding strength for the nitrided layer with matrix titanium. The abrasion test using an ultrasonic scaler showed very small scratch depth and width, demonstrating extremely high abrasion resistance.

The results show that a surface-nitrided titanium has sufficient abrasion resistance if it is used under clinical conditions.

Development of Arch Form Esthetic Orthodontic Wires by Light Polymerization

H.Toyoizumi, F.Watari, T.Imai, M.Kobayashi, S.Yamagata and J.Iida

The Journal of Japanese Society of Dental Materials and Devices, 21 (2002)

The arch form is indispensable for clinical application of the Fiber-Reinforced-Plastic (FRP) wire being developed in combination with biocompatible CaO-P₂O₅-SiO₂-Al₂O₃ (CPSA) glass fibers and polymer matrix. Since the production is limited to a straight from in the conventional hot drawing method, light polymerization method and urethanedimethacrylate (UDMA) resin were adopted for the fabrication of arch form FRP wires in this study, using the ready-made arch form metal wire. Dimensional accuracy and mechanical properties were then investigated.

Inter width of the FRP arch wires was smaller by 0.1-0.2mm (in front) and 0.4-0.7mm (in rear) compared to the original model. The cross sectional form was uniformly round (0.47-0.48mm ϕ). Dimensional accuracy in the molding was thus sufficiently good. On flexural test, Young's modulus could be controlled in the range of 5-40 Gpa, by changing the volume fraction of glass fiber 10-60%. The realization of an arch form FRP wire would contribute to its application to clinical treatment.

The Development of the Estetic Orthodontic Wire

S. Yamagata, J. Iida, T. Imai, F. Watari and M. Kobayashi

Zairyo-to-Kankyo. 51, 555-560 (2002)

The FRP as the esthetic orthodontic wire was fabricated with biocompatible CaO-P₂O₅-SiO₂-Al₂O₃ (CPSA) glass fibers and PMMA. In this study both the mechanical properties and biocompatibility of the FRP wire were investigated. All wires were approximately 0.5 mm in diameter Young's modulus could be regulated in proportion to the volume fraction of glass fibers from 20 GPa to 40 GPa under dry condition corresponding to the conventional metal wires. However, deload/load ratio at 1.0 mm in deflection was deteriorated from 80.9% to 23.3% after 30 days exposure to water. The coating layer could will function as the moisture protector so that the deterioration of the ratio was improved to 56.7%. In the histological study of long term implantation of CPSA FRP wires (4weeks), the organization had almost completed either by separation or by covering with the granulation tissue. Macrophages and foreign body giant cells were scarcely observed. Therefore it could be though that they had good biocompatibility.

Effect of the Addition on Intermediate Oxide on Firing Contraction of Porcelain Inlay Processed by Cold Isostatic Pressing Method

J.Konishi, F Watari, S. Ohkawa, M.Uo, and H.Sano

The Journal of Japanese Society of Dental Materials and Devices, 21(6),357-367 (2002)

To compensate for the sintering contraction of porcelain inlay processed with cold isostatic pressure, the effect of intermediate oxide addition was studied. After oxidation and firing at 970°C for 55sec for porcelain powder with the addition of 10wt% of B, Si, Ti, SiO, TiO, or SnO, SnO was chosen due to its color tone and stable form. The effect of various concentrations and firing times or temperatures on dimentional change and bi-axial flexure of the inlay were investigation. The contraction decreased with increase in the SnO contractions, showing expansion when 50wt% or more of SnO was added. There were so significant changes when the firing time was prolonged to 5 hours or the firing temperature was raised to 1100°C. The strength decreased from 75 to 30MPa as the SnO concentration increased from 10 to 80wt%, although the porcelain made from original powder showed 120MPa. The intermediate oxide addition seemed to effectively compensate for the firing contraction.

Effect of Debindered Spherical Particle on Porcelain Inlay Processed by Cold Isostatic Pressing

J.Konishi, C.Kawamoto, H.Komatsu, H.Sano, and F.Watari

The Japanese Journal of Conservative Dentistry, 45(6), 1213-1222 (2002)

Porcelain has been known as aesthetic, mechanical and chemical stable, and biocompatible material in dentistry. The process for porcelain restoratives, however, requires labor and specific technique. In the conventional method for porcelain restoratives, the porcelain powders are mixed with water, placed on the model, and fired many times. We have attempted to simplify the process by using the cold isostatic pressure, or CIP, method to compress porcelain powders and to sinter once. We previously reported that porcelain inlay processed with CIP showed equal mechanical strength to conventional porcelain inlays. The ratio of sintering contraction, however, was 8 to 12% and required improvement. The sintering contraction could be decreased by using sphericalized powder including a binder. Debinder before sintering might be effective to achieve uniform porcelain products. In the present study, the effect of debinder from sphericalyzed particles on the contraction ratio of porcelain inlay processed by the CIP method was investigated.

Roles of Aluminium and Chromium in Sulfidation and Oxidation of Sputter-Deposited Al- and Cr-Refractory Metal Alloys

H. Habazaki, H. Mitsui, K. Ito, K. Asami, K. Hashimoto and S. Mrowec

Corrosion Science, 44, 285-301 (2002)

Our recent results of the sulfidation and oxidation behavior of sputter-deposited Al- and Cr-refractory metal alloys at high temperatures are reviewed, and the roles of the aluminum and chromium in sulfidation and oxidation of these alloys are discussed in this paper. Niobium, molybdenum and tantalum are highly resistant to sulfide corrosion. Their sulfidation resistance is further enhanced by alloying with aluminum. Although Cr-refractory metal alloys also reveal high sulfidation resistance, their sulfidation rates do not become lower than those of the corresponding refractory metals. The sulfide scales formed on the Al-refractory metal and Cr-refractory metal alloys consist of two layers, comprising an outer Al₂S₃ or Cr₂S₃ layer and an inner refractory metal disulfide layer. The inner layer has a columnar structure, and the growth direction of the refractory metal disulfides is perpendicular to 001 direction. Intercalation of Al3+ ions into NbS2 and a decrease in the sulfur activity at the outer layer/inner layer interface by the presence of the Al₂S₃ layer are probably responsible for the improvement of the sulfidation resistance by the addition of aluminum. The oxidation resistance of niobium and tantalum is improved more effectively by the addition of chromium rather than aluminum. Although preferential oxidation of chromium does not occur, an outer protective Cr₂O₃ layer in the oxide scales is formed on Cr-rich Cr-Nb and Cr-Ta alloys due to outward diffusion of Cr³⁺ ions. In contrast, continuous alumina layer cannot be formed on the Al-Nb and Al-Ta alloys, and the alloys reveal a pest phenomenon at 1073 K, and at higher temperatures rapid oxidation occurs. Concerning the oxidation of molybdenum, the addition of aluminum, which has

higher activity for oxidation than chromium, is more effective in improving the oxidation resistance of molybdenum than chromium addition, since preferential oxidation of aluminum suppresses the formation of volatile molybdenum oxide.

Oxidation Behavior of Mo₅SiB₂-Based Alloy at Elevated Temperatures

K. Yoshimi, S. Nakatani, T. Suda, S. Hanada and H. Habazaki

Intermetallics, 10, 407-414 (2002)

A Mo₅SiB₂-based alloy having composition of Mo-12.3 mol% Si- 24.9 mol% B was produced by arc-melting in an Ar atmosphere, and its oxidation behavior was investigated at temperature between 973 and 1673 K. At and above 1273 K, transient and steady state oxidation stages were clearly observed. The occurrence of the transient and steady state oxidation is interpreted in terms of rapid volatilization of MoO₃ and B₂O₃ under ambient O₂ pressure at the initial stage and the passive oxidation after completely sealing the substrate by silicate glass. Development of two layers onto the substrate, i.e. SiO₂ glass scale and Mo solid solution interlayer including SiO₂ dispersions, strongly supports the interpretation. Dissolution of B into the SiO₂ scale was not confirmed because of low B concentration that was under a detectable limit of EPMA and TEM-EDS. It is suggested that the SiO₂ glass scale formed on the Mo₅SiB₂-based alloy is more protective than as expected.

Sorption and Recovery of Heavy Oils Using Carbonized Fir Fibers and Recycling

M. Inagaki, A. Kawahara and H. Konno

Carbon, 40, 105-111 (2002).

Fibers extracted from fir trees (Abis sachalinensis Fr. Schm) and carbonized at either 380 or 900°C were found to have a high performance for sorption, recovery and recycling of heavy oils, even the viscous ones. Sorption capacity showed strong dependence on bulk density of carbonized fibers, suggesting the importance of the space formed among entangled fibers: 60-80 g/g for bulk density of ca. 6 kg/m³ and 10-20 g/g for density of ca. 40 kg/m³. The sorption capacity of carbonized fir fibers for a less viscous heavy oil was almost comparable to that of exfoliated graphite which was also reported to have high capacity. For viscous oil, however, carbonized fir fibers had higher sorption capacities than exfoliated graphite, particularly when the bulk densities are high. Less viscous heavy oil could be recovered by simple filtration under suction and the fibers could be reused for the sorption of oil, although the sorption capacity decreased with recycling. Their recycling performance was also strongly dependent on their bulk density: the sorption capacity of 6 kg/m³ fibers after the eighth cycle became less than 60% from that of the first cycle, but for 35 kg/m³ fibers it was more than 90%. Viscous oil could be recovered only by washing with n-hexane and also with less viscous oil. After washing the fir fibers could be reused for the sorption of oil.

Microstructure and Oxidation Behavior of ReSi_{1.75} Synthesized by Spark Plasma Sintering

K. Kurokawa, H. Hara, H. Takahashi and H. Takahashi

Vacuum, 65(3/4), 497-502, (2002).

Synthesis and sintering of ReSi_{1.75} were simultaneously performed by a spark plasma sintering method, using the mixed powders of elemental Re and Si. The interface structure between Re and Si changed with temperature as follows: Re/ReSi_{1.75}/Si, Re/Re₅Si₃/ReSi_{1.75}, and Re/Re₅Si₃/ReSi/ReSi_{1.75}. On the basis of the results on the interfacial reaction, a compact body consisting of the single phase ReSi_{1.75} could be easily fabricated. In addition, oxidation tests of ReSi_{1.75} were carried out in air at temperatures ranging from 773 to 1473 K. Although a silica scale was formed on ReSi_{1.75} at all temperatures by the evaporation of Re₂O₇, the formation of a protective silica scale was observed at 1273 K and above. The effect of vapor pressures of metal oxides on formation of a silica scale was also discussed.

Degradation of Cr₂O₃ Scale Formed on Stainless Steel in H₂O-Containing Atmospheres

A. Yamauchi, K. Kurokawa, and H. Takahashi

Proc. of 15th International Corrosion Congress, CD-ROM #746, 1-8, (2002).

In oxidation of Type 430 at 1473 K in H₂O-containing atmospheres, there is an induction period in the early stage of oxidation, in which a Cr₂O₃ scale is formed. After the period, formation of a nodule-like scale is caused by degradation of the Cr₂O₃ scale. Then an external scale consisting of an iron oxides and an inner scale consisting of an Fe-Cr spinel oxide are formed, resulting in drastic increase in mass. In the present study, to discuss the degradation of a Cr₂O₃ scale by H₂O vapor, the evaporation behavior of Cr₂O₃ in H₂O-containing atmospheres was investigated. The sintered Cr₂O₃ was heated for up to 360 ks at 1473 K in N₂-3%O₂, N₂-2.4%O₂-19.7%H₂O, and N₂-19.7%H₂O, and the mass losses were measured by a micro balance. The mass losses in N2-3%O2 and N2-19.7%H2O were almost identical and the rates of the mass losses was about 8×10^{-9} kg/m²s. On the other hand, the rate of the mass loss in N₂-2.4%O₂-19.7%H₂O was 5×10⁻⁸ kg/m²s. Therefore, it can be concluded that the degradation of a Cr₂O₃ scale is likely to occur in mixed atmospheres of oxygen and H₂O vapor. Volatilization of Cr₂O₃ may be mainly based on the following reaction: $Cr_2O_3(s)+3/2O_2(g)+2H_2O(g)=2CrO_2(OH)_2(g)$. The evaporation rate of Cr₂O₃ in N₂-2.4%O₂-19.7%H₂O is roughly comparable to the growth rate of the Cr₂O₃ scale in N₂-3%O₂. Therefore, the steady growth of a Cr₂O₃ scale could be prevented by the evaporation of Cr₂O₃.

High-Temperature Oxidation Behavior of ReSi_{1.75}

K. Kurokawa, H. Hara, A. Shibayama, and H. Takahashi

High Temperature Materials (ECS PV2002-5), 240-246, (2002).

Oxidation tests of ReSi_{1.75} synthesized by applying a spark plasma sintering method were carried out in air at temperatures ranging from 773 to 1473 K. Although a silica scale was formed by the evaporation of Re₂O₇ at all temperatures, the scales formed at low temperatures were porous. The porosity decreased with increasing oxidation temperature. The formation of a protective silica scale was observed at 1273 K and above. Base on such scale structures, the mass loss by the evaporation of Re₂O₇ strongly depended on oxidation temperature. The addition of B remarkably improves the plasticity of a SiO₂ scale, resulting in excellent oxidation resistance of ReSi_{1.75}. The effect of vapor pressures of metal oxides on formation of a silica scale was also discussed in comparison with MoSi₂ and WSi₂.

Oxidation Behavior of Fe-25Cr Alloy under Mechanical Loading in Atmosphere Containing SO₂ at High Temperature

I.R. Sohn and T. Narita

Corrosion Science and Technology, 31, 80-85 (2002)

Fe-25Cr alloy was pre-treated in Ar or N2-0.1%SO₂ at 973K, and then external stresses were applied in the N₂-0.1%SO₂ at 973K. By the pre-treatment, 1 μ m thickness scale which consist of a mixture of oxides and sulfides of Cr and/or Fe were formed. With applying stress of 15MPa there was little strain for 36ks, although the scale grew somewhat and an Fe oxide formed at the metal/scale interface. At high stresses, 25 and 30MPa, the scale cracked due to plastic strain between 0.9% and 3.5%, and corrosion progressed very rapidly. In case of the Ar pre-treatment a thin Cr₂O₃ with 0.1 μ m formed on the Fe-25Cr. With applying stress the scale cracked, but corrosion was limited within the cracks. The thin Cr₂O₃ scale seems to be very effective on corrosion resistance of the Fe-25Cr under external loading, and it was also resistive against the creep deformation.

High Temperature Oxidation Behavior of TiAl Coated by Al-Cr Alloy in Molten Salt

M. UEDA, D. SUSUKIDA, S. KONDA, and T. OHTSUKA The 13th International Symposium on Molten Salt, 02-05, 724-733,2002.

Al-Cr alloys were electroplated on the TiAl alloy in an AlCl₃-NaCl-KCl molten salt containing $CrCl_2$ at 423 K. The deposit consisting of γ -Al₈Cr₅ single phase is obtained at potential of -0.1 V vs. Al/Al³⁺ and includes chromium content at 41 at%. The γ -Al₈Cr₅ and Al mixture phase is, however, formed at potential from -0.2 to =0.4 V. The oxidation resistance of the electrodeposit was evaluated by a high temperature oxidation test at 1173 K for 24 h. The TiAl specimen with the Al-Cr deposit formed at -0.1 V is covered by the Cr₂Al uniform layer and the thin dense Al₂O₃ layer after oxidation. For the TiAl specimen with the deposits formed from -0.2 to -0.4 V, however, the uniform protective layer does not form. The plating of the γ -Al₈Cr₅ single phase deposit is found to reduce the oxide formation by 1/40 in thickness from that on the TiAl without the Al-Cr deposit by the oxidation.

Coating of Ni-Aluminides on TiAl Intermetallics Through Up-hill Diffusion

T. Izumi, T. Nishimoto and T. Narita

Proc. of High Temperature Materials for Power Engineering, Liège, Belgium, 693-702 (2002).

A TiAl intermetallic was electrolytic-plated with 10µm Ni, followed by high Al activity pack cementation at 1273K for 5h to form a coated layer with an inner TiAl₂ / TiAl₃ / Al₂TiNi layer and an outer Ni₂Al₃ layer. The coated layer grew due to inward, up-hill diffusion of Al.

The Ni-aluminized TiAl was oxidized in air for up to 1,000h under a thermal cycling condition between room temperature and 1173K. Mass gain per unit surface area was 8 g/m² after 1,000h and there was little exfoliation of the Al_2O_3 scale. After oxidation for up to1,000h it was found that the coated layer maintains a duplex layer structure of an inner $TiAl_2/Al_2TiNi$ layer and an outer Al-rich β -NiAl layer; the inner layer contains more Al than the outer layer. Both the Ni_2Al_3 and the Al rich β -NiAl contain less than 0.5at% Ti, in accordance with the experimentally determined phase diagram.

Sulfidation Properties of TiAl-2at.%X(X=Si, Mn, Ni, Ge, Y, Zr, La and Ta) Alloys at 1173K and 1.3Pa sulfur Pressure in an H₂S-H₂ Gas Mixture

T. Izumi, T. Yoshioka, S. Hayashi and T. Narita

Intermetallics, 10,353-360 (2002)

TiAl-2at.%X(X=Si, Mn, Ni, Ge, Y, Zr, La and Ta) alloys were sulfidized at 1173K for 86.4ks at a 1.3Pa sulfur pressure in an H₂S-H₂ gas mixture. The structure, phases, and compositions of the external sulfide scale and alloy surface layer were measured using EPMA and X-RD. The sulfides formed were mainly TiS, Ti₃S₄ and Al₂S₃. The alloy surface layer consisted of multi-layered structures that can be classified into three groups: Group 1 of Mn, Ni, Y and Zr as well as TiAl binary alloy with alloy/TiAl₂/TiAl₃/sulfide scales; group 2 of Si and Ge with alloy/TiAl₂/Ti(Al,X)₃/sulfide scales, and group 3 of La and Ta with alloy/TiAl₂/TiAl₃/X-Al alloy/sulfide scales. The TiAl-2La and -2Ni alloys sulfidized faster than the TiAl, while the sulfidation amount for the TiAl-2X (X = Si, Mn, Ge, Y, Zr and Ta) alloys was almost the same as that of TiAl. The thickness of the alloy surface layer increased in the order: Ta < Si < Ni < Mn < Zr < (TiAl binary alloy) < Ge < La < Y.

Modifying Solidification Structures of Sn-Ag Alloys with Third Elements

T. Kobayashi, H. Xue, J. Tanaka, T. Takashima and T. Narita

Proc. of 8th Microjoining and Assembly Technology in Electronics, 209-214 (2002)

Modifying microstructures of Sn-Ag solders have been investigated by adding small addition of third elements under various solidification rates, and effect of Al addition of 0.1, 0.5, and 1.0mass% to the Sn-2.0mass%Ag solder showed a fine and homogeneous eutectic structures containing Ag₂Al precipitates. For the solders containing 0.5 and 1.0mass%Al the Ag₃Sn precipitated as glossy crystals in addition to fine precipitates. The primary β -Sn crystal has an average diameter of 6 μ m in contrast to about 40 μ m for a normal Sn-2.0mass%Ag solder, when solidified with cooling rates between 0.02 and 132K/s. The average size of 6 μ m was independent of cooling rates. The fine structure of the Sn-2.0mass%Ag solder containing (0.1~1.0) mass% Al is due to a fact that the melt formed very fine precipitates of Ag₂Al and probably Al₂O₃ particles, and they seem to act as nucleus for crystallization during solidification.

Growth Direction of Cellular and Dendritic Interface in a Constrained Growth Condition

H. Esaka, H. Daimon, Y. Natsume, K. Ohsasa and M. Tamura

Materials Transactions, 43 1312-1317 (2002)

In-situ observation of unidirectional solidification using transparent substance has been performed to investigate the growth direction of solid phase. Cell and/or dendrite, the preferred growth directions of which are not parallel to the heat flow direction, were observed with various solidification conditions. Dimensionless growth direction (π ' = (angle between heat flow direction and growth direction)/(angle between heat flow direction and preferred growth direction)) changes from zero to unity with increasing growth velocity at a constant temperature gradient. Introducing the normalized growth velocity (V/V_c , where V_c is the critical growth velocity for breaking down a planar interface), the relation between π ' and growth condition could be correlated and π ' could be expressed by a unique line with respect to the normalized growth velocity. Furthermore, the growth directions of cells or dendrites under the condition of unidirectional solidification have been analyzed by the phase-field model. The calculated results agree with the experimental results and the functional relationship between growth velocity and growth direction is qualitatively explained.

Investigation of the Mechanism of Alloy Dendrite effection due to Flowing Melt by Phase-Field Simulation

Y. Natsume, K. Ohsasa and T. Narita

Materials Transactions, 43 2228-2234 (2002)

Phase-field simulation of the dendrite growth of an Fe-0.15 mass%C binary alloy with fluid flow was carried out, and the mechanism of deflection of dendrites in the alloy system was examined. In the simulation, the primary arms growing in a flowing melt inclined toward the upstream direction, and the deflection angle increased with increase in flow velocity. Decrease in deflection angle with increase in growth velocity of the dendrite tip and accelerated growth of side branches were also observed in the simulation. These results of simulation were in good agreement with experimental results. The simulation showed that the change in the thermal field has little effect on the deflection and that the change in the solutal field is the main factor responsible for the deflection of a dendrite in an alloy system. The maximum deflection angle of a single dendrite in the simulation was less than 15°. The large deflection angles of grains (more than 20°-30°) in the experiments were thought to have been caused by nucleation in front of the dendrites and the subsequent competitive growth.

Probabilistic Parameter for Nucleation during olidification of Al Alloys

K.Ohsasa, H.Shirosawa and T.Narita

Int. J. Cast Metals Research, 15, 193-197 (2002)

The frequency of heterogeneous nucleation during the solidification of aluminum base alloys was estimated by comparing experimentally obtained macrostructures of castings with numerically simulated ones. Al-Si binary and Al base multi-component commercial alloys were used in the present study. A molten alloy was unidirectionally solidified from a water-cooled copper chill in an adiabatic mold. The location of columnar to equiaxed transition (CET) in the solidified alloy ingot was measured. A numerical simulation for grain structure formation based on the Monte Carlo method was carried out, and the frequency of heterogeneous nucleation in the alloy was evaluated by producing similar structure with the experimental one. The frequency of heterogeneous nucleation was expressed as a probabilistic function with an exponential form of undercooling that determines the probability of nucleation event in the simulation. The value of the exponent is regarded as the nucleation parameter. The nucleation parameter of Al-Si binary and multi-component commercial alloys varied with Si content.

Tempetature-enthalpy Curves of Multicomponent Casting Alloys

K.Ohsasa, K.Matsuura and H.Shirosawa

Proc. of the 65th World Foundry Congress, 723-733, (2002)

Temperature-enthalpy curves of aluminum base and iron base multi-component commercial alloys were calculated using the ThermoCalc for both an equilibrium state and nonequilibrium state assuming no diffusion in solid. The heat transfer simulations during the solidification of the alloys based on the enthalpy method were carried out using the calculated temperature-enthalpy curves. Thermal analysis experiment of the alloys under a furnace cooling condition was carried out and measured cooling curve was compared with simulated one. The simulated cooling curves obtained under the nonequilibrium condition showed similar shape with the experimental ones.

Reactive Casting and Welding of High-Melting-Point Intermetallic Compounds

K. Matsuura, K. Ohsasa and M. Kudoh

Proc. of the 65th World Foundry Congress, 1097-1104 (2002)

A new process for casting and welding of high-melting-point intermetallics has been proposed, and its feasibility has been investigated using NiAl as a demonstration material. When Al Liquid of 1023K and Ni liquid of 1773K, for example, were mixed at a molar ration of 1:1, the temperature of the liquid mixture quickly rose and exceeded 2300K due to the enthalpy of formation of NiAl, which is much higher than the melting point of NiAl, 1911K. This extremely superheated NiAl liquid was cast into round bar ingots to investigate their chemical and physical properties. When the NiAl was alloyed with Co, the ingot exhibited higher Vickers hardness, more excellent corrosion resistance and lower thermal conductivity, while the thermal expansion coefficient was not affected. When the metals such as Fe-base and Ni base alloys, the heat from the NiAl liquid melted the surface of the base metal and the NiAl and the base metal were welded after solidification. The joint strength exceeded 480Mpa, when the NiAl was welded to a dual phase stainless steel.